Dominik Pölz, BSc

Galerkin Boundary Element Formulations for Impedance Boundary Conditions in Acoustics

MASTER'S THESIS

to achieve the academic degree

Diplom-Ingenieur

Master's degree programme: Civil Engineering and Structural Engineering

submitted to

Graz University of Technology

Supervisor
Univ.-Prof. Dr.-Ing. Martin Schanz

Institute of Applied Mechanics

Supervising assistant
Dipl.-Ing. Thomas Traub

Graz, November 2015

Acknowledgement

I wish to express my sincere gratitude to my supervisor Prof. Martin Schanz for entrusting me with this thesis I could profit so much from. My deepest appreciation goes to my supervising assistant Thomas Traub for his expertise and dedication guided me through my first steps in the boundary element methods.

I thank every member of staff at the Institute of Applied Mechanics for continuously providing advice during my work on this thesis as well as my occupation as teaching assistant.

Last but not least, I wish to thank my friends, my brothers, and especially my parents, Christine and Friedrich, for their unconditional support throughout my studies and personal endeavours.

AFFIDAVIT

EIDESSTATTLICHE ERKLÄRUNG

I declare that I have authored this thesis independently, that I have not used other than the declared sources/resources, and that I have explicitly indicated all material which has been quoted either literally or by content from the sources used. The text document uploaded to TUGRAZonline is identical to the present master's thesis.

Ich erkläre an Eides statt, dass ich die vorliegende Arbeit selbstständig verfasst, andere als die angegebenen Quellen/Hilfsmittel nicht benutzt, und die den benutzten Quellen wörtlich und inhaltlich entnommenen Stellen als solche kenntlich gemacht habe. Das in TUGRAZonline hochgeladene Textdokument ist mit der vorliegenden Masterarbeit identisch.

Date/Datum

Signature/Unterschrift

Abstract

Acoustic wave phenomena play a major role in many applications of engineering sciences. One of the most prevalent topics in acoustics is the encounter between an acoustic wave and a surface. It is well known that soft surfaces tend to absorb larger parts of the incoming waves than acoustically hard ones. Consequently, one has to employ a mechanical model which is capable of reproducing these effects. Within this thesis, a very well-established and straightforward approach to modelling acoustic absorption on surfaces is discussed. Basically, this concept relies on a special impedance boundary condition to account for acoustically soft surfaces. Furthermore, a boundary integral formulation of such problems, which is obtained by means of the integral equation method, seems advantageous. Such a formulation requires a triangulation of the surface only, and it can be applied to unbounded domains easily. In this work, three Galerkin boundary element methods (BEM) for simulating acoustic waves in domains bounded by acoustically hard as well as absorbing surfaces are presented. Moreover, the characteristics of these procedures and the basic properties of the generated approximations are discussed. The considered methods are implemented in an existing BEM code and validated by means of numerical experiments. Finally, the applicability of the realized procedures is illustrated by treating an actual problem of architectural acoustics.

Zusammenfassung

In vielen Bereichen der Ingenieurwissenschaften spielt die Akustik eine wichtige Rolle, wobei besonders das Auftreffen einer Schallwelle auf eine Oberfläche einen mechanisch neuralgischen Punkt darstellt. Es ist gemeinhin bekannt, dass weiche Oberflächen größere Teile einfallender Schallwellen absorbieren als harte. Demnach stellt die Verwendung eines mechanischen Modells, welches diese Effekte abbilden kann, die oberste Prämisse dar. In dieser Masterarbeit wird ein erprobter und unkomplizierter Zugang zur Modellierung schallabsorbierender Oberflächen betrachtet. Die Grundidee dieses Konzepts stellt die Verwendung einer speziellen Impedanz-Randbedingung dar, welche akustisch weiche Berandungen darstellen kann. Weiters ist es sinnvoll, das zugrundeliegende Problem mittels der Integralgleichungsmethode auf Randintegralgleichungen zu transformieren, womit nur die Oberfläche zu diskretisieren ist und unbeschränkte Gebiete leicht behandelt werden können. In dieser Arbeit werden drei Galerkin-Randelementmethoden (BEM) vorgestellt, welche zur Simulation von Schallwellen in Gebieten, die von schallharten und schallabsorbierenden Oberflächen berandet werden, gut geeignet sind. Die besprochenen Verfahren werden in einen bestehenden BEM Code implementiert und anhand von numerischen Experimenten validiert. Um die Einsetzbarkeit der umgesetzten Verfahren zu verdeutlichen, wird abschließend ein reales Problem der Innenraumakustik behandelt.

CONTENTS

1 INTRODUCTION

1.1 Motivation

Acoustic wave phenomena play an important role in many engineering applications. Civil engineers continuously seek to optimize the design of structures to meet the rising demands in terms of architectural acoustics. This pursuit poses a central issue not only when it comes to designing magnificent concert halls, but is essential for the serviceability of any structure. Beyond the scope of civil engineering, the acoustic simulation of vehicles is one of the most prevalent topics in terms of acoustic design. Further topics are marine navigation and acoustic location by means of sonar.

A core part of acoustics is the interaction between acoustic waves and surfaces. Hard surfaces, like concrete walls, reflect the acoustic waves virtually perfectly, while softer surfaces, like foams, tend to absorb significant parts of them. Thus, it is of utmost importance to find models that reliably describe the mechanical behaviour of different surfaces.

Like many other problems in technical science and engineering, a multitude of acoustic wave phenomena can be described by partial differential equations. In most cases, i.e. for general domains and loading scenarios, exact solutions to these problems cannot be found. Hence, one resorts to find approximate solutions by means of numerical mathematics. There is quite a large body of methods for generating solutions to problems governed by differential equations, each of them possessing their respective advantages and drawbacks. Therefore the engineer has to have a certain understanding of these procedures to be able to choose the most viable of these methods for a certain problem at hand.

1.2 State of the art

Perhaps the most straightforward method for solving partial differential equations is the *finite difference method* (FDM, see e.g. [31]), which is based on a discretization of the differential operator itself. More sophisticated methods revolve around variational formulations of the differential equation and their discretization via suitable finite-dimensional trial spaces on the computational domain. The most famous representative of these methods is most certainly the *finite element method* (FEM, see e.g. [4, 16]), however, there are other relevant methods as well, like the class of *spectral methods*, see e.g. [5]. Two

powerful procedures belonging to this group are the Fourier and Chebyshev spectral methods, which make use of the distinguished properties of the underlying exceptional function spaces. One of the more outstanding approaches underlies the *boundary element method (BEM)*, which is the subject of this work. It is based on transforming the differential equation to an equivalent boundary integral equation on the surface of the computational domain. The most prominent boundary element methods in engineering sciences are based on collocation approaches to these operator equations. Additionally, there are boundary element methods that rely on variational formulations of these boundary integral equations and introduce, similarly to the previously mentioned procedures, finite-dimensional trial spaces on the surface of the domain.

Boundary element methods are based on the *integral equation method*, which translates the partial differential equation in the domain to boundary integral equations on the surface. By transferring the problem to the surface of the domain, procedures based on boundary integral equations inherit distinctive properties that set them apart from classical domain-based methods:

- The unknown fields are located only on the boundary, thus only the surface of the domain has to be discretized. For complicated domains the construction of admissible volume meshes might prove to be quite an involved task, while generating suitable triangulations of the surface is rather straightforward in most scenarios.
- Problems posed on unbounded domains can be treated easily, since only its surface is observed. Domain-based methods would require a modification of their formulation to be applicable in this scenario, and even then boundary integral equation methods remain superior in most cases.
- The dimension is reduced by one and the systems of equations are smaller in the process. Domain-based methods lead to algebraic systems with $N_\Omega = \mathcal{O}(h_\Omega^{-3})$ unknowns, while a similar boundary integral equation procedure would bring about $N_\Gamma = \mathcal{O}(h_\Gamma^{-2})$ unknowns, where h_Ω and h_Γ denote the respective discretization parameters. However, the underlying boundary integral operators are non-local which normally leads to fully populated system matrices, implying quadratic complexity $\mathcal{O}(N_\Gamma^2) = \mathcal{O}(h_\Gamma^{-4})$. Sparsely populated matrices associated with classical domain-based methods enjoy linear complexity $\mathcal{O}(N_\Omega) = \mathcal{O}(h_\Omega^{-3})$, thus growing slower by one order of magnitude. This circumstance is the most severe disadvantage of boundary integral procedures and completely cancels out the edge gained in reducing the dimension. Thus, the design of so-called *fast boundary element methods*, which seek sparse representations of the system matrices, have attracted a lot of attention throughout the last decades, see e.g. [27] or [14].
- Most occurring boundary integral operators have a singular nature. As a result their quadrature is significantly more expensive in terms of computational time than those encountered in more conventional methods.

Although the boundary element method is not nearly as versatile as the finite element method, it has already been successfully applied to a certain array of problems in modern engineering, see e.g. [29] or [18]. Perhaps the most notable field of application is electrodynamics, where it is classically used to solve Maxwell's equations efficiently [12]. Furthermore, the boundary element method is increasingly used for solving acoustic problems as well [33].

1.3 Outline

In this work conceivably the most straightforward way of dealing with acoustic absorption is covered. In this approach the absorption is accounted for by a certain boundary condition describing the mechanical properties of the surface by one parameter. In the process, a couple of inherently different boundary element methods for the arising initial-boundary value problem are constructed and examined.

Chapter 2 discusses the physical problem at hand and provides the final initial-boundary value problem under consideration. Moreover, the time dependency is resolved by transferring the problem to Laplace domain via Laplace transformation.

Chapter 3 addresses the boundary integral operators of interest throughout this work.

Chapter 4 is dedicated to the construction of the boundary integral equations describing solutions of the underlying boundary value problem in Laplace domain. Additionally, their variational formulations are presented.

Chapter 5 provides the discretization of the time dependency by shifting the problem to Laplace domain utilizing the convolution quadrature method.

Chapter 6 establishes the discretization of the surface of the spatial domain by means of boundary elements. In addition to a short introduction to Galerkin BEM, the employed trial spaces are introduced as well as their application to the variational formulations. Finally, the compuation of the coefficients in the respective system matrices and load vectors will be covered.

Chapter 7 presents the numerical results of algorithms based on the boundary element methods discussed previously. First, the convergence of the procedures is confirmed and afterwards the approach is used in an application of acoustic engineering.

Chapter 8 concludes this thesis and gives an outlook to topics not covered within this work.

2 PROBLEM STATEMENT

The first step in precisely defining the problem under consideration is to specify the observed domain in both space and time.

Let $\Omega^- \subset \mathbb{R}^3$ be a bounded and open interior domain, while its complement $\Omega^+ = \mathbb{R}^3 \setminus \overline{\Omega}$ is the exterior one. Throughout this work we explicitly focus on problems posed on Ω^-, however, in many applications of boundary integral equation methods problems related to Ω^+ are actually of higher interest. The boundary of the domain $\Gamma := \partial\Omega = \overline{\Omega} \cap (\mathbb{R}^3 \setminus \Omega)$[1] is equipped with an outward unit normal vector field $\mathbf{n}(\mathbf{x})$, $\mathbf{x} \in \Gamma$ defined almost everywhere on Γ. The expression *almost everywhere* or short *a.e.* on Γ refers to all $\mathbf{x} \in \Gamma$ that have nonzero Lebesgue measure. In the language of engineering this means that all geometric entities having one dimension or less are excluded, e.g. edges and corners.

In order to be capable of defining appropriate boundary conditions, one needs to introduce proper extensions of scalar-valued functions $v(\tilde{\mathbf{x}})$, $\tilde{\mathbf{x}} \in \Omega^-$ onto Γ. We consider the *interior Dirichlet trace*

$$\gamma_0^- v(\mathbf{x}) = \lim_{\Omega^- \ni \tilde{\mathbf{x}} \to \mathbf{x} \in \Gamma} v(\tilde{\mathbf{x}}) \quad \forall\, \mathbf{x} \in \Gamma$$

as well as the *interior Neumann trace*

$$\gamma_1^- v(\mathbf{x}) = \big(\mathbf{n}(\mathbf{x}), \gamma_0^- \operatorname{grad} v(\mathbf{x})\big) \quad \forall\, \mathbf{x} \in \Gamma$$

describing the extension of an interior function $v(\tilde{\mathbf{x}})$, $\tilde{\mathbf{x}} \in \Omega^-$ to its respective Dirichlet and Neumann datum. Within this thesis, we limit our considerations to a three-dimensional *Cartesian* coordinate system, which is orthonormal. Thus, the scalar product $(\cdot,\cdot)$ has the representation

$$(\mathbf{u}, \mathbf{v}) = \sum_{j=1}^{3} u_j v_j \tag{2.1}$$

where u_j, $j = 1,2,3$ denotes the j-th entry of $\mathbf{u}$.

Furthermore, let $\Upsilon = (0,T) \subset \mathbb{R}$ be the open timeline under consideration. For a scalar function $w(t)$, $t \in \Upsilon$, whenever we write $w(0)$ we do not refer to the explicit value of w at $t = 0$ but its *continuous extension* from within Υ, i.e.

$$w(0) := \lim_{\Upsilon \ni t \to 0} w(t) = \lim_{\substack{t \to 0 \\ t > 0}} w(t) \quad .$$

[1] Whenever we write Ω, we refer to Ω^- and Ω^+.

Note that this approach is applied to derivatives of w as well. In the case of homogeneous initial conditions w can be continuously extended to the negative time line by

$$w(t) \coloneqq 0 \quad \forall\, t \leq 0 \quad .$$

2.1 The acoustic wave equation

The following considerations are mainly adapted from [1] presenting a rather straightforward approach. For a more comprehensive derivation one might refer to [26] and for further reading on acoustics see e.g. [22, 23].

First, we introduce several conventions concerning the notation which do not interfere with the generality of the results:

- The fluid pressure acting on a surface is denoted by $u^t(\tilde{\mathbf{x}},t)$, the density by $\rho^t(\tilde{\mathbf{x}},t)$, and the velocity by $\mathbf{v}^t(\tilde{\mathbf{x}},t)$. All these fields are dependent on $(\tilde{\mathbf{x}},t) \in \Omega^- \times (0,\infty)$.
- Above quantities are decomposed into a constant mean value and a perturbation around it, such that

$$\begin{aligned} u^t(\tilde{\mathbf{x}},t) &= u_0 + u(\tilde{\mathbf{x}},t), \\ \rho^t(\tilde{\mathbf{x}},t) &= \rho_0 + \rho(\tilde{\mathbf{x}},t), \\ \mathbf{v}^t(\tilde{\mathbf{x}},t) &= \mathbf{v}_0 + \mathbf{v}(\tilde{\mathbf{x}},t) \end{aligned} \tag{2.2}$$

  holds for all $(\tilde{\mathbf{x}},t) \in \Omega^- \times (0,\infty)$.
- Note that the above fields always depend on space and time and if they are given without the argument list then this is done merely to provide better readability of the formulas.
- First derivatives with respect to time are denoted by $\partial_t \coloneqq \frac{\partial}{\partial t}$ and higher order ones by $\partial_t^p \coloneqq \frac{\partial^p}{\partial t^p}$, $p \in \mathbb{N}$ respectively.

2.1.1 Balance equations

Balance of mass

In the absence of an interior mass source or loss, the continuity equation in differential form

$$\partial_t \rho^t + \operatorname{div}\left(\rho^t \mathbf{v}^t\right) = 0$$

holds, cf. [15]. Inserting the assumed decomposition (2.2) yields the expression

$$\partial_t \rho + \rho_0 \mathrm{div}\mathbf{v} + \mathrm{div}(\rho \mathbf{v}) = 0 \tag{2.3}$$

which holds naturally for any $(\tilde{\mathbf{x}}, t) \in \Omega^- \times (0, \infty)$.

Balance of momentum

The balance of momentum is given by the relation

$$\partial_t \left(\rho^t \mathbf{v}^t\right) + \mathbf{v}^t \,\mathrm{div}\left(\rho^t \mathbf{v}^t\right) + \rho \mathbf{v}^t \,\mathrm{div}\mathbf{v}^t + \mathrm{grad}u^t - \mathbf{b} = \mathbf{0}$$

where $\mathbf{b}(\tilde{\mathbf{x}}, t)$ denotes the volumetric forces acting inside the body, see e.g. [15]. Again, we insert the decomposition (2.2) and obtain

$$\begin{aligned} \rho_0 \partial_t \mathbf{v} + \mathbf{v}_0 \partial_t \rho + \mathbf{v} \partial_t \rho + \rho \partial_t \mathbf{v} \\ + \rho_0 \mathbf{v}_0 \mathrm{div}\mathbf{v} + \rho_0 \mathbf{v} \mathrm{div}\mathbf{v} + \mathbf{v}\mathrm{div}(\rho \mathbf{v}) + \mathbf{v}_0 \mathrm{div}(\rho \mathbf{v}) \\ + (\rho_0 \mathbf{v}_0 + \rho_0 \mathbf{v} + \rho \mathbf{v}_0 + \rho \mathbf{v}) \,\mathrm{div}\mathbf{v} + \mathrm{grad}u - \mathbf{b} = \mathbf{0} \end{aligned} \tag{2.4}$$

which again is satisfied for any $(\tilde{\mathbf{x}}, t) \in \Omega^- \times (0, \infty)$.

2.1.2 Linearization

When considering a problem posed in the fields of civil or mechanical engineering it is mostly sufficient to resort to the theory of *linear acoustics*. The major assumption is that all perturbations have a marginal magnitude compared to their respective mean value, i.e.

$$\begin{aligned} u &\ll u_0 \\ \rho &\ll \rho_0 \\ \|\mathbf{v}\| &\ll \|\mathbf{v}_0\| \end{aligned}$$

where $\|\cdot\|$ denotes the standard l^2 norm induced by the scalar product (2.1). With this linearization available we revisit the balance equations. For the last term in (2.3)

$$\mathrm{div}(\rho \mathbf{v}) = (\mathrm{grad}\rho, \mathbf{v}) + \rho \mathrm{div}\mathbf{v}$$

we use the continuity of the scalar product and the estimate introduced above

$$(\mathrm{grad}\rho, \mathbf{v}) \leq \|\mathrm{grad}\rho\| \|\mathbf{v}\| \ll \|\mathrm{grad}\rho\| \|\mathbf{v}_0\|$$

and hence $\mathrm{div}(\rho \mathbf{v}) = 0$ within a linearized framework. We obtain the linearized continuity equation

$$\partial_t \rho + \rho_0 \mathrm{div}\mathbf{v} = 0 \quad . \tag{2.5}$$

and by applying similar arguments to (2.4) one ends up with the linearized balance of momentum equation

$$\rho_0 \partial_t \mathbf{v} + \text{grad} u = \mathbf{b} \quad . \tag{2.6}$$

The time derivative of (2.5) and the divergence of (2.6) form the system

$$\begin{aligned} \partial_t^2 \rho + \rho_0 \text{div} \partial_t \mathbf{v} &= 0 \\ \rho_0 \text{div} \partial_t \mathbf{v} + \text{divgrad} u &= \text{div} \mathbf{b} \end{aligned} \quad ,$$

and insertion of the first into to second equation yields

$$-\partial_t^2 \rho + \Delta u = \text{div} \mathbf{b} \tag{2.7}$$

where $\Delta = \text{divgrad}$ denotes the *Laplace operator*.

2.1.3 Constitutive equation

For linear acoustics it is mostly sufficient to consider isentropic flows only. The thermodynamic processes are adiabatic, i.e. there occurs no transfer of heat nor matter and there is no loss of energy. Within a linearized setting one finds

$$\frac{\rho}{\rho_0} = \frac{1}{\rho_0 c_0^2} u$$

where c_0 is the speed of sound determined by the relation

$$c_0 = \sqrt{\frac{K}{\rho_0}}$$

with the *bulk modulus* for adiabatic conditions K, see e.g. [26].

With the constitutive relation $u(\tilde{\mathbf{x}},t) = c^2 \rho(\tilde{\mathbf{x}},t)$ serving as closure condition in (2.7) one ends up with a pressure formulation of the linear scalar wave equation

$$\frac{1}{c_0^2} \partial_t^2 u(\tilde{\mathbf{x}},t) - \Delta u(\tilde{\mathbf{x}},t) = \text{div} \mathbf{b}(\tilde{\mathbf{x}},t) \quad \forall\, (\tilde{\mathbf{x}},t) \in \Omega^- \times (0,\infty) \quad .$$

In most applications the only volumetric force acting on the fluid is gravity. Since this force is constant, its divergence vanishes, yielding

$$c_0^{-2} \partial_t^2 u(\tilde{\mathbf{x}},t) - \Delta u(\tilde{\mathbf{x}},t) = 0 \quad \forall\, (\tilde{\mathbf{x}},t) \in \Omega^- \times (0,\infty)$$

which is a linear homogeneous partial differential equation of hyperbolic type with constant coefficients.

2.2 Impedance boundary condition

Throughout this work the acoustic absorption on the surface Γ will be accounted for by an impedance boundary condition. As stated in [23] the acoustic absorption of a wall or some other surface is described by the wall impedance $z(\mathbf{x}),\ \mathbf{x} \in \Gamma$. In a one dimensional setting it is the ratio of the acoustic pressure $u(x)$ and the scalar velocity $v(x)$

$$z = \frac{u(0)}{v(0)}$$

where the surface is assumed to be located at $x = 0$. This concept can be extended to higher spatial dimensions by only considering the very portion of the velocity vector $\mathbf{v}$ parallel to the normal vector, i.e.

$$z(\mathbf{x}) = \frac{\gamma_0^- u(\mathbf{x},t)}{\left(\mathbf{n}(\mathbf{x}), \gamma_0^- \mathbf{v}(\mathbf{x},t)\right)} \quad \forall\, \mathbf{x} \in \Gamma \tag{2.8}$$

which is assumed to be constant with respect to time. Performing the scalar product of the linearized momentum equation (2.6) with the normal vector as well as applying the Dirichlet trace we obtain

$$\rho_0 \partial_t \left(\mathbf{n}(\mathbf{x}), \gamma_0^- \mathbf{v}(\mathbf{x},t)\right) + \gamma_1^- u(\mathbf{x},t) = f(\mathbf{x},t) \quad \forall\, (\mathbf{x},t) \in \Gamma \times (0,\infty) \tag{2.9}$$

where $f(\mathbf{x},t) \coloneqq \left(\mathbf{n}(\mathbf{x}), \gamma_0^- \mathbf{b}(\mathbf{x},t)\right)$ is the exterior pressure applied to the surface. Insertion of (2.8) into (2.9) yields

$$\gamma_1^- u(\mathbf{x},t) + \frac{\rho_0}{z(\mathbf{x})} \partial_t \gamma_0^- u(\mathbf{x},t) = f(\mathbf{x},t) \quad \forall\, (\mathbf{x},t) \in \Gamma \times (0,\infty)$$

which is basically already the aspired boundary condition, however, in applied acoustics it is often more convenient to use a slightly different representation. The following relation holds

$$\frac{z(\mathbf{x})}{\rho_0 c_0} = \frac{1 + r(\mathbf{x})}{1 - r(\mathbf{x})} = \alpha(\mathbf{x}) \quad \forall\, \mathbf{x} \in \Gamma$$

where the coefficient of reflection $r(\mathbf{x}) \in \mathbb{C}$ is connected to the absorption coefficient $\alpha_s \in \mathbb{R}$ such that

$$\alpha_s(\mathbf{x}) = 1 - |r(\mathbf{x})|^2 \quad \forall\, \mathbf{x} \in \Gamma$$

holds, see [23]. Finally, this leads to

$$\alpha(\mathbf{x}) = \cos\theta \frac{1 - \sqrt{1 - \alpha_s(\mathbf{x})}}{1 + \sqrt{1 - \alpha_s(\mathbf{x})}} \quad \forall\, \mathbf{x} \in \Gamma$$

where θ is the incident wave angle. The actual values for α_s depend on the material the surface is made of and the frequency of the signal. Furthermore, note that $\alpha \in [0,1]$, where $\alpha = 0$ represents total reflection and $\alpha = 1$ total absorption of incoming waves. When it

comes to designing structures the actual values of α_s for a variety of materials as well as frequencies can be found in specific guidelines or national design codes, e.g. [24].

Thus, the acoustic impedance boundary condition reads as

$$\gamma_1^- u(\mathbf{x},t) + \frac{\alpha(\mathbf{x})}{c_0}\gamma_0^- \partial_t u(\mathbf{x},t) = f(\mathbf{x},t) \quad \forall\, (\mathbf{x},t) \in \Gamma \times (0,\infty)$$

where we introduce $\kappa(\mathbf{x}) = \frac{\alpha(\mathbf{x})}{c_0}$ for the sake of simplicity.

2.3 Initial-boundary value problem

Collecting the results derived in the prequel the complete initial-boundary value problem

$$\begin{aligned} c_0^{-2}\partial_t^2 u(\tilde{\mathbf{x}},t) - \Delta u(\tilde{\mathbf{x}},t) &= 0 && \forall\, (\tilde{\mathbf{x}},t) \in \Omega^- \times (0,\infty) \\ \partial_t u(\tilde{\mathbf{x}},0) = u(\tilde{\mathbf{x}},0) &= 0 && \forall\, \tilde{\mathbf{x}} \in \Omega^- \\ \gamma_1^- u(\mathbf{x},t) + \kappa(\mathbf{x})\gamma_0^- \partial_t u(\mathbf{x},t) &= f(\mathbf{x},t) && \forall\, (\mathbf{x},t) \in \Gamma \times (0,\infty) \end{aligned} \tag{2.10}$$

is obtained. The initial conditions are homogeneous, i.e. the fluid starts at a quiescent state, and the impedance boundary condition is of Robin-type. For a theoretical review of this problem, including a discussion about its solvability, see e.g. [13].

2.3.1 Laplace transformed boundary value problem

Problem (2.10), which is posed in time-domain may be transformed to *Laplace domain*. The translation from time to Laplace domain is called *Laplace transform*, which is an integral transformation defined by

$$\hat{f}(s) \coloneqq \mathcal{L}\{f\}(s) \coloneqq \lim_{a\to\infty} \int_0^a \exp(-st) f(t)\, dt$$

for some suitable $s \in \mathbb{C}$. To shorten the notation, we introduce the following notation associating a function in time domain to its respective Laplace transform

$$f(t) \circ\!\!-\!\!\bullet\, \hat{f}(s) \quad .$$

The Laplace transform comes in handy since several important operations in time domain correspond to much simpler ones in Laplace domain. Perhaps the most notable one is that differentiation in time domain corresponds to multiplication with the parameter in Laplace domain with a mere subtraction of the initial condition

$$\partial_t f(t) \circ\!\!-\!\!\bullet\, s\hat{f}(s) - f(0) \quad .$$

Moreover, we have the inverse Laplace transform

$$f(t) \coloneqq \mathcal{L}^{-1}\{\hat{f}\}(t) \coloneqq \lim_{b\to\infty} \frac{1}{2\pi i} \int_{a-ib}^{a+ib} \exp(ts)\hat{f}(s)ds \quad (t>0) \tag{2.11}$$

where i is the imaginary unit and $a \in \mathbb{R}$ has to be chosen, such that the integral converges. Note that $f(t)$ may be extended to the negative timeline by $f(t) = 0$ for $t \leq 0$. Similarly to above we abbreviate

$$\hat{f}(s) \bullet\!\!-\!\!\circ f(t) \quad .$$

Applying the Laplace transform to the partial differential equation $\mathcal{L}\{c^{-2}\partial_t^2 u - \Delta u\} = \mathcal{L}\{0\} = 0$ yields

$$c_0^{-2}\left(s^2\hat{u}(\tilde{\mathbf{x}}) - s\underbrace{u(\tilde{\mathbf{x}},0)}_{=0\ \forall\tilde{\mathbf{x}}\in\Omega} - \underbrace{\partial_t u(\tilde{\mathbf{x}},0)}_{=0\ \forall\tilde{\mathbf{x}}\in\Omega}\right) - \Delta\hat{u}(\tilde{\mathbf{x}}) = 0$$

for vanishing initial conditions. By employing the same procedure for the boundary condition we obtain an elliptic boundary value problem in Laplace domain

$$\begin{aligned} -\Delta\hat{u}(\tilde{\mathbf{x}}) + c_0^{-2}s^2\hat{u}(\tilde{\mathbf{x}}) &= 0 \qquad \forall\,\tilde{\mathbf{x}} \in \Omega^- \\ \gamma_1^-\,\hat{u}(\mathbf{x}) + s\kappa(\mathbf{x})\gamma_0^-\,\hat{u}(\mathbf{x}) &= \hat{f}(\mathbf{x}) \quad \forall\,\mathbf{x} \in \Gamma \end{aligned} \tag{2.12}$$

that corresponds to the intial-boundary value problem in time domain (2.10). Note that the partial differential operator $-\Delta + c_0^{-2}s^2$ in (2.12) is sometimes called *Yukawa operator*, cf. [18]. Actually, it is equivalent to the *Helmholtz operator* $-\Delta - c_0^{-2}\omega^2$ for complex-valued wave numbers, i.e. $s = -i\omega$. Throughout this entire work, these operators are not distinguished in a strict fashion. Whenever we refer to the Helmholtz operator we implicitly invoke the more general Yukawa operator.

3 REPRESENTATION FORMULA AND BOUNDARY INTEGRAL OPERATORS

In this chapter, the solution of the partial differential equation is transferred to an equivalent boundary integral equation. Furthermore, the occuring boundary integral operators are introduced.

3.1 Representation formula in time domain

To derive the representation formula in time domain, the wave equation is multiplied with a suitable test function $v(\tilde{\mathbf{x}},t)$. Additionally, a convolution with respect to time is performed and the resulting equation is integrated over the domain Ω^-

$$\begin{aligned}\int_{\Omega^-} \left(\left(c_0^{-2}\partial_t^2 u - \Delta u\right) * v\right)(\tilde{\mathbf{x}},\tau)\, d\tilde{\mathbf{x}} &= c_0^{-2}\int_{\Omega^-} (\partial_t^2 u * v)(\tilde{\mathbf{x}},\tau)\, d\tilde{\mathbf{x}} - \int_{\Omega^-} (\Delta u * v)(\tilde{\mathbf{x}},\tau)\, d\tilde{\mathbf{x}} \\ &= c_0^{-2}\int_{\Omega^-}\int_0^\tau \partial_t^2 u(\tilde{\mathbf{x}},t) v(\tilde{\mathbf{x}},\tau-t)\, dt\, d\tilde{\mathbf{x}} - \int_{\Omega^-}\int_0^\tau \Delta u(\tilde{\mathbf{x}},t) v(\tilde{\mathbf{x}},\tau-t)\, dt\, d\tilde{\mathbf{x}} \quad . \end{aligned} \tag{3.1}$$

Considering the first term in (3.1) we recall two rules for convolution

$$\begin{aligned}(u*v) &= (v*u) \quad , \\ \partial_t(u*v) &= \partial_t u * v + u(\tilde{\mathbf{x}},0)v(\mathbf{x},t) \quad ,\end{aligned} \tag{3.2}$$

see e.g. [10]. Using the second relation in (3.2) we obtain

$$\begin{aligned}\partial_t^2(u*v) &= \partial_t(\partial_t u * v + u(\tilde{\mathbf{x}},0)v(\tilde{\mathbf{x}},t)) \\ &= \partial_t^2 u * v + \underbrace{\partial_t u(\tilde{\mathbf{x}},0)}_{=0\ \forall \tilde{\mathbf{x}}\in\Omega^-} v(\tilde{\mathbf{x}},t) + \underbrace{u(\tilde{\mathbf{x}},0)}_{=0\ \forall \tilde{\mathbf{x}}\in\Omega^-} \partial_t v(\tilde{\mathbf{x}},t) \\ &= \partial_t^2 u * v\end{aligned}$$

where we inserted the vanishing initial conditions. Application of the first rule of (3.2) yields

$$\partial_t^2 u * v = \partial_t^2(u*v) = \partial_t^2(v*u) = \partial_t^2 v * u = u * \partial_t^2 v \quad , \tag{3.3}$$

thus we end up with

$$c_0^{-2} \int\limits_{\Omega^-} \int\limits_0^\tau \partial_t^2 u(\tilde{\mathbf{x}},t) v(\tilde{\mathbf{x}},\tau-t)\, dt\, d\tilde{\mathbf{x}} = c_0^{-2} \int\limits_{\Omega^-} \int\limits_0^\tau u(\tilde{\mathbf{x}},t) \partial_t^2 v(\tilde{\mathbf{x}},\tau-t)\, dt\, d\tilde{\mathbf{x}} \quad . \tag{3.4}$$

As we are switching our attention to the last term in (3.1) we consider

$$\int\limits_{\Omega^-} -\Delta u(\tilde{\mathbf{x}}) v(\tilde{\mathbf{x}}) d\tilde{\mathbf{x}} = \sum_{j=1}^{3} \int\limits_{\Omega^-} -\partial_{x_j}^2 u(\tilde{\mathbf{x}}) v(\tilde{\mathbf{x}}) d\tilde{\mathbf{x}}$$

and by applying integration by parts [30]

$$\int\limits_{\Omega^-} \partial_{x_j} u(\tilde{\mathbf{x}}) v(\tilde{\mathbf{x}}) d\tilde{\mathbf{x}} = \int\limits_{\Gamma} \gamma_0^- u(\mathbf{x}) \gamma_0^- v(\mathbf{x}) n_i(\mathbf{x}) ds_{\mathbf{x}} - \int\limits_{\Omega^-} u(\tilde{\mathbf{x}}) \partial_{x_j} v(\tilde{\mathbf{x}}) d\tilde{\mathbf{x}}$$

we obtain

$$\int\limits_{\Omega^-} -\Delta u(\tilde{\mathbf{x}},t) v(\tilde{\mathbf{x}},t) d\tilde{\mathbf{x}} = \sum_{j=1}^{3} \int\limits_{\Omega^-} \partial_{x_j} u(\tilde{\mathbf{x}}) \partial_{x_j} v(\tilde{\mathbf{x}}) d\tilde{\mathbf{x}} - \int\limits_{\Gamma} \gamma_1^- u(\mathbf{x}) \gamma_0^- v(\mathbf{x}) \quad . \tag{3.5}$$

By introducing the symmetric bilinear form

$$a(u,v) = \sum_{j=1}^{3} \int\limits_{\Omega^-} \partial_{x_j} u(\tilde{\mathbf{x}}) \partial_{x_j} v(\tilde{\mathbf{x}}) d\tilde{\mathbf{x}} = \int\limits_{\Omega^-} (\mathrm{grad} u(\tilde{\mathbf{x}}), \mathrm{grad} v(\tilde{\mathbf{x}}))\, d\tilde{\mathbf{x}}$$

equation (3.5) reveals itself as *Green's first formula*

$$a(u,v) = \int\limits_{\Omega^-} -\Delta u(\tilde{\mathbf{x}}) v(\tilde{\mathbf{x}}) d\tilde{\mathbf{x}} + \int\limits_{\Gamma} \gamma_1^- u(\mathbf{x}) \gamma_0^- v(\mathbf{x}) ds_{\mathbf{x}} \quad .$$

By using the symmetry of the bilinear form $a(u,v) = a(v,u)$ we obtain *Green's second formula* for the Laplace operator

$$\int\limits_{\Omega^-} -\Delta u(\tilde{\mathbf{x}}) v(\tilde{\mathbf{x}}) d\tilde{\mathbf{x}} + \int\limits_{\Gamma} \gamma_1^- u(\mathbf{x}) \gamma_0^- v(\mathbf{x}) ds_{\mathbf{x}} = \int\limits_{\Omega^-} -u(\tilde{\mathbf{x}}) \Delta v(\tilde{\mathbf{x}}) d\tilde{\mathbf{x}} + \int\limits_{\Gamma} \gamma_0^- u(\mathbf{x}) \gamma_1^- v(\mathbf{x}) ds_{\mathbf{x}} \tag{3.6}$$

and hence

$$\int\limits_{\Omega^-} -\Delta u(\tilde{\mathbf{x}}) v(\tilde{\mathbf{x}}) d\tilde{\mathbf{x}} = \int\limits_{\Gamma} \gamma_0^- u(\mathbf{x}) \gamma_1^- v(\mathbf{x}) ds_{\mathbf{x}} - \int\limits_{\Gamma} \gamma_1^- u(\mathbf{x}) \gamma_0^- v(\mathbf{x}) ds_{\mathbf{x}} + \int\limits_{\Omega^-} -u(\tilde{\mathbf{x}}) \Delta v(\tilde{\mathbf{x}}) d\tilde{\mathbf{x}} \quad . \tag{3.7}$$

Insertion of (3.4) and (3.7) into (3.1) yields

$$
\begin{aligned}
c_0^{-2} \int_{\Omega^-} \int_0^\tau \partial_t^2 u(\tilde{\mathbf{x}},t) v(\tilde{\mathbf{x}},\tau-t)\,dt\,d\tilde{\mathbf{x}} - \int_{\Omega^-} \int_0^\tau \Delta u(\tilde{\mathbf{x}},t) v(\tilde{\mathbf{x}},\tau-t)\,dt\,d\tilde{\mathbf{x}} \\
= c_0^{-2} \int_{\Omega^-} \int_0^\tau u(\tilde{\mathbf{x}},t) \partial_t^2 v(\tilde{\mathbf{x}},\tau-t)\,dt\,d\tilde{\mathbf{x}} + \int_\Gamma \int_0^\tau \gamma_0^- u(\mathbf{x},t) \gamma_1^- v(\mathbf{x},\tau-t) dt\,ds_{\mathbf{x}} \\
- \int_\Gamma \int_0^\tau \gamma_1^- u(\mathbf{x},t) \gamma_0^- v(\mathbf{x},\tau-t) dt\,ds_{\mathbf{x}} - \int_{\Omega^-} \int_0^t u(\tilde{\mathbf{x}},t) \Delta v(\tilde{\mathbf{x}},\tau-t) dt\,d\tilde{\mathbf{x}}
\end{aligned}
$$

and thus

$$
\begin{aligned}
\int_{\Omega^-} \int_0^\tau \underbrace{\left(c_0^{-2}\partial_t^2 u(\tilde{\mathbf{x}},t) - \Delta u(\tilde{\mathbf{x}},t)\right)}_{=0 \;\forall\,(\tilde{\mathbf{x}},t)\in\Omega^-\times(0,\infty)} v(\tilde{\mathbf{x}},\tau-t) dt\,d\tilde{\mathbf{x}} \\
= \int_{\Omega^-} \int_0^\tau u(\tilde{\mathbf{x}},t) \left(c_0^{-2}\partial_t^2 v(\tilde{\mathbf{x}},\tau-t) - \Delta v(\tilde{\mathbf{x}},\tau-t)\right) dt\,d\tilde{\mathbf{x}} \\
+ \int_\Gamma \int_0^\tau \gamma_0^- u(\mathbf{x},t) \gamma_1^- v(\mathbf{x},\tau-t) dt\,ds_{\mathbf{x}} - \int_\Gamma \int_0^\tau \gamma_1^- u(\mathbf{x},t) \gamma_0^- v(\mathbf{x},\tau-t) dt\,ds_{\mathbf{x}}
\end{aligned}
$$

which equals zero, since $u(\tilde{\mathbf{x}},t)$ is a solution of the homogeneous differential equation in $\Omega^- \times (0,\infty)$.

In order to provide a notation that is consistent with other literature, we swap the names of the variables. For $(\tilde{\mathbf{y}},\tau) \in \Omega^- \times (0,\infty)$ we have

$$
\begin{aligned}
&\int_0^t \int_{\Omega^-} u(\tilde{\mathbf{y}},\tau) \left(c_0^{-2}\partial_\tau^2 v(\tilde{\mathbf{y}},t-\tau) - \Delta v(\tilde{\mathbf{y}},t-\tau)\right) d\tilde{\mathbf{y}} d\tau \\
&+ \int_0^t \int_\Gamma \gamma_0^- u(\mathbf{y},t) \gamma_1^- v(\mathbf{y},t-\tau) ds_{\mathbf{y}} d\tau - \int_0^t \int_\Gamma \gamma_1^- u(\mathbf{y},t) \gamma_0^- v(\mathbf{y},t-\tau) ds_{\mathbf{y}} d\tau = 0 \quad . \qquad (3.8)
\end{aligned}
$$

Note that (3.8) describes a solution $u(\tilde{\mathbf{y}},\tau)$ of the differential equation, however, the differential operator $c_0^{-2}\partial_t^2 - \Delta$ has been shifted from $u(\tilde{\mathbf{y}},\tau)$ to the test function $v(\tilde{\mathbf{y}},t)$ by means of integration by parts. Furthermore, only the first term is related to the domain

Ω^-, while the remaining two are associated to the boundary Γ. If there exists a test function $v(\tilde{\mathbf{y}},t-\tau) := U(\tilde{\mathbf{x}}-\tilde{\mathbf{y}},t-\tau)$ such that

$$\int_0^t \int_{\Omega^-} \left(c_0^{-2}\partial_\tau^2 - \Delta_{\tilde{\mathbf{y}}}\right) U(\tilde{\mathbf{x}}-\tilde{\mathbf{y}},t-\tau)u(\tilde{\mathbf{y}},\tau)\,d\tilde{\mathbf{y}}d\tau = u(\tilde{\mathbf{x}},t) \tag{3.9}$$

for any $(\tilde{\mathbf{x}},t) \in \Omega^- \times (0,\infty)$, then the solution of the partial differential equation described by (3.8) is given by the *representation formula*

$$u(\tilde{\mathbf{x}},t) = \int_0^t \int_\Gamma U(\tilde{\mathbf{x}}-\mathbf{y},t-\tau)\,\gamma_1^- u(\mathbf{y},t)ds_\mathbf{y}d\tau - \int_0^t \int_\Gamma \gamma_{1,\mathbf{y}}^- U(\tilde{\mathbf{x}}-\mathbf{y},t-\tau)\,\gamma_0^- u(\mathbf{y},\tau)ds_\mathbf{y}d\tau \tag{3.10}$$

which characterizes the solution of the differential equation only using the Cauchy data and a test function satisfying (3.9). The representation formula is governed by two boundary integrals describing convolutions in both space and time and allows us to compute solutions in the domain Ω^- only by knowing data on the surface Γ. This distinguished property is pivotal for any boundary integral equation method.

The knowledge of a test function satisfying (3.9) is fundamental for transforming the differential equation to equivalent boundary integrals. With the sifting property of the *Dirac distribution* δ_0

$$\int_0^T \delta_0(t-\tau)f(\tau)d\tau = f(t) \quad \forall\, t \in (0,T)$$

we find that we seek a distributional solution of the partial differential equation

$$\left[\left(c_0^{-2}\partial_\tau^2 - \Delta_{\tilde{\mathbf{y}}}\right)U\right](\tilde{\mathbf{x}}-\tilde{\mathbf{y}},t-\tau) = \delta_0(\tilde{\mathbf{x}}-\tilde{\mathbf{y}})\delta_0(t-\tau) \quad \forall\, \tilde{\mathbf{x}},\tilde{\mathbf{y}} \in \mathbb{R}^3;\, t,\tau \in (0,\infty)$$

where U is commonly called *fundamental solution*, see [30]. For a brief introduction to distributions, especially the Dirac distribution, refer to [30] and [9] for its connection to the Laplace transformation.

The fundamental solution of the wave equation in three spatial dimensions reads as

$$U(\tilde{\mathbf{z}},t) = \frac{1}{4\pi\|\tilde{\mathbf{z}}\|}\delta_0\left(t - \frac{\|\tilde{\mathbf{z}}\|}{c_0}\right) \quad \forall\,(\tilde{\mathbf{z}},t) \in \mathbb{R}^3 \times (0,\infty) \tag{3.11}$$

see e.g. [10] or [8].

In this thesis we will solely focus on boundary element formulations in the Laplace domain, thus we will now shift our attention to deriving the representation formula of the Helmholtz equation and showing the equivalence of both formulations.

3.2 Representation formula in Laplace domain

Similarly to the previous approach, the Helmholtz equation is multiplied with a suitable test function $\hat{v}(\tilde{\mathbf{x}})$ and integrated over the entire domain Ω^-. For the sake of simplicity we set $\lambda := c_0^{-2}s^2$, yielding

$$0 = \int_{\Omega^-} \left(-\Delta\hat{u}(\tilde{\mathbf{x}}) + \lambda^2\hat{u}(\tilde{\mathbf{x}})\right)\hat{v}(\tilde{\mathbf{x}})d\tilde{\mathbf{x}} = \int_{\Omega^-} -\Delta\hat{u}(\tilde{\mathbf{x}})\hat{v}(\tilde{\mathbf{x}})d\tilde{\mathbf{x}} + \lambda^2\int_{\Omega^-}\hat{u}(\tilde{\mathbf{x}})\hat{v}(\tilde{\mathbf{x}})d\tilde{\mathbf{x}} \quad . \tag{3.12}$$

By applying Green's second formula (3.6) to the first term in (3.12) we obtain

$$0 = \int_{\Gamma} \gamma_0^-\,\hat{u}(\mathbf{x})\gamma_1^-\,\hat{v}(\mathbf{x})ds_{\mathbf{x}} - \int_{\Gamma}\gamma_1^-\,\hat{u}(\mathbf{x})\gamma_0^-\,\hat{v}(\mathbf{x})ds_{\mathbf{x}} + \int_{\Omega^-} -\hat{u}(\tilde{\mathbf{x}})\Delta\hat{v}(\tilde{\mathbf{x}})d\tilde{\mathbf{x}} + \lambda^2\int_{\Omega^-}\hat{u}(\tilde{\mathbf{x}})\hat{v}(\tilde{\mathbf{x}})d\tilde{\mathbf{x}}$$

leading to

$$0 = \int_{\Omega^-}\left(-\Delta\hat{u}(\tilde{\mathbf{y}}) + \lambda^2\hat{u}(\tilde{\mathbf{y}})\right)\hat{v}(\tilde{\mathbf{y}})d\tilde{\mathbf{y}} + \int_{\Gamma}\gamma_0^-\,\hat{u}(\mathbf{y})\gamma_1^-\,\hat{v}(\mathbf{y})ds_{\mathbf{y}} - \int_{\Gamma}\gamma_1^-\,\hat{u}(\mathbf{y})\gamma_0^-\,\hat{v}(\mathbf{y})ds_{\mathbf{y}} \tag{3.13}$$

where we relabeled variables again. Note that above equation equals zero, due to the fact that $\hat{u}(\tilde{\mathbf{y}})$ is a solution of the homogeneous differential equation for $\tilde{\mathbf{y}} \in \Omega^-$. If there exists a function $\hat{u}(\tilde{\mathbf{y}}) := \hat{U}_s(\tilde{\mathbf{x}} - \tilde{\mathbf{y}})$ such that

$$\int_{\Omega}\left((-\Delta_{\tilde{\mathbf{y}}} + \lambda^2)\hat{U}_s\right)(\tilde{\mathbf{x}} - \tilde{\mathbf{y}})\hat{v}(\tilde{\mathbf{y}})d\tilde{\mathbf{y}} = u(\tilde{\mathbf{x}}) \tag{3.14}$$

for any $\tilde{\mathbf{x}} \in \Omega$ we may obtain the representation formula

$$u(\tilde{\mathbf{x}}) = \int_{\Gamma}\hat{U}_s(\tilde{\mathbf{x}} - \mathbf{y})\,\gamma_1^-\,\hat{u}(\mathbf{y})(\mathbf{y})ds_{\mathbf{y}} - \int_{\Gamma}\gamma_{1,\mathbf{y}}^-\hat{U}_s(\tilde{\mathbf{x}} - \mathbf{y})\,\gamma_0^-\,\hat{u}(\mathbf{y})ds_{\mathbf{y}} \tag{3.15}$$

in Laplace domain. The fundamental solution is the distributional solution of the partial differential equation

$$\left(\left(-\Delta_{\tilde{\mathbf{y}}} + \frac{s^2}{c_0^2}\right)\hat{U}_s\right)(\tilde{\mathbf{x}} - \tilde{\mathbf{y}}) = \delta_0(\tilde{\mathbf{x}} - \tilde{\mathbf{y}}) \quad \forall\,\tilde{\mathbf{x}}, \tilde{\mathbf{y}} \in \mathbb{R}^3$$

and reads in three spatial dimensions as

$$\hat{U}_s(\tilde{\mathbf{z}}) = \frac{\exp\left(-\frac{s}{c_0}\|\tilde{\mathbf{z}}\|\right)}{4\pi\|\tilde{\mathbf{z}}\|} \quad \forall\,\tilde{\mathbf{z}} \in \mathbb{R}^3 \tag{3.16}$$

see e.g. [28]. Note that the fundamental solution is analytic for $\tilde{\mathbf{z}} \neq \mathbf{0}$ and singular at $\tilde{\mathbf{z}} = \mathbf{0}$. By using the Laplace transforms

$$\begin{aligned} \delta_0(t) \quad &\circ\!\!-\!\!\bullet \quad 1 \\ f(t-a)\Theta(t-a) \quad &\circ\!\!-\!\!\bullet \quad \exp(-as)\hat{f}(s) \quad \text{for } a \geq 0 \end{aligned}$$

see e.g. [9], where $\Theta(t)$ denotes the *Heaviside step function*, cf. appendix A. It can be shown that the Laplace transform of the fundamental solution in time domain, yields the fundamental solution for the Helmholtz equation

$$U(\tilde{\mathbf{z}},t) = \frac{1}{4\pi\|\tilde{\mathbf{z}}\|}\delta_0\left(t - \frac{1}{c_0}\|\tilde{\mathbf{z}}\|\right) \circ\!\!-\!\!\bullet \frac{\exp(-\frac{s}{c_0}\|\tilde{\mathbf{z}}\|)}{4\pi\|\tilde{\mathbf{z}}\|} = \hat{U}_s(\tilde{\mathbf{z}}) \quad .$$

As a direct consequence of this circumstance the representation formula of the Helmholtz equation with complex wave numbers equals the Laplace transform of the representation formula in time domain.

The following sections are dedicated to the introduction of the four standard boundary integral operators obtained by applying both trace operators to both of the operators occurring in the representation formula. A detailed discussion of these operators would exceed the scope of this thesis, for a thorough mathematical analysis refer to [30] or [28]. However, the basic idea of this approach is to augment the boundary around $\mathbf{x} \in \Gamma$ with a sphere B_ϵ of radius ϵ, such that $\Omega_\epsilon = \Omega \cup B_\epsilon$. The limit $\Omega \ni \tilde{\mathbf{x}} \to \mathbf{x} \in \Omega_\epsilon$ can then be carried out since $\mathbf{x}$ does not lie on the augmented boundary. In the process the limit $\epsilon \to 0$ is performed, to retrieve the original state with domain Ω and boundary Γ. This procedure is sketched in figure 3.1 for the two dimensional case.

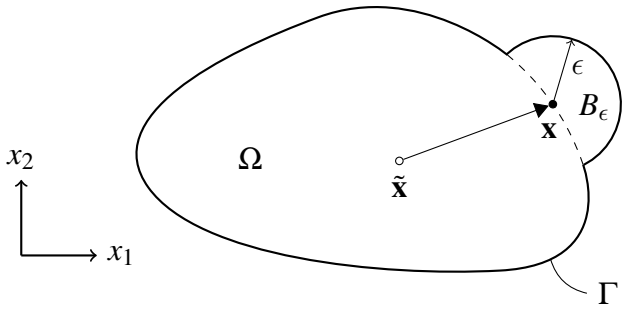

Figure 3.1: Augmented boundary in two dimensions. First the interior point is advanced to the original boundary $\Omega \ni \tilde{\mathbf{x}} \to \mathbf{x} \in \Omega_\epsilon$. To regain the original configuration the limit $\epsilon \to 0$ is performed in the process.

3.3 Single layer potential

For a given density $w \in H^{-1/2}(\Gamma)$ the single layer potential $\tilde{\mathcal{V}}_s : H^{-1/2}(\Gamma) \to H^1(\Omega^-)$ defines a solution of the homogeneous partial differential equation which has the fundamental solution $\hat{U}_s$. It reads as

$$u(\tilde{\mathbf{x}}) = \left(\tilde{\mathcal{V}}_s w\right)(\tilde{\mathbf{x}}) := \int_\Gamma \hat{U}_s(\tilde{\mathbf{x}} - \mathbf{y})\, w(\mathbf{y}) ds_\mathbf{y} \quad \forall\, \tilde{\mathbf{x}} \in \Omega^- \quad .$$

Application of the Dirichlet trace yields the operator $\gamma_0^- \tilde{\mathcal{V}}_s =: \mathcal{V}_s : H^{-1/2}(\Gamma) \to H^{1/2}(\Gamma)$ having the representation

$$(\mathcal{V}_s w)(\mathbf{x}) := \gamma_0^- \left(\tilde{\mathcal{V}}_s w\right)(\mathbf{x}) = \int_\Gamma \hat{U}_s(\mathbf{x} - \mathbf{y})\, w(\mathbf{y}) ds_\mathbf{y} \quad \forall\, \mathbf{x} \in \Gamma$$

which exists as weakly singular surface integral due to the singularity of the fundamental solution at $\mathbf{x} = \mathbf{y}$.

The single layer potential $\mathcal{V}_s$ is coercive, satisfying a Gårdings inequality

$$\langle (\mathcal{V}_s + \mathcal{T}) w, w \rangle_{H^{1/2}(\Gamma) \times H^{-1/2}(\Gamma)} \;\geq\; c \|w\|^2_{H^{-1/2}(\Gamma)} \quad \forall\, w \in H^{-1/2}(\Gamma)$$

with a compact operator $\mathcal{T} : H^{-1/2}(\Gamma) \to H^{1/2}(\Gamma)$, see [7] or [30, theorem 6.40].

3.4 Adjoint double layer potential

For a given density $w \in H^{-1/2}(\Gamma)$ we apply the interior Neumann trace to the single layer potential $\gamma_1^- \tilde{\mathcal{V}}_s : H^{-1/2}(\Gamma) \to H^{-1/2}(\Gamma)$ yielding

$$\gamma_1^- \left(\tilde{\mathcal{V}}_s w\right)(\mathbf{x}) = \sigma(\mathbf{x}) w(\mathbf{x}) + \left(\mathcal{K}'_s w\right)(\mathbf{x}) \quad \forall\, \mathbf{x} \in \Gamma$$

in the sense of $H^{-1/2}(\Gamma)$, with the adjoint double layer potential

$$\left(\mathcal{K}'_s w\right)(\mathbf{x}) := \int_\Gamma \gamma_{1,\mathbf{x}}^- \hat{U}_s(\mathbf{x} - \mathbf{y})\, w(\mathbf{y}) ds_\mathbf{y} \quad \forall\, \mathbf{x} \in \Gamma$$

which exists as weakly singular surface integral for our scalar-valued problem at hand, cf. [28]. Note that for vector-valued problems, e.g. linear elasticity or the Stokes system, the integral of the adjoint double layer potential exists only in the sense of a *Cauchy principal value*.

Furthermore, we have the jump term

$$\sigma(\mathbf{x}) = \frac{1}{2} \quad \text{for } \mathbf{x} \text{ a.e. in } \Gamma$$

or more precisely $\sigma(\mathbf{x}) = \frac{1}{2}$ when Γ is smooth in a neighbourhood of $\mathbf{x}$, see [30].

3.5 Double layer potential

For a given density function $v \in H^{1/2}(\Gamma)$ the double layer potential $\mathcal{W}_s : H^{1/2}(\Gamma) \to H^1(\Omega^-)$ describes a solution of the homogeneous partial differential equation which has the fundamental solution $\hat{U}_s$. It reads

$$u(\tilde{\mathbf{x}}) = (\mathcal{W}_s v)(\tilde{\mathbf{x}}) := \int_\Gamma \gamma_{1,\mathbf{y}}^- \hat{U}_s(\tilde{\mathbf{x}} - \mathbf{y})\, v(\mathbf{y}) ds_\mathbf{y} \quad \forall\, \tilde{\mathbf{x}} \in \Omega^- \quad .$$

We apply the interior Dirichlet trace to the double layer potential and obtain

$$\gamma_0^- (\mathcal{W}_s v)(\mathbf{x}) = [-1 + \sigma(\mathbf{x})] v(\mathbf{x}) + (\mathcal{K}_s v)(\mathbf{x}) \quad \forall\, \mathbf{x} \in \Gamma$$

with the operator $\mathcal{K}_s : H^{1/2}(\Gamma) \to H^{1/2}(\Gamma)$

$$(\mathcal{K}_s v)(\mathbf{x}) := \int_\Gamma \gamma_{1,\mathbf{y}}^- \hat{U}_s(\mathbf{x} - \mathbf{y})\, v(\mathbf{y}) ds_\mathbf{y} \quad \forall\, \mathbf{x} \in \Gamma$$

which exists as weakly singular surface integral for scalar-valued problems and exists, in general, only as a Cauchy principal value for vector-valued ones, see [28].

3.6 Hypersingular boundary integral operator

For a given density $v \in H^{1/2}(\Gamma)$ we apply the negative interior Neumann trace to the double layer potential $\gamma_1^- \mathcal{W}_s : H^{1/2}(\Gamma) \to H^{-1/2}(\Gamma)$ defining the hypersingular boundary integral operator

$$(\mathcal{D}_s v)(\mathbf{x}) := -\gamma_1^- (\mathcal{W}_s v)(\mathbf{x}) \quad \forall\, \mathbf{x} \in \Gamma \quad .$$

However, the integral

$$(\mathcal{D}_s v)(\mathbf{x}) = -\gamma_{1,\mathbf{x}}^- \int_\Gamma \gamma_{1,\mathbf{y}}^- \hat{U}_s(\tilde{\mathbf{x}} - \mathbf{y})\, v(\mathbf{y}) ds_\mathbf{y} \quad \forall\, \mathbf{x} \in \Gamma$$

does not exist as Cauchy principal value. Thus certain regularization techniques have to be employed. If the density v is globally continuous the hypersingular boundary integral operator has the representation

$$(\mathcal{D}_s v)(\mathbf{x}) = -\int_\Gamma \gamma_{1,\mathbf{x}}^- \gamma_{1,\mathbf{y}}^- \hat{U}_s(\mathbf{x} - \mathbf{y}) [v(\mathbf{y}) - v(\mathbf{x})] ds_\mathbf{y} \quad \forall\, \mathbf{x} \in \Gamma$$

which exists as Cauchy principal value, cf. [30]. Note that the sesquilinear form induced by the hypersingular boundary integral operator $b_\mathcal{D}(\cdot,\cdot)$, which is discussed in chapter 4, may

be regularized for globally continuous ansatz and test functions by means of integration by parts. In [30] one finds

$$\begin{aligned} b_{\mathcal{D}_s}(u,v) &:= \langle \mathcal{D}_s u, v\rangle_{H^{-1/2}(\Gamma)\times H^{1/2}(\Gamma)} \\ &= \int_{\Gamma\times\Gamma} \hat{U}_s(\mathbf{x}-\mathbf{y})\,(\mathbf{curl}_\Gamma u(\mathbf{y}), \mathbf{curl}_\Gamma \bar{v}(\mathbf{x}))\,ds_{\mathbf{y}} ds_{\mathbf{x}} \\ &\quad + \frac{s^2}{c_0^2}\int_{\Gamma\times\Gamma} \hat{U}_s(\mathbf{x}-\mathbf{y})\,u(\mathbf{y})\bar{v}(\mathbf{x})\,(\mathbf{n}(\mathbf{x}),\mathbf{n}(\mathbf{y}))\,ds_{\mathbf{y}} ds_{\mathbf{x}} \end{aligned} \tag{3.17}$$

with the surface curl

$$\mathbf{curl}_\Gamma u(\mathbf{x}) = \mathbf{n}(\mathbf{x}) \times \mathrm{grad}\tilde{u}(\mathbf{x}) \quad \forall\, \mathbf{x}\in\Gamma$$

where $\tilde{u}$ is a suitable extension of the given u on Γ into a three-dimensional neighbourhood of Γ.

The hypersingular boundary integral operator $\mathcal{D}_s$ is coercive, satisfying a Gårdings inequality

$$\langle (\mathcal{D}_s + \mathcal{T})\, v, v\rangle_{H^{-1/2}(\Gamma)\times H^{1/2}(\Gamma)} \;\geq\; c\|v\|^2_{H^{1/2}(\Gamma)} \quad \forall\, v\in H^{1/2}(\Gamma)$$

with a compact operator $\mathcal{T}: H^{1/2}(\Gamma)\to H^{-1/2}(\Gamma)$, see [7].

4 BOUNDARY INTEGRAL EQUATIONS

In this chapter a set of boundary integral equations employed to solve the underlying problem in Laplace domain (2.12) is derived. Furthermore, their variational formulations are presented, which are going to be the starting point of the actual boundary element formulation.

Note that at this stage it is not entirely obvious why we consider boundary integral equations in Laplace domain only. This approach is motivated due to the employed discretization of the time dependency which is detailed in chapter 5.

4.1 Variational formulation of operator equations

This short digression is merely intended to provide a glimpse into the basic idea underlying variational methods for operator equations, taken from [30, chapter 3].

Let H be a Hilbert space equipped with the scalar product $(\cdot,\cdot)_H$ inducing the norm $\|\cdot\|_H = \sqrt{(\cdot,\cdot)_H}$. In the subsequent part we consider a bounded linear operator $\mathcal{A} : H \to H'$, where H' denotes the dual space of H with respect to the duality pairing $\langle\cdot,\cdot\rangle_{H'\times H}$. For a given $f \in H'$ we wish to find the solution of the operator equation

$$\mathcal{A}u = f \quad . \tag{4.1}$$

However, instead of (4.1) we may consider the equivalent variational problem to find $u \in H$ such that

$$\langle \mathcal{A}u, v\rangle_{H'\times H} = \langle f, v\rangle_{H'\times H} \quad \forall\, v \in H \tag{4.2}$$

holds. Concerning the equivalence of the operator equation (4.1) and its variational formulation (4.2) we note that any solution $u \in H$ of (4.1) is obviously a solution of (4.2). In the reverse direction we consider $u \in H$ to be a solution of the variational problem (4.2) and by using the definition of the norm in H', cf. appendix A, we obtain

$$\|\mathcal{A}u - f\|_{H'} = \sup_{0\neq v\in H} \frac{|\langle \mathcal{A}u - f, v\rangle_{H'\times H}|}{\|v\|_H} = 0$$

which equals zero due to (4.2). Recalling the norm axiom $\|\mathcal{A}u - f\|_{H'} = 0 \iff \mathcal{A}u = f$ in H', we find that the solution of the variational formulation (4.2) is a solution of the operator equation (4.1) if $u \in H$ holds.

The operator $\mathcal{A} : H \to H'$ induces a bilinear form for real-valued functions or a sesquilinear form for complex-valued functions

$$b(u,v) \coloneqq \langle \mathcal{A}u, v \rangle_{H' \times H} \quad \forall u, v \in H$$

where the bilinear form has the mapping property $b(\cdot,\cdot) : H \times H \to \mathbb{R}$ whereas the sesquilinear form has the mapping property $b(\cdot,\cdot) : H \times H \to \mathbb{C}$.

Furthermore, by virtue of the *Riesz representation theorem* the right hand side in (4.2) induces a functional $F(v) \in H'$ for an arbitrary but fixed $f \in H'$, cf. [30, theorem 3.3].

If the sesquilinear form $b(\cdot,\cdot)$ is H-elliptic and bounded and $F(\cdot)$ is bounded, i.e. there exist positive constants c such that

$$\begin{aligned} b(v,v) &\geq c\|v\|_H^2 && \forall\, v \in H \\ b(u,v) &\leq c\|u\|_H \|v\|_H && \forall\, u, v \in H \\ F(v) &\leq c\|v\|_H && \forall\, v \in H \end{aligned}$$

then there exists a unique solution $u \in H$ by the *Lax-Milgram lemma*, see [30, theorem 3.4]. In many cases the H-ellipticity of $\mathcal{A}$ is too restrictive. The existence of a unique solution of (4.2) can also be ensured if $\mathcal{A}$ is injective and coercive, satisfying a Gårdings inequality

$$|b(v,v) + \langle \mathcal{T}v, v \rangle_{H' \times H}| \;\geq\; c\|v\|_H^2 \quad \forall\, v \in H$$

with a compact operator $\mathcal{T} : H \to H'$, as stated in [30, theorem 3.6].

4.2 Indirect method

Indirect methods are based on the observation that both the single layer potential $\left(\tilde{\mathcal{V}}_s w\right)(\tilde{\mathbf{x}})$ and the double layer potential $\left(\mathcal{W}_s v\right)(\tilde{\mathbf{x}})$ solve the homogeneous differential equation for $\tilde{\mathbf{x}} \in \Omega^-$ and for any $w \in H^{-1/2}(\Gamma)$ and $v \in H^{1/2}(\Gamma)$ respectively, see [28, theorem 3.1.1]. Thus, the task is to find either w or v such that the boundary condition

$$\gamma_1^- u(\mathbf{x}) + s\kappa(\mathbf{x})\gamma_0^- u(\mathbf{x}) = f(\mathbf{x}) \quad \forall\, \mathbf{x} \in \Gamma \tag{4.3}$$

is satisfied as well.

4.2.1 Single layer potential ansatz

For a density function $w \in H^{-1/2}(\Gamma)$ we consider solutions of the differential equation of the form

$$u(\mathbf{x}) \coloneqq \left(\tilde{\mathcal{V}}_s w\right)(\tilde{\mathbf{x}}) \quad \forall\, \tilde{\mathbf{x}} \in \Omega^- \tag{4.4}$$

whose insertion in (4.3) yields

$$\sigma(\mathbf{x})w(\mathbf{x}) + \left(\mathcal{K}'_s w\right)(\mathbf{x}) + s\kappa(\mathbf{x})\left(\mathcal{V}_s w\right)(\mathbf{x}) = f(\mathbf{x}) \quad \forall\, \mathbf{x} \in \Gamma \tag{4.5}$$

with the boundary integral operators $\mathcal{V}_s$ and $\mathcal{K}'_s$ as well as the function $\sigma(\mathbf{x})$ as defined in chapter 3.

We do not wish to consider (4.5) in operator form, but an equivalent variational formulation. It would seem to suggest itself to set up a variational formulation of (4.5) in the energy space $H^{-1/2}(\Gamma)$, however since the operator $\mathcal{K}'_s$ is of order zero the $L_2(\Gamma)$ scalar product cannot be extended to the required duality pairing. This would require the use of the $H^{-1/2}(\Gamma)$ scalar product, which is in many cases not feasible in terms of a technical computation. However, if the operators meet certain requirements, a formulation in $L_2(\Gamma)$ is possible. For further information on this topic see [28, chapter 3.8].

The modified variational formulation reads:
Assuming $f \in L_2(\Gamma)$, find $w \in L_2(\Gamma)$ such that

$$\frac{1}{2}(w,\mu)_{L_2(\Gamma)} + b_{\mathcal{K}'_s}(w,\mu) + s\, b^{\kappa}_{\mathcal{V}_s}(w,\mu) = (f,\mu)_{L_2(\Gamma)} \quad \forall\, \mu \in L_2(\Gamma) \tag{4.6}$$

holds with the two sesquilinear forms

$$\begin{aligned} b_{\mathcal{V}_s}(w,\mu) &= (\mathcal{V}_s w, \mu)_{L_2(\Gamma)} \\ b^{\kappa}_{\mathcal{K}'_s}(w,\mu) &= (\mathcal{K}'_s w, \mu)_{L_2(\Gamma),\kappa} \end{aligned}$$

where $(\cdot,\cdot)_{L_2(\Gamma)}$ denotes the regular scalar product in $L_2(\Gamma)$ and $(\cdot,\cdot)_{L_2(\Gamma),\kappa}$ the weighted one, see appendix A. Note that once the density function w has been determined, the solution at any $\tilde{\mathbf{x}} \in \Omega^-$ may be computed by virtue of (4.4).

4.2.2 Double layer potential ansatz

For any density function $v \in H^{1/2}(\Gamma)$ functions defined by

$$u(\mathbf{x}) \coloneqq \left(\mathcal{W}_s v\right)(\tilde{\mathbf{x}}) \quad \forall\, \tilde{\mathbf{x}} \in \Omega^- \tag{4.7}$$

are solutions of the homogeneous differential equation. By plugging this ansatz into (4.3) one obtains

$$-\left(\mathcal{D}_s v\right)(\mathbf{x}) + s\kappa(\mathbf{x})\left([-1+\sigma(\mathbf{x})]v(\mathbf{x}) + \left(\mathcal{K}_s v\right)(\mathbf{x})\right) = f(\mathbf{x}) \quad \forall\, \mathbf{x} \in \Gamma \tag{4.8}$$

with the boundary integral operators $\mathcal{K}_s$ and $\mathcal{D}_s$ as well as the function $\sigma(\mathbf{x})$ as defined chapter 3.

Similarly to the previous case, we wish to consider not the operator equation but a variational formulation. Although $\mathcal{K}_s$ is an operator of order zero, the occurrence of the function κ ensures that the left hand side is in the same space as the right hand side, i.e. $H^{-1/2}(\Gamma)$. A formulation in the natural energy space $H^{1/2}(\Gamma)$ is viable, since the $L_2(\Gamma)$ scalar product can be extended to the required duality pairing, cf. [28, chapter 3.4].

The variational formulation reads:
Find $v \in H^{1/2}(\Gamma)$ such that

$$-b_{\mathcal{D}_s}(v,\mu) - \frac{s}{2}(v,\mu)_{L_2(\Gamma),\kappa} + s\, b^{\kappa}_{\mathcal{K}_s}(v,\mu) = (f,\mu)_{L_2(\Gamma)} \quad \forall\, \mu \in H^{1/2}(\Gamma) \tag{4.9}$$

holds with the two sesquilinear forms

$$\begin{aligned} b^{\kappa}_{\mathcal{K}_s}(v,\mu) &= (\mathcal{K}_s v, \kappa\mu)_{L_2(\Gamma)} \\ b_{\mathcal{D}_s}(v,\mu) &= (\mathcal{D}_s v, \mu)_{L_2(\Gamma)} \end{aligned}$$

and the weighted scalar product $(\cdot,\cdot)_{L_2(\Gamma),\kappa}$. Note that $(\cdot,\cdot)_{L_2(\Gamma)}$ denotes the extension of the $L_2(\Gamma)$ scalar product to the duality pairing $\langle\cdot,\cdot\rangle_{H^{1/2}(\Gamma)\times H^{-1/2}(\Gamma)}$ and $\langle\cdot,\cdot\rangle_{H^{-1/2}(\Gamma)\times H^{1/2}(\Gamma)}$ respectively.

Once the density function v is known, we may compute the solution in Ω^- using (4.7).

4.3 Direct method

Direct methods are based on the representation formula

$$u(\tilde{\mathbf{x}}) = \left(\tilde{\mathcal{V}}_s \gamma_1^- u\right)(\tilde{\mathbf{x}}) - \left(\mathcal{W}_s \gamma_0^- u\right)(\tilde{\mathbf{x}}) \quad \forall\, \tilde{\mathbf{x}} \in \Omega^- \tag{4.10}$$

which may be used to compute the solution in Ω^- once the complete Dirichlet datum $\gamma_0^- u$ and Neumann datum $\gamma_1^- u$ are known. To provide a clearer notation we equip both the Dirichlet and the Neumann field with separate variables

$$\begin{aligned} u^D &:= \gamma_0^- u \\ u^N &:= \gamma_1^- u \quad . \end{aligned}$$

To derive equations that enable us to compute these yet unknown fields we apply the interior Dirichlet trace γ_0^- to (4.10), obtaining

$$u^D(\mathbf{x}) = \left(\mathcal{V}_s u^N\right)(\mathbf{x}) - \left(-\frac{1}{2}\mathcal{I} + \mathcal{K}_s\right) u^D(\mathbf{x}) \quad \text{for } \mathbf{x} \text{ a.e. in } \Gamma$$

as well as the interior Neumann trace γ_1^- yielding

$$u^N(\mathbf{x}) = \left(\frac{1}{2}\mathcal{I} + \mathcal{K}'_s\right) u^N(\mathbf{x}) - \left(-\left(\mathcal{D}_s u^D\right)(\mathbf{x})\right) \quad \text{for } \mathbf{x} \text{ a.e. in } \Gamma \quad .$$

Combination of both equations leads to the system

$$\begin{pmatrix} u^D \\ u^N \end{pmatrix} = \begin{pmatrix} \frac{1}{2}\mathcal{I} - \mathcal{K}_s & \mathcal{V}_s \\ \mathcal{D}_s & \frac{1}{2}\mathcal{I} + \mathcal{K}'_s \end{pmatrix} \begin{pmatrix} u^D \\ u^N \end{pmatrix} \quad \text{a.e. in } \Gamma \tag{4.11}$$

where

$$\mathcal{C}_s = \begin{pmatrix} \frac{1}{2}\mathcal{I} - \mathcal{K}_s & \mathcal{V}_s \\ \mathcal{D}_s & \frac{1}{2}\mathcal{I} + \mathcal{K}'_s \end{pmatrix}$$

is the *Calderón projection* holding a.e. on Γ, cf. [30].

From the first boundary integral equation in (4.11) we obtain a *Dirichlet to Neumann map*

$$u^N = \mathcal{V}_s^{-1} \left(\tfrac{1}{2}\mathcal{I} + \mathcal{K}_s\right) u^D \quad \text{for } \mathbf{x} \text{ a.e. in } \Gamma$$

with the *Steklov-Poincaré operator* $\mathcal{S}_s : H^{1/2}(\Gamma) \to H^{-1/2}(\Gamma)$

$$\mathcal{S}_s := \mathcal{V}_s^{-1} \left(\tfrac{1}{2}\mathcal{I} + \mathcal{K}_s\right) \quad \text{a.e. in } \Gamma \quad . \tag{4.12}$$

Insertion of (4.12) into the second boundary integral equation in (4.11) yields

$$u^N = \mathcal{D}_s u^D + \left(\tfrac{1}{2}\mathcal{I} + \mathcal{K}'_s\right) \mathcal{V}_s^{-1} \left(\tfrac{1}{2}\mathcal{I} + \mathcal{K}_s\right) u^D \quad \text{a.e. in } \Gamma$$

which is a symmetric representation of the Steklov-Poincaré operator $\mathcal{S}_s : H^{1/2}(\Gamma) \to H^{-1/2}(\Gamma)$

$$\mathcal{S}_s := \mathcal{D}_s + \left(\tfrac{1}{2}\mathcal{I} + \mathcal{K}'_s\right) \mathcal{V}_s^{-1} \left(\tfrac{1}{2}\mathcal{I} + \mathcal{K}_s\right) \quad \text{a.e. in } \Gamma \quad . \tag{4.13}$$

Note that both definitions of $\mathcal{S}_s$ given in (4.12) and (4.13) are equivalent and map some Dirichlet data $u^D \in H^{1/2}(\Gamma)$ to the respective Neumann data $u^N \in H^{-1/2}(\Gamma)$. Utilizing this operator we may describe the Neumann data in terms of the Dirichlet data

$$u^N(\mathbf{x}) = \left(\mathcal{S}_s u^D\right)(\mathbf{x}) \quad \text{for } \mathbf{x} \text{ a.e. in } \Gamma \quad . \tag{4.14}$$

By employing (4.14) in the boundary condition (4.3) we end up with

$$\left(\left(\mathcal{S}_s + s\,\kappa\mathcal{I}\right) u^D\right)(\mathbf{x}) = f(\mathbf{x}) \quad \text{for } \mathbf{x} \text{ a.e. in } \Gamma \quad . \tag{4.15}$$

Similarly to the indirect approach, we are interested not in the operator equation itself but a variational formulation. Since $\mathcal{S}_s$ is an operator of positive order one, a formulation in the natual energy space $H^{1/2}(\Gamma)$ is obvious, as the $L_2(\Gamma)$ scalar product can be extended the required duality pairing.

The variational formulation reads:
Find $u^D \in H^{1/2}(\Gamma)$, such that

$$b_{\mathcal{S}_s}(u^D, \mu) + s(u^D, \mu)_{L_2(\Gamma),\kappa} = (f, \mu)_{L_2(\Gamma)} \quad \forall\, \mu \in H^{1/2}(\Gamma) \tag{4.16}$$

holds with the sesquilinear form

$$b_{\mathcal{S}_s}(v,\mu) = (\mathcal{S}_s v, \mu)_{L_2(\Gamma)}$$

and the weighted scalar product $(\cdot,\cdot)_{L_2(\Gamma),\kappa}$. Note that $(\cdot,\cdot)_{L_2(\Gamma)}$ denotes the extension of the $L_2(\Gamma)$ scalar product to the duality pairing $\langle\cdot,\cdot\rangle_{H^{-1/2}(\Gamma)\times H^{1/2}(\Gamma)}$.

Since the Steklov-Poincaré operator (4.13) implies explicit knowledge of the inverse single layer potential operator $\mathcal{V}_s^{-1}$, we cannot set up the continuous incarnation of $\mathcal{S}_s$ explicitly. However, this trouble can be abolished by considering a variational formulation of both boundary integral equations characterizing (4.11). Hence we obtain the equivalent problem:
Find $(u_D, u_N) \in H^{1/2}(\Gamma) \times H^{-1/2}(\Gamma)$, such that

$$\begin{aligned} \tfrac{1}{2}(u^D,\tau)_{L_2(\Gamma)} + b_{\mathcal{K}_s}(u^D,\tau) &= b_{\mathcal{V}_s}(u^N,\tau) \\ b_{\mathcal{D}_s}(u^D,\mu) + b_{\mathcal{K}'_s}(u^N,\mu) + \tfrac{1}{2}(u^N,\mu)_{L_2(\Gamma)} + s(u^D,\mu)_{L_2(\Gamma),\kappa} &= (f,\mu)_{L_2(\Gamma)} \end{aligned} \tag{4.17}$$

holds for all $(\mu,\tau) \in H^{1/2}(\Gamma) \times H^{-1/2}(\Gamma)$ with the four sesquilinear forms

$$\begin{aligned} b_{\mathcal{V}_s}(w,\tau) &= (\mathcal{V}_s w,\tau)_{L_2(\Gamma)} & b_{\mathcal{K}_s}(v,\tau) &= (\mathcal{K}_s v,\tau)_{L_2(\Gamma)} \\ b_{\mathcal{K}'_s}(w,\mu) &= (\mathcal{K}'_s w,\mu)_{L_2(\Gamma)} & b_{\mathcal{D}_s}(v,\mu) &= (\mathcal{D}_s v,\mu)_{L_2(\Gamma)} \end{aligned}$$

and the weighted scalar product $(\cdot,\cdot)_{L_2(\Gamma),\kappa}$. Similarly to before $(\cdot,\cdot)_{L_2(\Gamma)}$ denotes the extension of the $L_2(\Gamma)$ scalar product to the duality pairing $\langle\cdot,\cdot\rangle_{H^{1/2}(\Gamma)\times H^{-1/2}(\Gamma)}$ and $\langle\cdot,\cdot\rangle_{H^{-1/2}(\Gamma)\times H^{1/2}(\Gamma)}$ respectively.

Once the Cauchy data (u^D,u^N) are known, we may compute the solution in Ω^- by virtue of the representation formula (4.10).

5 TIME DISCRETIZATION

It is more convenient to treat the discretization in time first, as it influences the spatial discretization significantly. The different techniques for resolving the time dependency will be shown on the model Dirichlet problem

$$\gamma_0^- u(\mathbf{x},t) = g^D(\mathbf{x},t) \quad \forall\, (\mathbf{x},t) \in \Gamma \times \Upsilon.$$

As an example we consider the single layer potential ansatz, which reads as

$$u(\tilde{\mathbf{x}},t) \coloneqq \left(\tilde{\mathcal{V}} * \varphi\right)(\tilde{\mathbf{x}},t) \coloneqq \int_0^t \int_\Gamma U\left(\tilde{\mathbf{x}}-\mathbf{y}, t-\tau\right) \varphi(\mathbf{y},t) ds_{\mathbf{y}} d\tau \quad \forall\, (\tilde{\mathbf{x}},t) \in \Omega^- \times (0,\infty)$$

and defines solutions to the partial differential equation for any suitable φ. There are three main classes of methods to solve this problem.

- *Time-stepping methods:* The underlying idea is to discretize the original initial-boundary value problem by some sort of time-stepping scheme and then apply the boundary integral equation method to solve a boundary value problem at each time step. There is a multitude of techniques to approximate the occurring source terms, which lead to domain integrals, e.g. the *dual reciprocity method*, cf. [11]. In this method one would approximate the source term $-\partial_{tt} u$ by some radial basis functions and solve Laplace's equation for each time step.

  Another approach belonging to this group is to introduce simple locally supported ansatz functions $\varphi(\mathbf{x},t) \coloneqq \varphi_{\mathbf{x}}(\mathbf{x})\varphi_t(t)$ and perform the convolution in time analytically, see e.g. [20].

- *Laplace transform methods:* This group of procedures relies on a Laplace, or Fourier, transform of the data, in our case g_D to Laplace, or Fourier, domain. Since convolution corresponds to multiplication in these domains, a series of decoupled boundary value problems has to be solved for each observed frequency ω

  $$\left(\mathcal{V}_\omega \hat{\varphi}\right)(\tilde{\mathbf{x}}) = \hat{g}^D_\omega \quad \forall\, \tilde{\mathbf{x}} \in \Omega^- \quad .$$

  The solution in time domain may be recovered by applying the inverse Laplace, or Fourier, transform.

  Another procedure that is also based on the solution of boundary integral equations in Laplace domain is the *convolution quadrature method* (CQM, [19]). There are different formulations of it and most of them operate both in time and Laplace domain simultaneously.

- *Space-time integral equations:* The main idea is to consider a variational formulation of the underlying problem on the entire space-time cylinder, i.e.

$$\langle \gamma_0^- u, v \rangle_{\Gamma\times\Upsilon} = \langle g^D, v \rangle_{\Gamma\times\Upsilon} \quad \text{for all suitable } v$$

and for our model problem we would obtain

$$(\mathcal{V} * \varphi, \partial_t v)_{L_2(\Gamma\times\Upsilon)} = (g^D, \partial_t v)_{L_2(\Gamma\times\Upsilon)} \quad \text{for all suitable } v, \tag{5.1}$$

cf. [8]. Although this approach seems rather straightforward it is actually quite involved. Since the solution of the entire time interval is computed in one step, the dimension is increased by one, thus the system matrix is much larger. Furthermore, the $L_2(\Gamma\times\Upsilon)$ scalar product, which is an integral along the lateral boundary of the space-time cylinder, can be very complex when dealing with integral equations. For a parabolic equation one would have to solve six-dimensional integrals, while in our hyperbolic case the integrals are five-dimensional, due to the occurrence of the Dirac distribution in the fundamental solution.

An exhaustive introduction to the time discretization of boundary integral equations can be found in [8]. Throughout this work we only consider the CQM based on a shift to Laplace domain [2].

5.1 Convolution quadrature method

The following derivations of the convolution quadrature method are directly adapted from [17].

Consider the model problem

$$(f * g)(t) \coloneqq \int_0^t f(t-\tau) g(\tau) d\tau \tag{5.2}$$

which is the convolution of two scalar functions $f(t)$ and $g(t)$ for $t \in \Upsilon$. It is assumed that both functions vanish for negative arguments, i.e. they are causal. Recalling the Laplace transform pairing

$$f(t-\tau)\Theta(t-\tau) \circ\!\!-\!\!\bullet \exp(-\tau s)\hat{f}(s)$$

as well as the inverse Laplace transform (2.11), we obtain the alternative representation of (5.2)

$$(f * g)(t) = \int_0^t \lim_{b\to\infty} \frac{1}{2\pi i} \int_{a-ib}^{a+ib} \exp(s(t-\tau))\hat{f}(s) ds \; g(\tau) d\tau$$

while exchanging the order of integration yields

$$(f*g)(t) = \frac{1}{2\pi i} \lim_{b\to\infty} \int_{a-ib}^{a+ib} \hat{f}(s) \int_0^t \exp(s(t-\tau))g(\tau)\,d\tau\,ds \quad .$$

Note that $a \in \mathbb{R}$ has to be chosen such that the real parts of all singularities of $\hat{f}(s)$ are smaller than a. For the sake of shortness we abbreviate the inner integral

$$x(t,s) = \int_0^t \exp(s(t-\tau))g(\tau)\,d\tau \quad . \tag{5.3}$$

The function $x(t,s)$ defined above solves the initial value problem

$$\partial_t x(t,s) = s\,x(t,s) + g(t) \quad , \quad x(0,s) = 0 \quad . \tag{5.4}$$

To prove this claim we multiply the ordinary differential equation in (5.4) with a function $u(t,s) \coloneqq \exp(-ts)$ yielding

$$u(t,s)\partial_t x(t,s) - u(t,s)x(t,s)s = u(t,s)g(t) \quad , \tag{5.5}$$

and introduce another function $z(t,s) \coloneqq u(t,s)x(t,s)$ with

$$\begin{aligned} \partial_t z(t,s) &= \partial_t u(t,s)x(t,s) + u(t,s)\partial_t x(t,s) \\ &= -u(t,s)x(t,s)s + u(t,s)\partial_t x(t,s) \end{aligned} \tag{5.6}$$

where we used $\partial_t u(t,s) = -\exp(-ts)s = -u(t,s)s$. By inserting (5.6) in (5.5) we get

$$\partial_t z(t,s) = u(t,s)g(t) = \exp(-ts)g(t)$$

and thus

$$z(t,s) = u(t,s)x(t,s) = \int \exp(-\tau s)g(\tau)\,d\tau + C \quad .$$

Dividing by $u(t,s) = \exp(-ts) \neq 0$ yields

$$x(t,s) = \int \exp(s(t-\tau))g(\tau)\,d\tau + C$$

and by applying the fundamental theorem of calculus as well as the initial condition $x(0,s) = 0$ we finally obtain the integral representation

$$x(t,s) = \int_0^t \exp(s(t-\tau))g(\tau)\,d\tau$$

showing that above integral solves the initial-value problem (5.4).

The time interval $\overline{\Upsilon} = [0,T]$ is divided into N_t equidistant subintervals $\Delta t = \frac{T}{N_t}$ and the n-th time step is given by $t_n = n\Delta t,\ n = 0,\ldots,N_t$. The convolution at each individual time step reads

$$(f * g)(t_n) = \frac{1}{2\pi i} \lim_{b\to\infty} \int_{a-ib}^{a+ib} \hat{f}(s) x(t_n, s)\, ds \tag{5.7}$$

by virtue of (5.3) and the discretization of the time interval introduced above. We abbreviate $x_n := x(t_n, s)$, which may be interpreted as solution of the initial-value problem (5.4) governed by an ordinary differential equation. Hence, its solution may be approximated by a finite difference method, where the application of a linear multistep method seems reasonable. The general definition of a k-th order multistep procedure for the generic differential equation of first order

$$y'(t) = f(t,y)$$

can be written as

$$\sum_{j=0}^{k} \alpha_j y_{n+j} = \Delta t \sum_{j=0}^{k} \beta_j f(t_{n+j}, y_{n+j}) \quad . \tag{5.8}$$

Application of (5.8) to (5.4) yields

$$\sum_{j=0}^{k} \alpha_j x_{n+j} = \Delta t \sum_{j=0}^{k} \beta_j \left(s x_{n+j} + g_{n+j} \right) \tag{5.9}$$

which is multiplied by the n-th power of some $\xi \in \mathbb{C}$ and summed up over all nonnegative integers n, i.e. all possible discrete times, yielding

$$\sum_{n=0}^{\infty} \sum_{j=0}^{k} \alpha_j x_{n+j} \xi^n = \Delta t \sum_{n=0}^{\infty} \sum_{j=0}^{k} \beta_j \left(s x_{n+j} + g_{n+j} \right) \xi^n \quad . \tag{5.10}$$

Moreover, expression (5.10) is rearranged

$$\sum_{j=0}^{k} \alpha_j \sum_{n=0}^{\infty} x_{n+j} \xi^n = \Delta t \sum_{j=0}^{k} \beta_j \sum_{n=0}^{\infty} \left(s x_{n+j} + g_{n+j} \right) \xi^n \quad .$$

Assuming vanishing initial conditions, i.e. $x_0 = x_1 = \cdots = x_{k-1} = 0$ as well as $g_0 = g_1 = \cdots = g_{k-1} = 0$, we obtain the identities

$$\begin{aligned} \sum_{n=0}^{\infty} x_{n+k} \xi^n &= \xi^{-k} \sum_{n=0}^{\infty} x_n \xi^n \\ \sum_{n=0}^{\infty} g_{n+k} \xi^n &= \xi^{-k} \sum_{n=0}^{\infty} g_n \xi^n \end{aligned}$$

whose insertion in (5.1) results in

$$\sum_{j=0}^{k} \alpha_j \xi^{-j} \sum_{n=0}^{\infty} x_n \xi^n = \Delta t \sum_{j=0}^{k} \beta_j \xi^{-j} \left(s \sum_{n=0}^{\infty} x_n \xi^n + \sum_{n=0}^{\infty} g_n \xi^n \right)$$

and consequently

$$\left(\sum_{j=0}^{k} \alpha_j \xi^{-j} - s\Delta t \sum_{j=0}^{k} \beta_j \xi^{-j} \right) \sum_{n=0}^{\infty} x_n \xi^n = \Delta t \sum_{j=0}^{k} \beta_j \xi^{-j} \sum_{n=0}^{\infty} g_n \xi^n \quad . \tag{5.11}$$

Dividing (5.11) by $\Delta t \sum_{j=0}^{k} \beta_j \xi^{-j}$ and defining the characteristic rational function

$$\gamma(\zeta) = \sum_{j=0}^{k} \alpha_j \xi^{-j} \left(\sum_{j=0}^{k} \beta_j \xi^{-j} \right)^{-1}$$

yields the power series representation

$$\sum_{n=0}^{\infty} x_n \xi^n = \left(\frac{\gamma(\xi)}{\Delta t} - s \right)^{-1} \sum_{n=0}^{\infty} g_n \xi^n \quad . \tag{5.12}$$

Insertion of (5.12) into (5.7) leads to

$$\sum_{n=0}^{\infty} (f * g)(t_n) \xi^n = \frac{1}{2\pi i} \lim_{b \to \infty} \int_{a-ib}^{a+ib} \hat{f}(s) \left(\frac{\gamma(\xi)}{\Delta t} - s \right)^{-1} ds \sum_{n=0}^{\infty} g_n \xi^n \quad .$$

The line integral in above formula may be converted to a closed contour integral, along the path C if $\hat{f}(s)$ satisfies the assumption $|\hat{f}(s)| \to 0$ for $\Re(s) \geq a$ and $|s| \to \infty$. If this assumption holds true, which is a prerequisite for the existence of the Laplace transform, we may add the integration along a semicircle since it only adds a zero. It shall be kept in mind that all singularities are situated in the plane left of the integration line defined by a, with the sole exception of the additional singularity at $s = \frac{\gamma(\xi)}{\Delta t}$. By making use of Cauchy's integral formula we obtain

$$\sum_{n=0}^{\infty} (f * g)(t_n) \xi^n = \frac{1}{2\pi i} \oint_C \hat{f}(s) \left(\frac{\gamma(\xi)}{\Delta t} - s \right)^{-1} ds \sum_{n=0}^{\infty} g_n \xi^n = \hat{f}\left(\frac{\gamma(\xi)}{\Delta t} \right) \sum_{n=0}^{\infty} g_n \xi^n \quad . \tag{5.13}$$

Since we wish to get rid of the infinite sum, we perform a power series representation of $\hat{f}\left(\frac{\gamma(\xi)}{\Delta t}\right)$ yielding

$$\hat{f}\left(\frac{\gamma(\xi)}{\Delta t} \right) = \sum_{n=0}^{\infty} \omega_n \xi^n$$

whose insertion in (5.13) leads to

$$\sum_{n=0}^{\infty} (f*g)(t_n)\xi^n = \sum_{m=0}^{\infty} \omega_m \xi^m \sum_{n=0}^{\infty} g_n \xi^n = \sum_{n=0}^{\infty} \xi^n \sum_{m=0}^{n} \omega_{n-m} g_m$$

where the Cauchy product of two power series was used. Consequently, one ends up with an approximation of the convolution integral of the form

$$(f*g)(t_n) = \sum_{m=0}^{n} \omega_{n-m} g_m \quad . \tag{5.14}$$

Above representation may serve as a starting point for directly computing solutions in time domain, see [17]. However, the approach used within this thesis seeks a different representation of the convolution.

The convolution weights in (5.14) may be computed numerically by employing Cauchy's differentiation formula

$$\frac{\partial^n}{\partial \xi^n}\left(\hat{f}\left(\frac{\gamma(\xi)}{\Delta t}\right)\right) = \frac{n!}{2\pi i}\oint_C \frac{\hat{f}(\gamma(s)/\Delta t)}{(s-\xi)^{n+1}} ds$$

which allows the calculation of the n-th partial derivatives. The evaluation at $\xi = 0$ yields

$$\left.\frac{\partial^n}{\partial \xi^n}\left(\hat{f}\left(\frac{\gamma(\xi)}{\Delta t}\right)\right)\right|_{\xi=0} = \frac{n!}{2\pi i}\oint_C \frac{\hat{f}(\gamma(s)/\Delta t)}{s^{n+1}} ds \quad .$$

By choosing C to be a circle centered at the origin with a radius of $R < 1$ we obtain $s = R\exp(i\varphi),\ \varphi \in [0, 2\pi)$ and thus

$$\omega_n(\hat{f}) := \frac{1}{2\pi}\int_0^{2\pi} \hat{f}\left(\frac{\gamma(R\exp(i\varphi))}{\Delta t}\right)(R\exp(i\varphi))^{-n} d\varphi \quad . \tag{5.15}$$

By approximating (5.15) with the trapezoidal rule of $N_t + 1$ quadrature points we obtain the following representation of the convolution weights

$$\omega_n(\hat{f}) := \frac{R^{-n}}{N_t+1}\sum_{l=0}^{N_t} \hat{f}(s_l)\zeta^{nl} \tag{5.16}$$

where we introduced the principal root of order N_t of unity

$$\zeta = \exp\left(\frac{2\pi i}{N_t+1}\right)$$

as well as the Laplace parameter

$$s_l = \frac{\gamma\left(R\zeta^{-l}\right)}{\Delta t} \quad .$$

Recalling the definition of the inverse discrete Fourier transform (IDFT)

$$u_k = \frac{1}{N+1}\sum_{j=0}^{N} \hat{u}_j \zeta^{jk} \tag{5.17}$$

we realize that (5.16) is actually a weighted IDFT with a scaling factor R^{-n}.

5.1.1 Decoupled system in Laplace domain

In this section we apply the CQM approach introduced previously to an abstract operator convolution equation. Hence, we will gain a decoupled system in Laplace domain, which will serve as a starting point for the spatial discretization of the boundary integral equations in Laplace domain. This approach is introduced in [2].

Consider the abstract operator equation

$$(\mathcal{A} * u)(\mathbf{x},t) = f(\mathbf{x},t) \quad \forall\, (\mathbf{x},t) \in \Gamma \times (0,\infty) \tag{5.18}$$

and by discretization of the time interval as discussed at the beginning of this section as well as application of (5.14) one obtains

$$(\mathcal{A} * u)(\mathbf{x},t_n) = f(\mathbf{x},t_n) \approx \sum_{m=0}^{n} \omega_{n-m}(\hat{\mathcal{A}}) u(\mathbf{x},t_m)$$

where we emphasize that the weights ω_n depend on the operator $\hat{\mathcal{A}}$. Assuming $\omega_n = 0$ for all $n < 0$ we may extend above sum to N_t, leading to

$$\sum_{m=0}^{N_t} \omega_{n-m}(\hat{\mathcal{A}}) u(\mathbf{x},t_m) \coloneqq f(\mathbf{x},t_n) \quad .$$

Insertion of the definition of the weights (5.16) yields

$$\sum_{m=0}^{N_t} \frac{R^{-(n-m)}}{N_t+1} \sum_{l=0}^{N_t} \hat{\mathcal{A}}(s_l)\zeta^{(n-m)l} u(\mathbf{x},t_m) = f(\mathbf{x},t_n)$$

and by changing the order of summation one finds

$$\frac{R^{-n}}{N_t+1} \sum_{l=0}^{N_t} \hat{\mathcal{A}}(s_l)\zeta^{nl} \sum_{m=0}^{N_t} R^m \zeta^{-ml} u(\mathbf{x},t_m) = f(\mathbf{x},t_n) \quad . \tag{5.19}$$

By employing the definition of the discrete Fourier transform one may interpret the term

$$\sum_{m=0}^{N_t} R^m \zeta^{-ml} u(\mathbf{x}, t_m) = \hat{u}(\mathbf{x}, s_l)$$

occurring in (5.19) as weighted DFT. Thus

$$\frac{R^{-n}}{N_t+1} \sum_{l=0}^{N_t} \hat{\mathcal{A}}(s_l) \zeta^{nl} \hat{u}(\mathbf{x}, s_l) = f(\mathbf{x}, t_n)$$

and by interpreting the right hand side in above equation as weighted IDFT

$$f(\mathbf{x}, t_n) = \frac{R^{-n}}{N_t+1} \sum_{l=0}^{N_t} \hat{f}(\mathbf{x}, s_l) \zeta^{nl}$$

we end up with

$$\frac{R^{-n}}{N_t+1} \sum_{l=0}^{N_t} \hat{\mathcal{A}}(s_l) \hat{u}(\mathbf{x}, s_l) \zeta^{nl} = \frac{R^{-n}}{N_t+1} \sum_{l=0}^{N_t} \hat{f}(\mathbf{x}, s_l) \zeta^{nl} \quad . \tag{5.20}$$

By equating the coefficients in (5.20) we obtain a decoupled system of operator equations in Laplace domain

$$\hat{\mathcal{A}}(s_l) \hat{u}(\mathbf{x}, s_l) = \hat{f}(\mathbf{x}, s_l) \quad \forall\, \mathbf{x} \in \Gamma \quad . \tag{5.21}$$

Thus we may transform the operator equation in time domain (5.18) to Laplace domain by means of the transformation rules given by the CQM, and solve a set of decoupled equations. Once the solution of (5.21) is computed for all prescribed s_l one may retrieve the approximate solution in time domain by applying the inverse transformation. Due to the fact that in this approach boundary integral equations have to be solved only in Laplace domain, chapter 4 only presented boundary integral equations of the Laplace transformed wave equation, i.e. the Helmholtz equation.

A crucial question is still the choice of the multistep procedure in (5.9). In many applications one opts for backward finite difference methods which belong to the class of implicit multistep methods, i.e. $\beta_0 = 0$. Throughout this work we employ the second-order BDF-2 scheme which is the highest order A-stable multistep procedure, see e.g. [31]. The characteristic polynomial of the BDF-2 scheme reads

$$\gamma(\xi) = \frac{1}{2}\xi^2 - 2\xi + \frac{3}{2} \quad . \tag{5.22}$$

5.1.2 Algorithmic description of a CQM calculation

Within this section we collect the most important results of this chapter and present a short algorithmic overview over the CQM.

The first step is to decompose the time interval into N_t equidistant steps such that $t_n = n\Delta t,\ n = 0,\ldots,N_t$. Moreover, there are four core quantities required for applying the weighted DFT as suggested by the CQM:

- The principal root of order N_t of unity

$$\zeta = \exp\left(\frac{2\pi i}{N_t+1}\right) \quad .$$

- The characteristic polynomial of the underlying multistep method, which is the BDF-2 in our case

$$\gamma(\xi) = \frac{1}{2}\xi^2 - 2\xi + \frac{3}{2} \quad .$$

- The radius of integration

$$R = \max(\Delta t^{3/N_t}, \epsilon^{-1/(2N_t)}) \quad .$$

  with $\epsilon = 10^{-12}$, cf. [2] and [3].

- The definition of the Laplace parameter

$$s_l = \frac{\gamma(R\zeta^{-l})}{\Delta t} \quad .$$

With these quantities at hand we may provide algorithm 1 for solving a convolution based boundary integral equation by means of the CQM.

Algorithm 1 Solving a convolution BIE in time via CQM

1: discretize time interval $t_n = n\,\Delta t$
2: compute right hand side at discrete time steps $f(\mathbf{x},t_n)$
3: transform data to Laplace domain $\hat{f}(\mathbf{x},s_l) = \sum_{n=0}^{N_t} R^n \zeta^{-nl} f(\mathbf{x},t_n)$
4: **for** $l = 0$ to $N_t/2$ **do**
5: compute $s_l = \Delta t^{-1}\gamma(R\zeta^{-l})$
6: solve boundary integral equation $\hat{A}(s_l)\hat{u}(\mathbf{x},s_l) = \hat{f}(\mathbf{x},s_l) \quad \forall\, \mathbf{x} \in \Gamma$
7: **end for**
8: construct remaining solution $\hat{u}(\mathbf{x},s_{N_t+1-l}) := \overline{\hat{u}(\mathbf{x},s_l)} \quad ,\ l = 1,\ldots,N_t/2-1$
9: transform solution to time domain $u(\mathbf{x},t_n) = \frac{R^{-n}}{N_t+1}\sum_{l=0}^{N_t}\hat{u}(\mathbf{x},s_l)\zeta^{-nl}$

Note that in above algorithm the complex symmetry was used. It states that spectra in Laplace domain are symmetric with respect to complex conjugation if the results in time domain are purely real. Thus one has to solve for one half of the actual frequencies only, see e.g. [6].

Moreover, the weighted DFT and weighted IDFT employed in above algorithm may be realized using the so-called *fast Fourier transform*, which is a fast incarnation of the matrix-vector product required for the DFT and IDFT respectively. To achieve the weighting one just has to modify the data accordingly, i.e. define $\tilde{f}(\mathbf{x},t_n) := R^n f(\mathbf{x},t_n)$ and use $\tilde{f}$ in a regular FFT algorithm.

Furthermore all boundary integral equations need to be known in Laplace domain only. In many applications this proves to be a significant advantage, since in most cases the fundamental solution and thus the boundary integral equations are much simpler in Laplace domain than in time domain. Moreover, there are many problems where the fundamental solution is only known in Laplace domain. Another compelling advantage of the employed method is its inherent parallelizability, as the solution of the decoupled boundary value problems may be delegated to different computers for each frequency. For further details on this approach to the CQM as well as a thorough error analysis refer to [2].

The following chapter is dedicated to row 6 in above algorithm, i.e. it presents the solution of boundary integral equations of elliptic boundary value problems. The discretization of these integral equations is realized using boundary element methods (BEM).

6 SPATIAL DISCRETIZATION

In chapter 4 we derived variational formulations of boundary integral equations, each stated on a respective Hilbert space H. All these problems basically read as

$$\text{find } u \in H : b(u,v) = F(v) \quad \forall\, v \in H$$

or equivalently

$$\text{find } u \in H : \langle \mathcal{A}u, v\rangle_{H'\times H} = \langle f, v\rangle_{H'\times H} \quad \forall\, v \in H \tag{6.1}$$

with the abstract sesquilinear form $b(\cdot,\cdot) : H \times H' \to \mathbb{C}$

$$b(u,v) = \langle \mathcal{A}u, v\rangle_{H'\times H}$$

and the functional $F \in H'$. Table 6.1 identifies the operator as well as the function space for the boundary integral equations under consideration.

Integral equation	$\mathcal{A}$	H
Indirect SLP	$\mathcal{K}'_s + \frac{1}{2}\mathcal{I} + s\kappa\mathcal{V}_s$	$L_2(\Gamma)$
Indirect DLP	$-\mathcal{D}_s + s\kappa\left(\mathcal{K}_s - \frac{1}{2}\mathcal{I}\right)$	$H^{1/2}(\Gamma)$
Direct method	$\mathcal{D}_s + \left(\mathcal{K}'_s + \frac{1}{2}\mathcal{I}\right)\mathcal{V}_s^{-1}\left(\mathcal{K}_s + \frac{1}{2}\mathcal{I}\right) + s\kappa\mathcal{I}$	$H^{1/2}(\Gamma)$

Table 6.1: Identification of abstract operator $\mathcal{A}$ and Hilbert space H with boundary integral equations derived in chapter 4.

The abstract statement (6.1) serves as the starting point for establishing a discretization by means of boundary elements.

6.1 Galerkin-Bubnov methods

In order to find an approximate solution of (6.1), we consider for $K \in \mathbb{N}$ a sequence

$$H_K := \operatorname{span}\{\varphi_k\}_{k=1}^K \subset H$$

of finite-dimensional conforming trial spaces. The approximate solution $u_K \in H_K$

$$u_K(\mathbf{x}) := \sum_{k=1}^K u_k \varphi_k(\mathbf{x}) \quad \forall\, \mathbf{x} \in \Gamma \tag{6.2}$$

is then defined as the solution of the *Galerkin-Bubnov* variational problem

$$\text{find } u_K \in H_K : \langle \mathcal{A}u_K, v_K \rangle_{H' \times H} = \langle f, v_K \rangle_{H' \times H} \quad \forall\, v_K \in H_K \quad . \tag{6.3}$$

Galerkin-Bubnov methods employ the same space H_K for both the trial functions u_K as well as the test functions v_K. Boundary element procedures based on Galerkin-Bubnov methods are commonly referred to as *Galerkin BEM* simply.

Due to the conformity $H_K \subset H$ equation (6.1) holds for any $v_K \in H_K$ in particular, i.e.

$$\langle \mathcal{A}u, v_K \rangle_{H' \times H} = \langle f, v_K \rangle_{H' \times H} \quad \forall\, v_K \in H_K \tag{6.4}$$

and subtraction of (6.4) from (6.1) yields the *Galerkin orthogonality*

$$\langle \mathcal{A}(u - u_K), v_K \rangle_{H' \times H} = 0 \quad \forall\, v_K \in H_K \quad . \tag{6.5}$$

If the operator $\mathcal{A}$ is H-elliptic, i.e.

$$\langle \mathcal{A}u, u \rangle_{H' \times H} \geq c \|u\|_H^2 \quad \forall\, u \in H,$$

which again holds especially for any $v_K \in H_K \subset H$, we find

$$c\|u - u_K\|_H^2 \leq \langle \mathcal{A}(u - u_K), u - u_K \rangle_{H' \times H}$$

and by using the Galerkin orthogonality (6.5) and the boundedness of $\mathcal{A}$ we obtain

$$\begin{aligned} \langle \mathcal{A}(u - u_K), u - u_K \rangle_{H' \times H} &= \langle \mathcal{A}(u - u_K), u - v_K \rangle_{H' \times H} + \langle \mathcal{A}(u - u_K), v_K - u_K \rangle_{H' \times H} \\ &= \langle \mathcal{A}(u - u_K), u - v_K \rangle_{H' \times H} \\ &\leq c\|u - u_K\|_H \|u - v_K\|_H \end{aligned}$$

which holds for all $v_K \in H_K$. This leads to the error estimate

$$\|u - u_K\|_H \leq c \inf_{v_K \in H_K} \|u - v_K\|_H \quad . \tag{6.6}$$

Above statement is known as *Cea's Lemma* and implies that the error of the discretization is connected to the smallest error in the entire space H_K only by a constant. This *quasi-optimality* of the error is an eminently powerful property that serves as a starting point for estimating the orders of convergence of the discretizations of variational formulations. Equation (6.6) also holds if $\mathcal{A}$ is not elliptic, but only coercive and satisfies a certain stability criterion, see [30, theorem 8.10].

The convergence of the approximate solution $u_K \to u \in H$ as $K \to \infty$ then follows from the approximation property of the trial space H_K

$$\lim_{K \to \infty} \inf_{v_K \in H_K} \|v - v_K\|_H = 0 \quad \forall\, v \in H \quad . \tag{6.7}$$

Hence, the sequence of conforming trial spaces $\{X_K\}_{K\in\mathbb{N}}$ has to be constructed such that (6.7) is ensured.

The following sections are dedicated to presenting the fundamental tools for setting up standard boundary element spaces as well as commenting on their approximation properties. It shall be noted that the following explanations are explicitly adapted to three spatial dimensions, for the general case refer to [30] or [28].

6.2 Boundary elements

For $\Gamma = \partial\Omega$ with $\Omega \subset \mathbb{R}^3$, we consider a sequence $\{\Gamma_N\}_{N\in\mathbb{N}}$ of triangulations

$$\Gamma_N = \bigcup_{l=1}^{N} \overline{\tau}_l \tag{6.8}$$

which are assumed to be *admissible*, i.e. two neighbouring elements with $\overline{\tau}_l \cap \overline{\tau}_k$, $l \neq k$, either share a common point or a common edge. Within this work, we only consider plane triangular boundary elements, although rectangular or curved elements are frequently used as well. Examples for the employed meshes are depicted in figure 6.1.

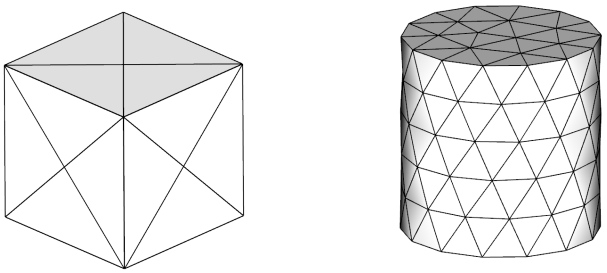

Figure 6.1: Rather simple decompositions of a cube and a cylinder intro plane triangular elements. Note that $\Gamma_N \neq \Gamma$ for the cylinder.

By $\{\mathbf{x}_k\}_{k=1}^{M}$ we denote the set of all vertices of the triangulation Γ_N. Moreover, we consider the two index sets

$$\begin{aligned} J(l) &:= \{k : \mathbf{x}_k \in \overline{\tau}_l\} \quad l = 1,\dots,N \\ I(k) &:= \{l : \mathbf{x}_k \in \overline{\tau}_l\} \quad k = 1,\dots,M \end{aligned}$$

where $J(l)$ denotes the indices of all vertices belonging to an element $\overline{\tau}_l$ and $I(k)$ is the index set of all elements sharing the node $\mathbf{x}_k$, as shown in figure 6.2.

We define the surface area of an element

$$\Delta_l := \int_{\tau_l} ds_{\mathbf{x}}$$

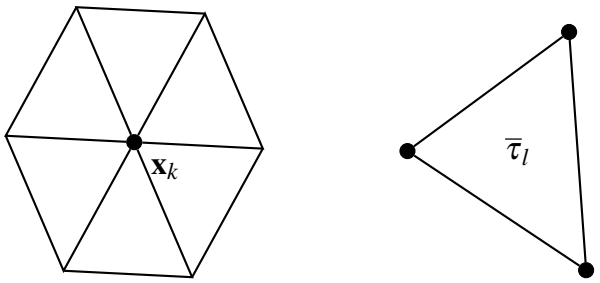

(a) Index set $I(k)$. (b) Index set $J(l)$.

Figure 6.2: Index sets $I(k)$ and $J(l)$ for triangular elements.

and the local mesh size

$$h_l := \Delta_l^{1/2}$$

for $l = 1,\ldots,N$, as well as the global mesh size of the triangulation

$$h := \max_{l=1,\ldots,N} h_l \quad .$$

Using the minimal mesh size

$$h_{min} := \min_{l=1,\ldots,N} h_l$$

we call the sequence of triangulations (6.8) *globally quasi-uniform* if there exists a constant c, independent of N, such that

$$\frac{h}{h_{min}} \leq c$$

holds. Throughout this work, only admissible and globally quasi-uniform triangulations are considered.

In essence, boundary elements are finite elements on the surface of the domain. Similarly to most finite element methods, one employs a reference element τ to describe all elements $\tau_l,\ l = 1,\ldots,N$ of the triangulation. We consider the reference element τ, which is a triangle in the two dimensional parameter domain

$$\tau := \left\{(\hat{x}_1,\hat{x}_2) \in \mathbb{R}^2 : 0 < \hat{x}_2 < \hat{x}_1 < 1\right\}$$

which is mapped onto an actual boundary element using the parametrization $\chi_l : \tau \to \tau_l$

$$\chi_l(\hat{\mathbf{x}}) = \mathbf{x}_{l_0} + \hat{x}_1(\mathbf{x}_{l_1} - \mathbf{x}_{l_0}) + \hat{x}_2(\mathbf{x}_{l_2} - \mathbf{x}_{l_1})$$

where $\mathbf{x}_{l_k}$, $k = 0,1,2$ denote the vertices of the element τ_l numbered counterclockwise with respect to the normal vector. This mapping process is depicted in figure 6.3.

This allows a representation

$$\begin{pmatrix} x_1 \\ x_2 \\ x_3 \end{pmatrix} = \begin{pmatrix} x_{l_1,1} - x_{l_0,1} & x_{l_2,1} - x_{l_1,1} \\ x_{l_1,2} - x_{l_0,2} & x_{l_2,2} - x_{l_1,2} \\ x_{l_1,3} - x_{l_0,3} & x_{l_2,3} - x_{l_1,3} \end{pmatrix} \begin{pmatrix} \hat{x}_1 \\ \hat{x}_2 \end{pmatrix} + \begin{pmatrix} x_{l_0,1} \\ x_{l_0,2} \\ x_{l_0,3} \end{pmatrix}$$

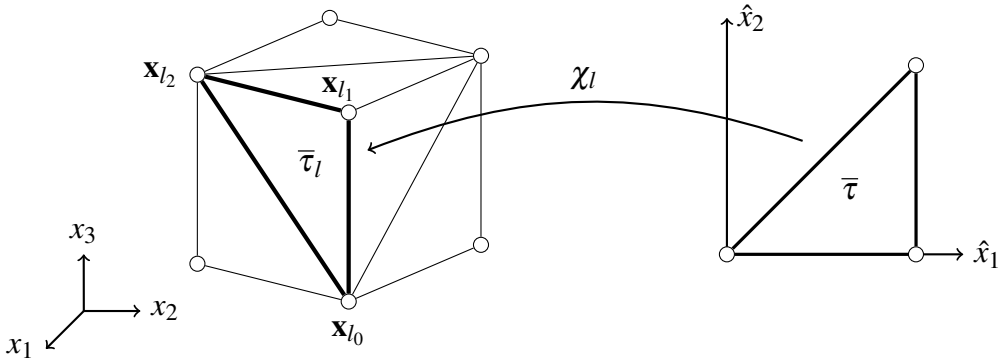

Figure 6.3: Triangular element τ_l described in terms of τ using the parametrization χ_l.

or in short

$$\tau_l \ni \mathbf{x} = \chi_l(\hat{\mathbf{x}}) = \mathbf{x}_{l_0} + \mathbf{J}_l \hat{\mathbf{x}} \quad \text{for } \hat{\mathbf{x}} \in \tau$$

where $\mathbf{J}_l \in \mathbb{R}^{3\times 2}$ is the *Jacobi matrix*

$$\mathbf{J}_l[j,k] = \frac{\partial \chi_{l,j}}{\partial \xi_k} \quad , j = 1,2,3;\ k = 1,2 \quad .$$

6.2.1 Boundary integrals

Consider a boundary element τ_l defined via the parametrization $\chi_l : \tau \to \tau_l$ and a function $f : \tau_l \to \mathbb{C}$. The surface integral of f over τ_l is

$$\int_{\tau_l} f(\mathbf{x}) ds_{\mathbf{x}} = \int_{\tau} \tilde{f}_l(\hat{\mathbf{x}})\, g_l\, d\hat{\mathbf{x}} \tag{6.9}$$

where g_l is the square root of the determinant of the Gramian matrix and

$$\tilde{f}_l(\hat{\mathbf{x}}) = f(\mathbf{x}_{l_0} + \mathbf{J}_l \hat{\mathbf{x}})$$

where we write $\tilde{f}_l \coloneqq f \circ \chi_l$. The Gramian matrix is defined by

$$\mathbf{G}_l = \mathbf{J}_l^T \mathbf{J}_l \in \mathbb{R}^{2\times 2}$$

and as a result the factor used in (6.9) is

$$g_l \coloneqq \sqrt{\det \mathbf{G}_l} \quad .$$

Note that the Jacobi matrix, and thus the Gramian matrix, are constant for each mapping since we only employ parametrizations χ_l linear in $\hat{\mathbf{x}}$.

Considering the surface area, we learn

$$\Delta_l := \int_{\tau_l} ds_{\mathbf{x}} = g_l \int_{\tau} d\hat{\mathbf{x}} = g_l \int_0^1 \int_0^{\hat{x}_1} d\hat{x}_2 d\hat{x}_1 = \frac{g_l}{2} \quad .$$

With this notation available, we may provide an explicit formula for the surface curl occurring in the regularized sesquilinear form of the hypersingular boundary integral operator (3.17)

$$\mathbf{curl}_\Gamma u \circ \chi_l = \mathbf{J}_l \mathbf{G}_l^{-1} \mathrm{grad}_{\hat{\mathbf{x}}} \tilde{u}_l \times \tilde{\mathbf{n}}$$

with $\tilde{u}_l = u \circ \chi_l$ and $\tilde{\mathbf{n}} = \mathbf{n} \circ \chi_l$. Furthermore we define $\mathrm{grad}^\perp := \left(\hat{\partial}_2, -\hat{\partial}_1\right)$ and there holds

$$g_l \mathbf{curl}_\Gamma u \circ \chi_l = \mathbf{J}_l \mathrm{grad}^\perp \tilde{u}$$

for sufficiently smooth function u, see [28]. Note that most of the previous considerations become more involved when allowing elements that employ parametrizations of higher than linear order.

6.3 Boundary element spaces

Throughout this thesis we employ three different approximation spaces, which are introduced in the following sections. In general those spaces will be denoted by $S_h^{c_p}$ or $S_h^{d_p}$, where h refers to the spatial mesh size and p to the polynomial degree of the basis functions. Furthermore, the letter c denotes globally continuous spaces, while d represents a globally discontinuous space.

Recalling the abstract approximation space H_K from the first part of this chapter, any function within this space may be represented by

$$H_K \ni u_K(\mathbf{x}) = \sum_{k=1}^{K} u_k \varphi_k(\mathbf{x}) \quad \forall\, \mathbf{x} \in \Gamma \quad .$$

Thus any function within H_K is uniquely identified by its vector of expansion coefficients

$$\begin{array}{rcl} \mathbb{C}^K \ni \mathsf{u} & = & \begin{bmatrix} u_1 & u_2 & \dots & u_{K-1} & u_K \end{bmatrix} \\ \mathsf{u} & \leftrightarrow & u_K \in H_K \end{array} \quad . \tag{6.10}$$

The isomorphism (6.10) enables us to represent any function $u_K(\mathbf{x}),\ \mathbf{x} \in \Gamma$ belonging to a K-dimensional approximation space by its vector of K expansion coefficients.

6.3.1 Discontinuous boundary elements

By $S_h^{d_0} = \operatorname{span}\{\varphi_k^{d_0}\}_{k=1}^N$ we denote the space of piecewise constant boundary elements spanned by the basis functions

$$\varphi_k^{d_0}(\mathbf{x}) = \begin{cases} 1 & \mathbf{x} \in \tau_k \\ 0 & \text{elsewhere} \end{cases} \qquad k = 1, \ldots, N,$$

which has, despite being the simplest trial space, already very powerful approximation properties. A visualization of a basis function belonging to this space is depicted in figure 6.4.

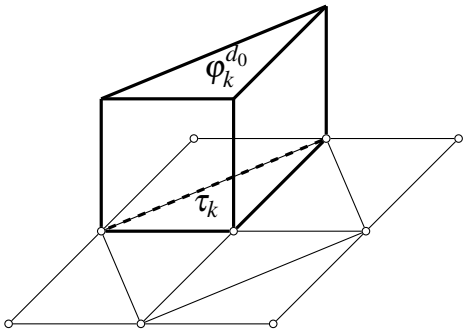

Figure 6.4: Piecewise constant basis function $\varphi_k^{d_0}$ associated to the globally discontinuous space $S_h^{d_0}$.

It is worthwhile to note that the support[1] of each basis function is precisely one element, i.e.

$$\operatorname{supp}(\varphi_k^{d_0}) = \overline{\tau}_k \quad k = 1, \ldots, N$$

thus the intersection of the supports of two different basis functions within this space always has zero measure, i.e.

$$\operatorname{supp}(\varphi_k^{d_0}) \cap \operatorname{supp}(\varphi_l^{d_0}) \text{ is either a vertex, an edge or zero for } k \neq l$$

due to the admissibility criterion stated before. As a result $S_h^{d_0}$ is an orthogonal space with respect to the $L_2(\Gamma)$ scalar product, implying

$$(\varphi_k^{d_0}, \varphi_l^{d_0})_{L_2(\Gamma)} = \int_\Gamma \varphi_k^{d_0}(\mathbf{x}) \varphi_l^{d_0}(\mathbf{x})\, d\mathbf{x} = \int_{\operatorname{supp}(\varphi_k^{d_0}) \cap \operatorname{supp}(\varphi_l^{d_0})} \varphi_k^{d_0}(\mathbf{x}) \varphi_l^{d_0}(\mathbf{x})\, d\mathbf{x} = 0 \quad \text{for } k \neq l$$

whereas

$$(\varphi_k^{d_0}, \varphi_k^{d_0})_{L_2(\Gamma)} = \int_{\tau_k} \underbrace{\left|\varphi_k^{d_0}(\mathbf{x})\right|^2}_{=1 \ \forall \ \mathbf{x} \in \tau_k} d\mathbf{x} = \int_{\tau_k} d\mathbf{x} = \Delta_k$$

[1] The support of a function is defined in appendix A.

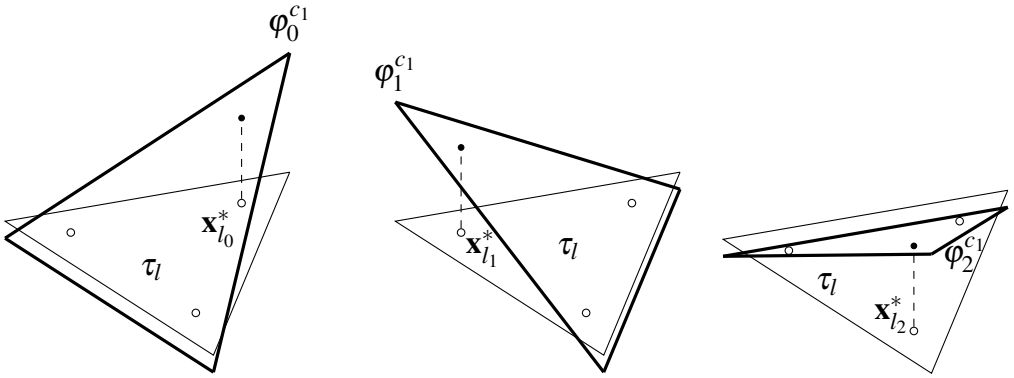

Figure 6.5: The three piecewise linear basis functions $\varphi_k^{d_1}$ of an element τ_l associated to the globally discontinuous space $S_h^{d_1}$.

holds. This circumstance leads to a diagonal mass matrix

$$\mathsf{M}_h[k,l] = \Delta_k \delta_{kl}, \quad \mathsf{M}_h = \begin{bmatrix} \Delta_1 & & \\ & \ddots & \\ & & \Delta_N \end{bmatrix} .$$

Moreover, we employ the space of linear discontinuous functions $S_h^{d_1} = \operatorname{span}\{\varphi_k^{d_1}\}_{k=1}^{3N}$ for the approximation of the right hand side. Such a space is constructed by placing three interior vertices $\mathbf{x}^*_{l_k}$, $k = 1,2,3$ within an element τ_l and setting up three linear polynomials $\varphi_{l_k}^{d_1}$, $k = 1,2,3$ such that the Kronecker delta property

$$\varphi_{l_k}^{d_1}(\mathbf{x}^*_{l_j}) = \delta_{kj} \quad k,j = 1,2,3 \tag{6.11}$$

holds. The actual positioning of these vertices does not matter from an analytical point of view as long as they do not coincide, which would cause the functions to become linearly dependent. However, if these points are too close to each other, the basis leads to ill-conditioned matrices and is thus useless from a numerical point of view. Therefore, the vertices should be spaced in a reasonable fashion, cf. [10]. These three functions are depicted in figure 6.5.

Again, the support of one basis function is precisely one element, but there are two other basis functions sharing this support as well. Consequently, this function space is not orthogonal, however, the mass matrix is composed of non-overlapping element matrices and thus may be inverted in an element-wise manner.

For the family of globally discontinuous boundary element spaces $S_h^{d_p}$ with polynomial

degree p and for $0 \leq t \leq s \leq p+1$ there holds the approximation property

$$\inf_{w_h \in S_h^{dp}} \|w - w_h\|_{H^{-t}(\Gamma)} \leq c\, h^{s+t} \|w\|_{H^s(\Gamma)} \quad \forall\, w \in H^s_{pw}(\Gamma) \tag{6.12}$$

see [28, theorem 4.3.19]. We especially emphazise the two properties

$$\begin{array}{rcll} \inf\limits_{w_h \in S_h^{dp}} \|w - w_h\|_{L_2(\Gamma)} & \leq & c\, h^{\min(p+1,s)} \|w\|_{H^s(\Gamma)} & s \geq 0 \\ \inf\limits_{w_h \in S_h^{dp}} \|w - w_h\|_{H^{-1/2}(\Gamma)} & \leq & c\, h^{1/2+\min(p+1,s)} \|w\|_{H^s(\Gamma)} & s \geq 1/2 \end{array} \qquad \forall\, w \in H^s_{pw}(\Gamma)$$

which state the convergence in two crucial spaces for the problem at hand. Furthermore, it can be observed that this space does not enjoy an approximation property in $H^{1/2}(\Gamma)$, since it is not contained in it. As a consequence, the next chapter introduces another function space designed for this demand.

6.3.2 Continuous boundary elements

Due to the fact that the discontinuous boundary elements are not contained within the space $H^{1/2}(\Gamma)$ we have to consider continuous boundary elements for problems involving this space, i.e. the double layer potential ansatz as well as the direct method.

By $S_h^{c_1} = \operatorname{span}\{\varphi_k^{c_1}\}_{k=1}^M$ we denote the space of piecewise linear globally continuous boundary elements, spanned by the basis

$$\varphi_k^{c_1}(\mathbf{x}) = \begin{cases} 1 & \mathbf{x} = \mathbf{x}_k \\ 0 & \mathbf{x} = \mathbf{x}_l \neq \mathbf{x}_k \\ \text{linear} & \text{elsewhere} \end{cases}, \quad k = 1, \ldots, M,$$

which are depicted in figure 6.6. The support of each function is given by

$$\operatorname{supp}(\varphi_k^{c_1}) = \bigcup_{l \in I(k)} \overline{\tau}_l$$

and highly depends on the connectivity of the elements, i.e. the shape regularity of the triangulation.

The three basis functions defined on the reference element read as

$$\begin{aligned} \psi_0^{c_1}(\hat{\mathbf{x}}) &= 1 - \hat{x}_1 \\ \psi_1^{c_1}(\hat{\mathbf{x}}) &= \hat{x}_1 - \hat{x}_2 \\ \psi_2^{c_1}(\hat{\mathbf{x}}) &= \hat{x}_2 \end{aligned}$$

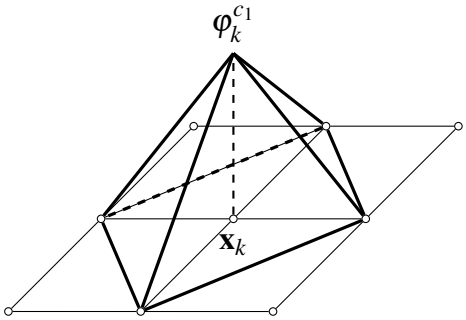

Figure 6.6: Piecewise linear basis function $\varphi_k^{c_1}$ associated to the globally continuous space $S_h^{c_1}$.

thus vanishing at each vertex they are not associated with, implying a Kronecker delta property similar to (6.11) but with respect to the vertices $\mathbf{x}_k$, $k = 1, \ldots, M$.

For $t \in [0,1]$ and $s \in [t,2]$ the space of globally continuous piecewise linear boundary elements $S_h^{c_1}$ enjoys the approximation property

$$\inf_{v_h \in S_h^{c_1}} \|v - v_h\|_{H^t(\Gamma)} \leq c\, h^{s-t} \|v\|_{H^s(\Gamma)} \quad \forall\, v \in H^s(\Gamma) \tag{6.13}$$

see [30, theorem 10.9]. In particular there holds

$$\inf_{v_h \in S_h^{c_1}} \|v - v_h\|_{H^{1/2}(\Gamma)} \leq c\, h^{s-1/2} \|v\|_{H^s(\Gamma)} \quad \forall\, v \in H^s(\Gamma)$$

for $s \in [\frac{1}{2}, 2]$ which states the convergence in the energy space of the indirect double layer potential ansatz and the direct method.

6.4 Boundary element methods

Inserting the ansatz (6.2) into the abstract variational formulation (6.1) yields

$$\langle \mathcal{A} u_K, v_K \rangle_{H' \times H} = \langle f, v_K \rangle_{H' \times H} \quad \forall\, v_K \in H_K$$

and by inserting (6.2) we obtain its fully discretized version

$$\begin{aligned}
\langle \mathcal{A} \sum_{k=1}^{K} u_k \varphi_k, \sum_{k=1}^{K} v_k \varphi_k \rangle_{H' \times H} &= \langle f, \sum_{k=1}^{K} v_k \varphi_k \rangle_{H' \times H} \\
\sum_{k=1}^{K} \overline{v_k} \langle \mathcal{A} \sum_{l=1}^{K} u_l \varphi_l, \varphi_k \rangle_{H' \times H} &= \sum_{k=1}^{K} \overline{v_k} \langle f, \varphi_k \rangle_{H' \times H} \\
\sum_{k=1}^{K} \overline{v_k} \sum_{l=1}^{K} u_l \langle \mathcal{A} \varphi_l, \varphi_k \rangle_{H' \times H} &= \sum_{k=1}^{K} \overline{v_k} \langle f, \varphi_k \rangle_{H' \times H}
\end{aligned}$$

for all $v_k \in \mathbb{C},\ k = 1,\dots,K$ by virtue of the isomorphism (6.10). Employing the linear independence of the basis functions

$$\sum_{l=1}^{K} v_k \varphi_k(\mathbf{x}) = 0 \quad \forall\, \mathbf{x} \in \Gamma \iff v_k = 0 \quad ,\ k = 1,\dots,K$$

we obtain

$$\sum_{l=1}^{K} u_l \langle \mathcal{A}\varphi_l, \varphi_k \rangle_{H' \times H} = \langle f, \varphi_k \rangle_{H' \times H} \quad ,\ k = 1,\dots,K \tag{6.14}$$

which tells us that both the sesquilinear form as well as the functional only have to be evaluated in terms of the basis functions which leads to a system of K equations. Considering the coefficient matrix

$$\mathsf{A}[k,l] = \langle \mathcal{A}\varphi_l, \varphi_k \rangle_{H' \times H}$$

and the coefficient vector

$$\mathsf{f}[k] = \langle f, \varphi_k \rangle_{H' \times H}$$

we end up with the algebraic system

$$\mathsf{A}\mathsf{u} = \mathsf{f} \quad . \tag{6.15}$$

By solving system (6.15) for u and utilizing (6.10) we obtain the solution u_K of the approximated abstract variational formulation (6.3). This general routine is employed to the boundary integral equations of chapter 4 to derive boundary element methods for them.

6.4.1 Approximation of the functional

In many scenarios it is more convenient not to deal with the actual functional $F(v)$ in (6.1) but a discretized version $F_h(v)$. This occurs due to the fact that the function $f \in H^{-1/2}(\Gamma)$ on the right hand side might be rather involved, thus a representation of f within a computational algorithm is more cumbersome than translating f to some $f_h \in S_h^{d_p}$ and merely representing it by means of the isomorphism (6.10). Throughout the following considerations we assume $f \in L_2(\Gamma)$ for the sake of simplicity, which is a reasonable claim in many engineering applications. The two main strategies for approximating functions employed throughout this work are interpolation and L_2-projection.

Interpolation of the right hand side

The interpolation operator $\mathcal{I}_h^{d_p}$ is defined by

$$f(\mathbf{x}_k^*) - \mathcal{I}_h^{d_p} f(\mathbf{x}_k^*) = 0 \quad k = 1,\dots,\dim(S_h^{d_p})$$

where $\mathbf{x}_k^*$ is a set of $\dim(S_h^{d_p}) = \frac{N}{2}(p+1)(p+2)$ non-coincing points at which the error is forced to vanish. For the space of piecewise constant functions these points are the centers of each element, while for the space of piecewise linear basis functions these points are the ones where the Kronecker delta property (6.11) is satisfied. With the representation

$$S_h^{d_p} \ni \mathcal{I}_h^{d_p} f(\mathbf{x}) = \sum_{k=1}^{\dim(S_h^{d_p})} f_k \varphi_k^{d_p}(\mathbf{x}) \quad \forall\, \mathbf{x} \in \Gamma \quad ,$$

this leads to a set of $\dim(S_h^{d_p})$ equations

$$\sum_{k=1}^{\dim(S_h^{d_p})} f_k \varphi_k^{d_p}(\mathbf{x}_l^*) = f(\mathbf{x}_l^*) \quad l = 1, \ldots, \dim(S_h^{d_p})$$

and since we constructed the spaces such that $\varphi_k^{d_p}(\mathbf{x}_l^*) = \delta_{kl},\ k,l = 1,\ldots,\dim(S_h^{d_p})$ the set of equations becomes decoupled, thus

$$f_k = f(\mathbf{x}_k^*) \quad k = 1, \ldots, \dim(S_h^{d_p}) \quad .$$

By setting up a coefficient vector $\mathsf{f} = [f_1 \ldots f_{N(p+1)(p+2)/2}]$ and invoking the isomorphism (6.10) we obtain the interpolating function $\mathcal{I}_h^{d_p} f(\mathbf{x}),\ \mathbf{x} \in \Gamma$.

Orthogonal projection of the right hand side

On the other hand the L_2-projection operator $\mathcal{Q}_h^{d_p} : L_2(\Gamma) \to S_h^{d_p}$ is defined by

$$\mathcal{Q}_h^{d_p} f = \arg \min_{f_h \in S_h^{d_p}} \|f - f_h\|_{L_2(\Gamma)}$$

which is the unique solution of the variational problem

$$(\mathcal{Q}_h^{d_p} f, q_h)_{L_2(\Gamma)} = (f, q_h)_{L_2(\Gamma)} \quad \forall\, q_h \in S_h^{d_p} \quad .$$

By inserting the representation

$$S_h^{d_p} \ni \mathcal{Q}_h^{d_p} f(\mathbf{x}) = \sum_{k=1}^{\dim(S_h^{d_p})} f_k \varphi_l^{d_p}(\mathbf{x}) \quad \forall\, \mathbf{x} \in \Gamma \quad ,$$

and employing the routines resulting in (6.14) we obtain the algebraic system

$$\mathsf{M}_h \mathsf{f} = \mathsf{b}_h$$

with the mass matrix

$$\mathsf{M}_h[k,l] = (\varphi_k^{d_p}, \varphi_l^{d_p})_{L_2(\Gamma)}$$

and the coefficient vector

$$\mathsf{b}_h[k] = (f, \varphi_k^{d_p})_{L_2(\Gamma)} \quad .$$

By solving above system for f we find the projection $\mathcal{Q}_h^{d_p} f(\mathbf{x}),\ \mathbf{x} \in \Gamma$ via (6.10).

It shall be kept in mind that the error estimate (6.12) holds and if f is sufficiently smooth we obtain

$$\|f - \mathcal{Q}_h^{d_p} f\|_{L_2(\Gamma)} \leq c\, h^{p+1} \|f\|_{H^{p+1}(\Gamma)} \quad . \tag{6.16}$$

It is important to realize that replacing $F(v)$ by $F_h(v)$ introduces another error to the discretization. If the approximation of the functional converges at a slower rate than the unperturbed variational formulation using $F(v)$ then the originally expected order of convergence cannot be maintained. For a discussion of this topic see e.g. [30, theorem 8.2]. Due to the sparsity of the mass matrix the computational cost of replacing f by $\mathcal{Q}_h^{d_1} f$ is actually negligibly small compared to the actual boundary element stiffness matrices in (6.15). The orthogonal projection of f onto the space of piecewise linear discontinuous boundary elements implies the optimal error estimate

$$\|f - \mathcal{Q}_h^{d_1} f\|_{L_2(\Gamma)} \leq c\, h^2 \|f\|_{H^2(\Gamma)} \quad . \tag{6.17}$$

for a sufficiently smooth f.

By collecting various results in [30, chapter 12] one may show that by using the L_2-projection on the space of piecewise linear discontinuous functions one does not influence the rates of convergence of the methods presented throughout the rest of this thesis.

6.4.2 Indirect single layer potential Galerkin BEM (SLP BEM)

Choosing $S_h^{d_0} \subset L_2(\Gamma) \subset H^{-1/2}(\Gamma)$ we obtain a fully discrete form of the boundary integral equation associated with the single layer potential ansatz (4.6):
Find $w_h \in S_h^{d_0}$ such that

$$\frac{1}{2}(w_h, \mu_h)_{L_2(\Gamma)} + b_{\mathcal{K}'_s}(w_h, \mu_h) + s\, b^{\kappa}_{\mathcal{V}_s}(w_h, \mu_h) = (f_h, \mu_h)_{L_2(\Gamma)} \quad \forall\ \mu_h \in S_h^{d_0}, \tag{6.18}$$

which leads to the algebraic system

$$\frac{1}{2}\mathsf{M}_h \mathsf{w} + \mathsf{K}'_h \mathsf{w} + s\mathsf{V}_h^{\kappa} \mathsf{w} = \mathsf{f}_h$$

or equivalently $\mathsf{A}_h\mathsf{w} = \mathsf{f}_h$ with

$$\mathsf{A}_h := \frac{1}{2}\mathsf{M}_h + s\mathsf{K}'_h + \mathsf{V}_h^\kappa \quad .$$

The entries of the stiffness matrices $\mathsf{V}_h^\kappa, \mathsf{K}'_h \in \mathbb{C}^{M\times M}$, the mass matrix $\mathsf{M}_h \in \mathbb{C}^{M\times M}$ as well as the load vector $\mathsf{f}_h \in \mathbb{C}^M$ read as

$$\begin{aligned}
\mathsf{V}_h^\kappa[k,l] &= \int_{\mathrm{supp}(\varphi_k^{d_0})\times\mathrm{supp}(\varphi_k^{d_0})} \hat{U}_s(\mathbf{x}-\mathbf{y})\,\kappa(\mathbf{x})\varphi_k^{d_0}(\mathbf{x})\varphi_l^{d_0}(\mathbf{y})\,ds_\mathbf{y}\,ds_\mathbf{x} \\
\mathsf{K}'_h[k,l] &= \int_{\mathrm{supp}(\varphi_k^{d_0})\times\mathrm{supp}(\varphi_k^{d_0})} \gamma_{1,\mathbf{x}}^- \hat{U}_s(\mathbf{x}-\mathbf{y})\,\varphi_k^{d_0}(\mathbf{x})\varphi_l^{d_0}(\mathbf{y})\,ds_\mathbf{y}\,ds_\mathbf{x} \\
\mathsf{M}_h[k,l] &= \int_{\mathrm{supp}(\varphi_k^{d_0})\cap\mathrm{supp}(\varphi_l^{d_0})} \varphi_k^{d_0}(\mathbf{x})\varphi_l^{d_0}(\mathbf{x})\,ds_\mathbf{x} = \Delta_k\delta kl \\
\mathsf{f}_h[k] &= \int_{\mathrm{supp}(\varphi_k^{d_0})} f_h(\mathbf{x})\varphi_k^{d_0}(\mathbf{x})\,ds_\mathbf{x} = \int_{\mathrm{supp}(\varphi_k^{d_0})} f_h(\mathbf{x})\,ds_\mathbf{x} \quad .
\end{aligned}$$

6.4.3 Indirect double layer potential Galerkin BEM (DLP BEM)

By employing $S_h^{c_1} \subset H^{1/2}(\Gamma)$ we get a discretized version of the boundary integral equation of the double layer potential ansatz (4.9):
Find $v_h \in S_h^{c_1}$ such that

$$-b_{\mathcal{D}_s}(v_h,\mu_h) - \frac{s}{2}(v_h,\mu_h)_{L_2(\Gamma),\kappa} + s\,b_{\mathcal{K}_s}^\kappa(v_h,\mu_h) = (f_h,\mu_h)_{L_2(\Gamma)} \quad \forall\ \mu_h \in S_h^{c_1}, \tag{6.19}$$

which is equivalent to the algebraic system

$$-\mathsf{D}_h\mathsf{w} - \frac{s}{2}\mathsf{M}_h^\kappa\mathsf{w} + s\mathsf{K}_h^\kappa\mathsf{w} = \mathsf{f}_h$$

or $\mathsf{A}_h\mathsf{w} = \mathsf{f}_h$ with

$$\mathsf{A}_h := -\mathsf{D}_h - \frac{s}{2}\mathsf{M}_h^\kappa + s\mathsf{K}_h^\kappa \quad .$$

The entries of the stiffness matrices $\mathsf{K}_h^\kappa, \mathsf{D}_h \in \mathbb{C}^{N\times N}$, the weighted mass matrix $\mathsf{M}_h^\kappa \in \mathbb{C}^{N\times N}$ as well as the load vector $\mathsf{f}_h \in \mathbb{C}^N$ read as

$$
\begin{aligned}
\mathsf{K}_h^{\kappa}[k,l] &= \int\limits_{\mathrm{supp}(\varphi_k^{c_1})\times\mathrm{supp}(\varphi_k^{c_1})} \gamma_{1,\mathbf{y}}^{-}\hat{U}_s(\mathbf{x}-\mathbf{y})\,\kappa(\mathbf{x})\varphi_k^{c_1}(\mathbf{x})\varphi_l^{c_1}(\mathbf{y})\,ds_{\mathbf{y}}\,ds_{\mathbf{x}} \\
\mathsf{D}_h[k,l] &= \int\limits_{\mathrm{supp}(\varphi_k^{c_1})\times\mathrm{supp}(\varphi_k^{c_1})} \hat{U}_s(\mathbf{x}-\mathbf{y})\left(\mathbf{curl}_{\Gamma}\varphi_l^{c_1}(\mathbf{y}),\mathbf{curl}_{\Gamma}\varphi_k^{c_1}(\mathbf{x})\right)\,ds_{\mathbf{y}}\,ds_{\mathbf{x}} \\
&+ \frac{s^2}{c_0^2}\int\limits_{\mathrm{supp}(\varphi_k^{c_1})\times\mathrm{supp}(\varphi_k^{c_1})} \hat{U}_s(\mathbf{x}-\mathbf{y})\,\varphi_k^{c_1}(\mathbf{y})\varphi_l^{c_1}(\mathbf{x})\,(\mathbf{n}(\mathbf{x}),\mathbf{n}(\mathbf{y}))\,ds_{\mathbf{y}}\,ds_{\mathbf{x}} \\
\mathsf{M}_h^{\kappa}[k,l] &= \int\limits_{\mathrm{supp}(\varphi_k^{c_1})\cap\mathrm{supp}(\varphi_l^{c_1})} \kappa(\mathbf{x})\varphi_k^{c_1}(\mathbf{x})\varphi_l^{c_1}(\mathbf{x})\,ds_{\mathbf{x}} \\
\mathsf{f}_h[k] &= \int\limits_{\mathrm{supp}(\varphi_k^{c_1})} f_h(\mathbf{x})\varphi_k^{c_1}(\mathbf{x})\,ds_{\mathbf{x}} \quad .
\end{aligned}
$$

6.4.4 Direct Galerkin BEM

Since a direct formulation relies on two function spaces, we have to consider both spaces employed for the indirect method simultaneously. By choosing $S_h^{d_0} \subset H^{-1/2}(\Gamma)$ and $S_h^{c_1} \subset H^{1/2}(\Gamma)$ we obtain the discretized version of (4.17):
Find $(u_h^D, u_h^N) \in S_h^{c_1} \times S_h^{d_0}$, such that

$$
\begin{aligned}
\tfrac{1}{2}(u_h^D,\tau_h)_{L_2(\Gamma)} + b_{\mathcal{K}_s}(u_h^D,\tau_h) &= b_{\mathcal{V}_s}(u_h^N,\tau_h) \\
b_{\mathcal{D}_s}(u_h^D,\mu_h) + b_{\mathcal{K}'_s}(u_h^N,\mu_h) + \tfrac{1}{2}(u_h^N,\mu_h)_{L_2(\Gamma)} + s(u_h^D,\mu_h)_{L_2(\Gamma),\kappa} &= (f_h,\mu_h)_{L_2(\Gamma)}
\end{aligned}
\tag{6.20}
$$

holds for all $(\mu_h,\tau_h) \in S_h^{c_1} \times S_h^{d_0}$, corresponding to the system

$$
\begin{aligned}
\frac{1}{2}\mathsf{M}_h\mathsf{u} + \mathsf{K}_h\mathsf{u} &= \mathsf{V}_h\mathsf{t} \\
\mathsf{D}_h\mathsf{u} + \mathsf{K}_h^T\mathsf{t} + \frac{1}{2}\mathsf{M}_h^T\mathsf{t} + s\mathsf{M}_h^{\kappa}\mathsf{u} &= \mathsf{f}
\end{aligned}
$$

or alternatively

$$
\begin{bmatrix} \mathsf{V}_h & -\frac{1}{2}\mathsf{M}_h - \mathsf{K}_h \\ \frac{1}{2}\mathsf{M}_h^T + \mathsf{K}_h^T & \mathsf{D}_h + s\mathsf{M}_h^{\kappa} \end{bmatrix} \begin{bmatrix} \mathsf{t} \\ \mathsf{u} \end{bmatrix} = \begin{bmatrix} \mathsf{0} \\ \mathsf{f} \end{bmatrix} \tag{6.21}
$$

where we identify $u_h^D \leftrightarrow \mathsf{u}$ and $u_h^N \leftrightarrow \mathsf{t}$.

The entries of the stiffness matrices $\mathsf{V}_h \in \mathbb{C}^{N\times N}, \mathsf{K}_h \in \mathbb{C}^{N\times M}, \mathsf{D}_h \in \mathbb{C}^{M\times M}$, the mass matrix $\mathsf{M}_h \in \mathbb{C}^{N\times M}$, the weighted mass matrix $\mathsf{M}_h^\kappa \in \mathbb{C}^{M\times M}$ as well as the load vector $\mathsf{f}_h \in \mathbb{C}^M$ read as

$$\begin{aligned}
\mathsf{V}_h[k,l] &= \int_{\mathrm{supp}(\varphi_k^{d_0})\times\mathrm{supp}(\varphi_l^{d_0})} \hat{U}_s(\mathbf{x}-\mathbf{y})\,\varphi_k^{d_0}(\mathbf{x})\varphi_l^{d_0}(\mathbf{y})\,ds_{\mathbf{y}}\,ds_{\mathbf{x}} \\
\mathsf{K}_h[k,l] &= \int_{\mathrm{supp}(\varphi_k^{d_0})\times\mathrm{supp}(\varphi_l^{c_1})} \gamma_{1,\mathbf{y}}^{-}\hat{U}_s(\mathbf{x}-\mathbf{y})\,\varphi_k^{d_0}(\mathbf{x})\varphi_l^{c_1}(\mathbf{y})\,ds_{\mathbf{y}}\,ds_{\mathbf{x}} \\
\mathsf{D}_h[k,l] &= \int_{\mathrm{supp}(\varphi_k^{c_1})\times\mathrm{supp}(\varphi_l^{c_1})} \hat{U}_s(\mathbf{x}-\mathbf{y})\left(\mathbf{curl}_\Gamma\varphi_k^{c_1}(\mathbf{y}),\mathbf{curl}_\Gamma\varphi_l^{c_1}(\mathbf{x})\right)\,ds_{\mathbf{y}}\,ds_{\mathbf{x}} \\
&\quad + \frac{s^2}{c_0^2}\int_{\mathrm{supp}(\varphi_k^{c_1})\times\mathrm{supp}(\varphi_l^{c_1})} \hat{U}_s(\mathbf{x}-\mathbf{y})\,\varphi_k^{c_1}(\mathbf{y})\varphi_l^{c_1}(\mathbf{x})\,(\mathbf{n}(\mathbf{x}),\mathbf{n}(\mathbf{y}))\,ds_{\mathbf{y}}\,ds_{\mathbf{x}} \\
\mathsf{M}_h[k,l] &= \int_{\mathrm{supp}(\varphi_k^{d_0})\cap\mathrm{supp}(\varphi_l^{c_1})} \varphi_k^{d_0}(\mathbf{x})\varphi_l^{c_1}(\mathbf{x})\,ds_{\mathbf{x}} \\
\mathsf{M}_h^\kappa[k,l] &= \int_{\mathrm{supp}(\varphi_k^{c_1})\cap\mathrm{supp}(\varphi_l^{c_1})} \kappa(\mathbf{x})\varphi_k^{c_1}(\mathbf{x})\varphi_l^{c_1}(\mathbf{x})\,ds_{\mathbf{x}} \\
\mathsf{f}_h[k] &= \int_{\mathrm{supp}(\varphi_k^{c_1})} f_h(\mathbf{x})\varphi_k^{c_1}(\mathbf{x})\,ds_{\mathbf{x}} \quad .
\end{aligned}$$

For further details on the symmetries of these matrices see appendix D.

Due to the coercivity of the single layer potential the matrix V_h is invertible and allows the computation of a Schur complement of the block matrix in (6.21). Thus, the first row yields the discrete incarnation of the first representation of the Steklov-Poincaré operator

$$\mathsf{t} = \mathsf{V}_h^{-1}\left(\frac{1}{2}\mathsf{M}_h + \mathsf{K}_h\right)\mathsf{u} \quad .$$

By inserting above equation into the second row of (6.21) we obtain

$$\left[\mathsf{D}_h + s\mathsf{M}_h^\kappa + \left(\frac{1}{2}\mathsf{M}_h^T + \mathsf{K}_h^T\right)\mathsf{V}_h^{-1}\left(\frac{1}{2}\mathsf{M}_h + \mathsf{K}_h\right)\right]\mathsf{u} = \mathsf{f} \quad .$$

Note that all entries of the coefficient matrix of the hypersingular boundary integral operator D_h are given with the regularized version of the kernel. Actually, it is only necessary to consider this kernel when the integral is in fact singular, i.e.

$$\inf_{(\mathbf{x},\mathbf{y})\in\mathrm{supp}(\varphi_k^{c_1})\times\in\mathrm{supp}(\varphi_l^{c_1})} \|\mathbf{x}-\mathbf{y}\| = 0 \quad .$$

In cases with positive distance it is sufficient to consider a non-regularized version of the kernel, which is not based on the computationally expensive regularization by means of integration by parts.

6.4.5 Matrix assembly

Although the definition of the matrix coefficients above suggests an assembly loop over the support of each basis function, this approach is highly deprecated. It is advantageous to assemble the matrices in an element-wise manner, similary to most finite element methods.

To this extent we consider a generic stiffness matrix for globally continuous piecewise linear ansatz and test functions

$$\begin{aligned} \mathsf{A}_h[k,l] &= \int\limits_{\mathrm{supp}(\varphi_k^{c1})\times\mathrm{supp}(\varphi_l^{c1})} k(\mathbf{x},\mathbf{y},\mathbf{y}-\mathbf{x})\varphi_k^{c1}(\mathbf{x})\varphi_l^{c1}(\mathbf{y})\; ds_{\mathbf{y}}\, ds_{\mathbf{x}} \\ &= \sum_{m\in I(k)}\sum_{n\in I(l)} \int\limits_{\tau_m\times\tau_n} k(\mathbf{x},\mathbf{y},\mathbf{y}-\mathbf{x})\varphi_k^{c1}(\mathbf{x})\varphi_l^{c1}(\mathbf{y})\; ds_{\mathbf{y}}\, ds_{\mathbf{x}} \end{aligned}$$

which can be obtained by assembling the stiffness matrix of each element pairing $\tau_m \times \tau_l$

$$\mathsf{A}_h^{\tau_m\times\tau_n}[k,l] = \int\limits_{\tau\times\tau} k\left(\chi_m(\hat{\mathbf{x}}),\chi_n(\hat{\mathbf{y}}),\chi_m(\hat{\mathbf{x}})-\chi_n(\hat{\mathbf{y}})\right)\psi_k^{c1}(\hat{\mathbf{x}})\psi_l^{c1}(\hat{\mathbf{y}})\; g_n d\hat{\mathbf{y}}\, g_m d\hat{\mathbf{x}} \;,\; k,l=1,2,3$$

to the global matrix using connectivity relations. Note that due to the non-local support of the kernel k the stiffness matrices are fully populated. Unlike finite element methods there is not only one element matrix for each element $\tau_m,\ n=1,\ldots,N$, but one element matrix for each element pairing $\tau_m\times\tau_n,\ m,n=1,\ldots,N$.

6.4.6 Comparison of indirect and direct Galerkin BEM

Based on the explanations in [28] the indirect and direct methods show the following distinctions:

- Indirect methods for the Robin boundary value problem require the assembly of two matrices, while the direct method is built around three matrices. However, the matrix V_h is symmetric in the direct approach, while V_h^K does not share this property due to the underlying weighted scalar product in the indirect single layer potential ansatz. Furthermore, the indirect approaches require the solution of smaller matrices, since each trial space of the two indirect methods occurs in the direct formulation simultaneously.

- The unknowns of the direct method are the Dirichlet and Neumann data, while the indirect approaches compute an abstract density function, without any inherent physical meaning. To retrieve the Cauchy data one would have to apply the respective traces to the ansatz and compute them in a secondary step.

- To compute solutions in the domain Ω, the direct method has to evaluate the representation formula, which is based on two boundary integral operators. The presented indirect methods evolve around one potential only, thus having a significant edge when the solution has to be computed at a multitude of interior points.

- The rate of convergence of indirect methods may be significantly slower than equivalent direct formulations on non-smooth surfaces. This occurs due to the fact that indirect methods yield quasi-optimal approximations of abstract density functions. As an example we consider the indirect single layer potential ansatz yielding the estimate for the unknown density w in the energy norm

$$\inf_{v_h \in S_h^{dp}} \|w - w_h\|_{H^{-1/2}(\Gamma)} \leq c\, h^{1/2+\min(p+1,s)} \|w\|_{H^s(\Gamma)}$$

  for $s \geq \frac{1}{2}$. If the density w is not smooth enough the maximal rate of convergence $\frac{1}{2} + p + 1$ cannot be reached. As stated in [28] the density w inherits singularities of both the exterior as well as the interior boundary value problem on non-smooth surfaces, which might reduce the regularity of the density vastly. Direct methods, on the other hand, approximate the actual Cauchy data quasi-optimally, thus the singularities inherited in the direct method are precisely the singularities of actual solutions of the boundary value problem. Consequently the regularity of the Cauchy data might be higher than the associated density, hence leading to better orders of convergence. This behaviour is thoroughly investigated in [32] for Laplace's equation in two dimensions.

To draw a conclusion of above aspects, we state certain problems where each of these methods may prove advantageous.

- If the problem is to find the unknown Cauchy data only, the direct method seems more appealing than the indirect one.

- In problems where the solution has to be evaluated at a great number of interior points an indirect formulation is more suitable than the direct one.

Another important application of indirect methods is to test the correctness of the implementation of the individual boundary integral operators within a code as stated in [17].

6.5 Computation of matrix coefficients

The following explanations are adapted from [28]. We introduce the generic boundary integral operator

$$(\mathcal{A}u)(\mathbf{x}) = \int_\Gamma k(\mathbf{x},\mathbf{y},\mathbf{y}-\mathbf{x})u(\mathbf{y})ds_\mathbf{y} \quad \forall\, \mathbf{x}\in\Gamma$$

where the kernel k is some sort of directional derivative of the fundamental solution $\hat{U}_s$. All integrals that occurred in the prequel may be assigned to type

$$(\varphi_j,\varphi_i)_{L_2(\Gamma),\alpha} = \int_\Gamma \alpha(\mathbf{x})\varphi_i(\mathbf{x})\varphi_j(\mathbf{x})ds_\mathbf{x} \tag{6.22}$$

or

$$(\mathcal{A}\varphi_j,\varphi_i)_{L_2(\Gamma),\alpha} = \int_\Gamma \alpha(\mathbf{x})\varphi_i(\mathbf{x}) \int_\Gamma k(\mathbf{x},\mathbf{y},\mathbf{y}-\mathbf{x})\varphi_j(\mathbf{y})ds_\mathbf{y}ds_\mathbf{x} \tag{6.23}$$

respectively, where (6.22) corresponds to a weighted mass matrix and (6.23) to a weighted stiffness matrix, where α is the weighting function. Moreover, φ_i represents the basis function or some function depending on the basis, e.g. the surface curl. Note that since all basis functions are real-valued the complex conjugation of the $L_2(\Gamma)$ scalar product is obsolete. Above integrals may be decomposed into the sum over all elements, i.e.

$$\begin{aligned}(\varphi_j,\varphi_i)_{L_2(\Gamma),\alpha} &= \sum_{l=1}^{N}(\varphi_j,\varphi_i)_{L_2(\tau_l),\alpha}\\ (\mathcal{A}\varphi_j,\varphi_i)_{L_2(\Gamma),\alpha} &= \sum_{l=1}^{N}(k\varphi_j,\varphi_i)_{L_2(\tau_l),\alpha} \quad .\end{aligned}$$

Within a computer-based calculation it is convenient do reduce any integration to an element-wise level. This leads to the following representation of the abstract operator

$$(\mathcal{A}u)(\mathbf{x}) = \sum_{m=1}^{N}\int_{\tau_m} k(\mathbf{x},\mathbf{y},\mathbf{y}-\mathbf{x})u(\mathbf{y})ds_\mathbf{y} \quad \forall\, \mathbf{x}\in\Gamma$$

and thus the integrals

$$(\varphi_j,\varphi_i)_{L_2(\Gamma),\alpha} = \sum_{l=1}^{N}\int_{\tau_l} \alpha(\mathbf{x})\varphi_i(\mathbf{x})\varphi_j(\mathbf{x})ds_\mathbf{x} \tag{6.24}$$

and

$$(\mathcal{A}\varphi_j,\varphi_i)_{L_2(\Gamma),\alpha} = \sum_{l=1}^{N}\sum_{m=1}^{N}\int_{\tau_l} \alpha(\mathbf{x})\varphi_i(\mathbf{x}) \int_{\tau_m} k(\mathbf{x},\mathbf{y},\mathbf{y}-\mathbf{x})\varphi_j(\mathbf{y})ds_\mathbf{y}ds_\mathbf{x} \quad . \tag{6.25}$$

Hence, we seek integration formulas that are capable of efficiently computing the terms of above sums for each element τ_l or element pairing $\tau_l \times \tau_m$ respectively. Due to the singularity of the kernel k at $\mathbf{x} = \mathbf{y}$ the computation of (6.25) is more involved that (6.24) and thus treated first.

To this extent we introduce the distance between two elements $\tau_l,\ \tau_m \in \Gamma_N$

$$\operatorname{dist}(\tau_l, \tau_m) \coloneqq \inf_{(\mathbf{x},\mathbf{y}) \in \tau_l \times \tau_m} \|\mathbf{x} - \mathbf{y}\|$$

and realize that (6.25) has a singular nature only if $\operatorname{dist}(\tau_l, \tau_m) = 0$. A common approach to computing these singular integrals is to employ transformations that lift the singularity at $\mathbf{x} = \mathbf{y}$ and allow regular integration of the transformed integral. To do so we distinguish four relations of the boundary element pair $\tau_l \times \tau_m$ as depicted in figure 6.7:

- coinciding boundary elements, i.e. $\tau_l = \tau_m \iff l = m$, `coincident case`
- boundary elements sharing a common edge, `edge adjacent case`
- boundary elements sharing a common point, `vertex adjacent case`
- boundary elements with a positive distance, `regular case`

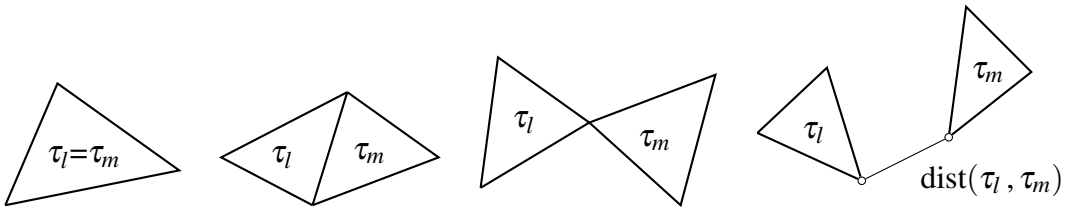

(a) coincident (b) edge adjacent (c) vertex adjacent (d) regular

Figure 6.7: Cases of relations of boundary element pair $\tau_l \times \tau_m$.

The derivations of suitable transformations would exceed the scope of this work by far and can be found in [28]. We merely sketch the crucial steps of the transformations to motivate the choice of quadrature rules in the sequel.

First and foremost, the relative coordinate $\mathbf{z} = \mathbf{y} - \mathbf{x}$ is introduced in order to fix the singularity at $\mathbf{z} = \mathbf{0}$. In reference coordinates we find

$$\mathbf{z} = \chi_m(\hat{\mathbf{y}}) - \chi_l(\hat{\mathbf{x}}) \quad , \hat{\mathbf{y}}, \hat{\mathbf{x}} \in \tau \quad . \tag{6.26}$$

Without loss of generality we assume for the vertex adjacent case

$$\chi_l\left(\left[\begin{smallmatrix}0\\0\end{smallmatrix}\right]\right) = \chi_m\left(\left[\begin{smallmatrix}0\\0\end{smallmatrix}\right]\right)$$

while for the edge adjacent we assume

$$\chi_l\left(\left[\begin{smallmatrix}s\\0\end{smallmatrix}\right]\right) = \chi_m\left(\left[\begin{smallmatrix}s\\0\end{smallmatrix}\right]\right) \quad \forall\, s \in [0,1] \quad .$$

For the coincident case we find with (6.26)

$$\mathbf{z} = \chi_l(\hat{\mathbf{y}}) - \chi_l(\hat{\mathbf{x}})$$

and due to the bijectivity of χ_l we learn that the singularity is located at the plane

$$\hat{\mathbf{y}} - \hat{\mathbf{x}} = \mathbf{0}$$

in reference coordinates. Considering the general integrand

$$k_1(\hat{\mathbf{x}},\hat{\mathbf{y}}) = \psi_i(\hat{\mathbf{x}})\psi_j(\hat{\mathbf{y}})\; k\left(\chi_l(\hat{\mathbf{x}}), \chi_m(\hat{\mathbf{y}}), \chi_m(\hat{\mathbf{y}}) - \chi_l(\hat{\mathbf{x}})\right)\; g_l(\hat{\mathbf{x}}) g_m(\hat{\mathbf{y}})$$

we have for the case of coincident elements the integral

$$I_{\tau\times\tau}(k_1) \coloneqq \int_\tau \int_\tau k_1(\hat{\mathbf{x}},\hat{\mathbf{y}})\, d\hat{\mathbf{y}} d\hat{\mathbf{x}} = \int_0^1 \int_0^{\hat{x}_1} \int_0^1 \int_0^{\hat{y}_1} k_1(\hat{\mathbf{x}},\hat{\mathbf{y}})\, d\hat{\mathbf{y}} d\hat{\mathbf{x}} \tag{6.27}$$

which reads in relative coordinates

$$I_{\tau\times\tau}(k_1) = \int_0^1 \int_0^{\hat{x}_1} \int_{-\hat{x}_1}^{1-\hat{z}_1} \int_{-\hat{x}_2}^{\hat{z}_1+\hat{x}_1-\hat{x}_2} k_1(\hat{\mathbf{x}},\hat{\mathbf{z}}+\hat{\mathbf{x}})\, d\hat{\mathbf{z}} d\hat{\mathbf{x}} \quad . \tag{6.28}$$

As stated in [28] the domain of integration in (6.28) is decomposed into six subdomains and each of them transformed onto the four-dimensional unit simplex

$$D \coloneqq \left\{(w_1,w_2,w_3,w_4) \in \mathbb{R}^4 : 0 \le w_1 \le 1, 0 \le w_2 \le w_1, 0 \le w_3 \le w_2, 0 \le w_4 \le w_3\right\} \quad .$$

Afterwards the simplex coordinates $(\xi,\eta_1,\eta_2,\eta_3)$ are used to transform the four dimensional unit hypercube $(0,1)^4$ onto D

$$\begin{pmatrix} w_1 \\ w_2 \\ w_3 \\ w_4 \end{pmatrix} = \begin{pmatrix} \xi \\ \xi\eta_1 \\ \xi\eta_1\eta_2 \\ \xi\eta_1\eta_2\eta_3 \end{pmatrix} = \xi \begin{pmatrix} 1 \\ \eta_1 \\ \eta_1\eta_2 \\ \eta_1\eta_2\eta_3 \end{pmatrix} \quad .$$

This transformation lifts the singularity and enables the use of standard integration techniques. The actual transformations as well as their derivations for each of the three cases of singularity can be found in [28].

As a result all singular integrals are actually posed on the four-dimensional hypercube $(0,1)^4$. As we are switching our attention on the numerical quadrature of the occurring integrals, we require formulas that can efficiently compute such integrals approximately.

6.5.1 Numerical quadrature

Virtually any larger boundary element code does not compute the integral in (6.22) and (6.23) exactly but approximates them by numerical quadrature. This approach is motivated by the fact that only few of these integrals can actually be integrated exactly. Moreover, it allows the implementation of a general framework applicable to a broad class of boundary integral operators and right hand sides.

Tensor Gaußian quadrature

Throughout this work we only consider Gauß-Legendre quadrature rules. The abscissas and integration weights for this quadrature can be computed by the program `GAULEG` for virtually arbitrary orders, see [25].

For the integration of a function $f : [0,1] \to \mathbb{C}$

$$I(f) = \int_0^1 f(x)\,dx$$

we consider the Gaußian quadrature rules

$$I_n(f) = \sum_{i=0}^{n} \omega_{i,n} f(x_{i,n})$$

where $\omega_{i,n}$ are the integration weights and $x_{i,n}$ are the sampling points. Note that each 2-tuple $(x_{i,n}, \omega_{i,n}),\ i = 0,\dots,n$ belongs to the quadrature rule of order n.

For the integral of the function $f : [0,1]^4 \to \mathbb{C}$

$$I(f) = \int_{(0,1)^4} f(\mathbf{x})\,d\mathbf{x} = \int_0^1 \int_0^1 \int_0^1 \int_0^1 f(x_1,x_2,x_3,x_4)\,dx_1 dx_2 dx_3 dx_4$$

we introduce the vector of orders $\mathbf{n} = (n_i)_{i=1}^4 \in \mathbb{N}^4$. This enables the definition of the *tensor Gaußian quadrature*

$$I_{\mathbf{n}}(f) = \sum_{i=0}^{n_1} \sum_{j=0}^{n_2} \sum_{k=0}^{n_3} \sum_{l=0}^{n_4} \omega_{i,n_1} \omega_{j,n_2} \omega_{k,n_3} \omega_{l,n_4} f\left(x_{i,n_1}, x_{j,n_2}, x_{k,n_3}, x_{l,n_4}\right)$$

which may have different orders for each direction. Note that although this concept is only introduced for four dimensions it can be applied in a straightforward manner to arbitrary dimensions.

Actually, we integrate over the unit hypercube in four dimensions only when computing entries of the stiffness matrix associated with singular integrals. Matrix coefficients corresponding to regular integration and coefficients of the vector of the right hand side are still formulated on the reference triangle. There are two main approaches to this issue:

- On the one hand one could employ special integration rules for triangles. In this approach the set of 3-tuples $\{(\omega_i, x_i, y_i)\}_{i=0}^{n}$ is considered, which can be computed using the condition that all monomials of maximal order p can be integrated exactly on the reference triangle

$$\int_0^1 \int_0^x x^a y^b \, dy dx = \sum_{i=0}^{n} \omega_i x_i^a y_i^b \quad \forall\, a,b \in \mathbb{N}_0 : a+b \leq p \quad .$$

  where $\mathbb{N}_0$ is the set of nonnegative integers. The number of sampling points $n+1$ is chosen such that polynomials of degree p can be integrated exactly, thus $n+1 = \frac{1}{2}(p+1)(p+2)$.

- On the other hand we might employ suitable parametrizations that map the domain used in the tensor Gaußian quadrature onto the triangle. The parametrization $\chi_{\boldsymbol{\xi}} : (0,1)^2 \to \tau$ maps the unit square onto the reference triangle and reads

$$\tau \ni \hat{\mathbf{x}} = \mathbf{T}_{\boldsymbol{\xi}} \boldsymbol{\xi} = \begin{bmatrix} 1 & 0 \\ 0 & \xi \end{bmatrix} \begin{bmatrix} \xi \\ \eta \end{bmatrix} = \begin{bmatrix} \xi \\ \xi\eta \end{bmatrix} \quad \text{for } (\xi,\eta) \in (0,1)^2 \quad .$$

  Note that the transformation determinant of above mapping $\det \mathbf{T} = \xi$ vanishes at $\xi = 0$. For instance, this circumstance is used to lift singularities in collocation boundary element methods, known as *Lachat-Watson transformation*, cf. [11]. With this mapping at hand we may transfer the integral (6.22) to the reference triangle and then to $(0,1)^2$, yielding

$$\int_\tau \tilde{\alpha}(\hat{\mathbf{x}}) \psi_i(\hat{\mathbf{x}}) \psi_j(\hat{\mathbf{x}}) \, g_l d\hat{\mathbf{x}} = \int_0^1 \int_0^1 \tilde{\alpha}\begin{pmatrix} \xi \\ \xi\eta \end{pmatrix} \psi_i\begin{pmatrix} \xi \\ \xi\eta \end{pmatrix} \psi_j\begin{pmatrix} \xi \\ \xi\eta \end{pmatrix} g_l \xi \, d\xi d\eta$$

  and employ regular tensor Gaußian quadrature as introduced above. Note that this approach may be applied to those coefficients of the stiffness matrices (6.23) that imply regular integration as well.

Thus all integrals occurring in the boundary element methods presented in the prequel can be transformed to suitable reference elements and approximated with appropriate quadrature rules.

It shall be kept in mind that the numerical quadrature introduces another error to the boundary element discretization since both the boundary integral operators as well as the $L_2(\Gamma)$

scalar product are not realized exactly. Thus the choice of the order of the employed Gaußian quadratures has to be chosen such that the originally expected order of convergence of the methods is not altered. In [28, chapter 5.3.4] one finds a detailed mathematical analysis of this topic, while a more engineering-like approach is provided in [18]. In the latter work, the distance of two elements is approximated and the required order is estimated based on three different levels for the distance normalized by the local mesh size of the elements. This strategy is only employed for regular integration, as a fixed order is used for the singular one. This approach seems quite viable in a sense that it allows a very straightforward and rapid implementation within a boundary element code.

7 NUMERICAL EXAMPLES

The methods presented in the prequel are implemented in the existing BEM library `HyENA` [21] and their correctness is confirmed throughout this chapter.

First, the convergence of the numerical procedures has to be confirmed in Laplace domain. Once this is established we consider an actual time-dependent problem to confirm the correctness of the CQM implementation. Finally, a real problem of architectural acoustics is examined.

7.1 Convergence in Laplace domain

To set up a simple reference problem in Laplace domain we consider the unit cube

$$\Omega^- = \left\{\tilde{\mathbf{x}} \in \mathbb{R}^3 : \tilde{\mathbf{x}} \in (-0.5, 0.5)^3 \text{ [m]}\right\}$$

as computational domain, equipped the piecewise constant κ-function

$$\kappa(\mathbf{x}) = \begin{cases} 0.25 \text{ [s m}^{-1}\text{]} & \text{for } \mathbf{x} \in \Gamma : x_1 = \ \ 0.5 \text{ [m]} \vee x_2 = \ \ 0.5 \text{ [m]} \vee x_3 = \ \ 0.5 \text{ [m]} \\ 1.50 \text{ [s m}^{-1}\text{]} & \text{for } \mathbf{x} \in \Gamma : x_1 = -0.5 \text{ [m]} \vee x_2 = -0.5 \text{ [m]} \vee x_3 = -0.5 \text{ [m]} \end{cases}$$

as well as the wave velocity $c_0 = 1$ [m s^{-1}].

Since the fundamental solution is a solution of the underlying differential equation, we may exploit this circumstance to generate exact solutions in order to confirm convergence. We recall the fundamental solution of the Helmholtz equation (3.16)

$$\hat{U}_s(\tilde{\mathbf{z}}) = \frac{\exp\left(-\frac{s}{c_0}\|\tilde{\mathbf{z}}\|\right)}{4\pi\|\tilde{\mathbf{z}}\|} \quad \forall\, \tilde{\mathbf{z}} \in \mathbb{R}^3 \quad .$$

In order not to interfere with the singularity of the fundamental solution at $\tilde{\mathbf{z}} = \mathbf{0}$, we consider a *source point* sufficiently far from the domain. We set

$$\tilde{\mathbf{y}}_0 = (2,2,2)^T \text{ [m]} \quad \in \Omega^+$$

and thus obtain a solution of the Helmholtz equation

$$u(\tilde{\mathbf{x}}) := \frac{\exp\left(-\frac{s}{c_0}\|\tilde{\mathbf{x}} - \tilde{\mathbf{y}}_0\|\right)}{4\pi\|\tilde{\mathbf{x}} - \tilde{\mathbf{y}}_0\|} \quad \forall\, \tilde{\mathbf{x}} \in \Omega^- \quad .$$

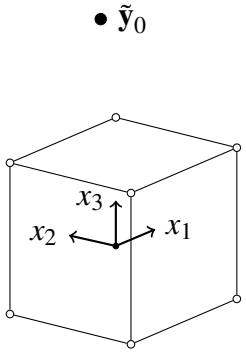

Figure 7.1: Schematic sketch of the unit cube and source under consideration.

The resulting configuration is depicted in figure 7.1.

To acquire the boundary condition imposed by this solution, we simply insert it into the Robin boundary condition in Laplace domain

$$f(\mathbf{x}) = \gamma_1^- u(\mathbf{x}) + s\kappa(\mathbf{x})\gamma_0^- u(\mathbf{x}) \quad \forall\, \mathbf{x} \in \Gamma$$

yielding

$$f(\mathbf{x}) = \frac{(\mathbf{n}(\mathbf{x}), \tilde{\mathbf{y}}_0 - \mathbf{x}) \exp(-\frac{s}{c_0}\|\mathbf{x}-\tilde{\mathbf{y}}_0\|)}{4\pi\|\mathbf{x}-\tilde{\mathbf{y}}_0\|^2} \left(\frac{1}{\|\mathbf{x}-\tilde{\mathbf{y}}_0\|} + \frac{s}{c_0} \right) + s\kappa(\mathbf{x}) \frac{\exp\left(-\frac{s}{c_0}\|\mathbf{x}-\tilde{\mathbf{y}}_0\|\right)}{4\pi\|\mathbf{x}-\tilde{\mathbf{y}}_0\|} \quad \forall\, \mathbf{x} \in \Gamma \quad (7.1)$$

which serves as the right hand side that the numerical procedures have to satisfy.

To obtain some sort of average error over several frequencies, we consider those frequencies imposed by the CQM transform for $\Upsilon = (0,8)$ [s] and $\Delta t = 1$ [s]. Although this decomposition of the time interval would actually make little sense, it merely serves as tool to obtain somewhat arbitrary frequencies to test at. All errors shown in the sequel are actually the average values of those five frequencies.

For the direct method we consider the error in the Cauchy data measured in the $L_2(\Gamma)$ norm

$$e_D \coloneqq \|\gamma_0^- u - u_h^D\|_{L_2(\Gamma)} \quad , \quad e_N \coloneqq \|\gamma_1^- u - u_h^N\|_{L_2(\Gamma)} \quad .$$

Furthermore, we consider a set of 24 interior points $\tilde{\mathbf{x}}_l$, $l = 1, \ldots, 24$ located on a cube of side 0.2 with its center at the origin. By defining the vector of interior solutions

$$\mathbf{u}^{\text{int}} \coloneqq \begin{bmatrix} u(\tilde{\mathbf{x}}_1) & \ldots & u(\tilde{\mathbf{x}}_{24}) \end{bmatrix}^T$$

we may compute relative average error at the interior points by

$$e_\Omega \coloneqq \frac{\|\mathbf{u}^{\text{int}} - \mathbf{u}_h^{\text{int}}\|_2}{\|\mathbf{u}^{\text{int}}\|_2} \quad .$$

All three boundary element methods introduced previously are used to solve the Robin boundary value problem with the right hand side (7.1). Two of the employed triangulations are depicted in figure 7.2 and all results can be found in tables 7.1 - 7.5.

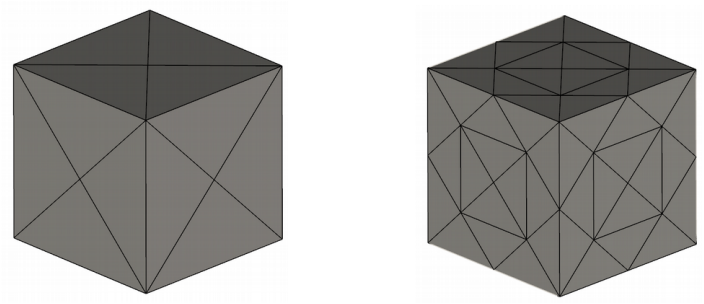

Figure 7.2: Triangulations of the unit cube with $N = 24$ and $N = 96$.

Indirect SLP BEM

	interpolation		L_2-projection	
N	e_Ω	eoc	e_Ω	eoc
24	5.45E-01		7.84E-02	
96	1.20E-01	2.18	2.37E-02	1.73
384	3.16E-02	1.93	8.66E-03	1.45
1536	8.59E-03	1.88	2.98E-03	1.54
6144	2.37E-03	1.86	9.93E-04	1.58
24576	6.66E-04	1.83	3.27E-04	1.60
eoc_{opt}		2		2

Table 7.1: Error and convergence for the inner evaluation for the unit cube, SLP BEM.

Table 7.1 shows the error and rate of convergence for the indirect SLP BEM. The optimal order of convergence eoc_{opt}, which would actually be $\mathcal{O}(h^3)$ for variational formulations in $H^{-1/2}(\Gamma)$ discretized by the space of piecewise constant basis functions, cannot be reached. The reasons for this are twofold. On the one hand the underlying variational formulation is defined not on the natural energy space $H^{-1/2}(\Gamma)$ but on $L_2(\Gamma) =: H$. Due to the approximation property (6.12) we may only expect linear convergence of sufficiently smooth density functions in the $L_2(\Gamma)$ norm. As stated in appendix C, the optimal rate of convergence of the interior evaluation is the rate of convergence of the density function in H times two. Due to the definition of the variational formulation on $L_2(\Gamma)$ the optimal rate of convergence drops to $\mathcal{O}(h^2)$ for sufficiently smooth densities. However, the boundary of the cube has edges and corners, thus we might expect that the density function is not smooth enough to reach the optimal quadratic convergence. The experimental order of

convergence is roughly $\mathcal{O}(h^{5/3})$ and although there is an evident difference between the interpolated and the L_2-projected right hand side, this deviation becomes smaller as the mesh is refined. Ultimately this difference will vanish as both approximations are equivalent in terms of their rate of convergence, however, the L_2-projection yields a smaller absolute error.

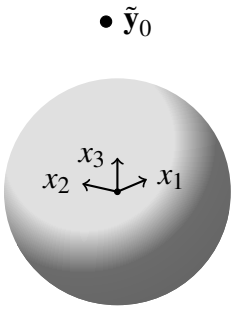

Figure 7.3: Schematic sketch of the unit sphere and source under consideration.

To support these claims, we consider a unit sphere rather than a unit cube, depicted in figure 7.3. Although the triangulation by plane triangles is neither exact nor smooth the interior angles get less pronounced at each step of refinement. Therefore we expect this circumstance to play only a minor role for the following considerations. All computational parameters are identical to the unit cube, however, the κ-function is simply $\kappa := 1\ [\mathrm{s\,m^{-1}}]$ on the entire boundary. Two of the considered meshes are depicted in figure 7.4 and table 7.2 shows the errors and rates of convergence for the inner evaluation. It can be observed that the Robin boundary value problem, whose variational formulation is posed on $L_2(\Gamma)$, is capable of reaching its optimal quadratic rate convergence on the approximated sphere. To underline that the formulation on $L_2(\Gamma)$ is indeed a drawback, we also consider a Dirichlet problem posed on the same sphere, which is also solved by the indirect SLP BEM. As stated in [28, chapter 3.4.1], the SLP ansatz for the Dirichlet problem allows a variational formulation on $H^{-1/2}(\Gamma)$, thus implying cubic convergence for the error of the interior evaluation, for smoothly bounded domains, cf. [28, example 4.2.15]. This exact behaviour can be observed in table 7.2 as well.

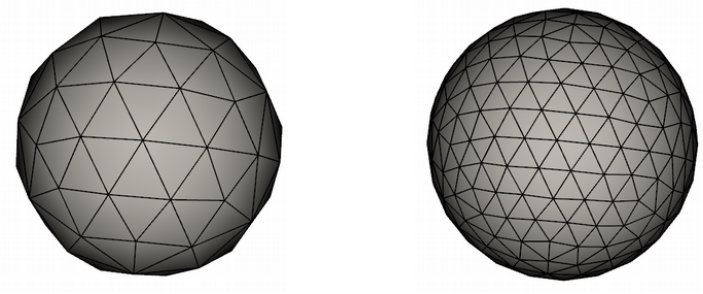

Figure 7.4: Triangulations of the unit sphere with $N = 122$ and $N = 488$.

	Robin BVP		Dirichlet BVP	
N	e_Ω	eoc	e_Ω	eoc
122	2.33E-02		1.42E-03	
488	5.66E-03	2.04	1.76E-04	3.01
1952	1.38E-03	2.04	2.16E-05	3.03
7808	3.40E-04	2.02	2.71E-06	3.00
theory		2		3

Table 7.2: Error and rate of convergence for SLP BEM for the unit sphere. In both cases we opted for a projected right hand side $f_h = \mathcal{Q}_h^{d_1} f$.

Indirect DLP BEM

	interpolation		L_2-projection	
N	e_Ω	eoc	e_Ω	eoc
24	4.70E-01		1.69E-02	
96	1.02E-01	2.21	4.84E-03	1.80
384	2.39E-02	2.09	5.42E-04	3.16
1536	5.86E-03	2.03	6.72E-05	3.01
6144	1.45E-03	2.01	8.35E-06	3.01
24576	3.62E-04	2.01	1.02E-06	3.03
eoc_{opt}		3		3

Table 7.3: Error and convergence for the interior evaluation for the unit cube, DLP BEM.

In table 7.3 both the error and rate of convergence of the indirect DLP BEM are given. The optimal order of convergence is again $\mathcal{O}(h^3)$, which can only be reached when using the L_2-projected right hand side. In the case of an interpolated right hand side, the convergence drops to a mere quadratic rate. This behaviour can be predicted by collecting the results in [30, chapter 12], assuming that the density function is sufficiently smooth. The experimental evidence suggests that the smoothness of the underlying density function in the DLP BEM is a lesser problem compared to the SLP BEM for the observed unit cube.

Note that the computational cost of the L_2-projection of the right hand side is negilibly small compared to the occurring boundary integral operators. Thus, it is highly recommendend to resort to a projected right hand side rather than an interpolated one.

Direct BEM

Tables 7.4 and 7.5 show the errors and rates of convergence of the direct BEM for the Cauchy data as well as the interior evaluation. We observe quadratic convergence in the

Dirichlet data and a linear one in the Neumann data for both approximations of the right hand side. However, the interpolated right hand side restricts the rate of convergence of the interior evaluation to $\mathcal{O}(h^2)$, while the projected right hand side enables the method to reach cubic convergence. These experimental results match the theoretical ones given in [30, chapter 12].

	interpolation				L_2-projection			
N	e_D	eoc	e_N	eoc	e_D	eoc	e_N	eoc
24	3.79E-04		1.07E-03		1.14E-04		9.80E-04	
96	8.41E-05	2.17	4.93E-04	1.12	3.27E-05	1.80	4.82E-04	1.12
384	2.04E-05	2.04	2.36E-04	1.07	8.23E-06	1.99	2.34E-04	1.07
1536	5.06E-06	2.01	1.15E-04	1.03	2.05E-06	2.01	1.15E-04	1.03
6144	1.26E-06	2.00	5.72E-05	1.01	5.10E-07	2.01	5.72E-05	1.01
24576	3.15E-07	2.00	2.85E-05	1.00	1.27E-07	2.00	2.85E-05	1.00
theory		2		1		2		1

Table 7.4: Error and convergence for the Cauchy data for the unit cube, direct BEM.

	interpolation		L_2-projection	
N	e_Ω	eoc	e_Ω	eoc
24	4.81E-01		2.47E-02	
96	1.01E-01	2.26	3.73E-03	2.73
384	2.38E-02	2.08	4.35E-04	3.10
1536	5.85E-03	2.03	5.22E-05	3.06
6144	1.45E-03	2.01	5.90E-06	3.14
24576	3.62E-04	2.00	4.87E-07	3.60
theory		2		3

Table 7.5: Error and convergence for the interior evaluation for the unit cube, direct BEM.

7.2 Convergence in time domain

The construction of the simple reference problem in time domain used throughout this section can be found in appendix E. Moreover, the considered configuration is depcited in figure 7.5.

For all following numerical experiments we consider the set of parameters

$$\begin{aligned} L &= 3.0\ [\mathrm{m}], & \kappa_0 &= 0.5\ [\mathrm{s\,m^{-1}}], & \kappa_1 &= 2.0\ [\mathrm{s\,m^{-1}}], \\ c_0 &= 1.0\ [\mathrm{m\,s^{-1}}], & T &= 4.0\ [\mathrm{s}], & p &= 3 \quad . \end{aligned}$$

The boundary conditions for the three dimensional problem that has to be solved by the presented methods read

$$\begin{aligned}
\gamma_1^- u(\mathbf{x},t) + \kappa_0 \gamma_0^- \partial_t u(\mathbf{x},t) &= f_0(t) \quad \forall \quad (\mathbf{x},t) \in \{\mathbf{x} \in \Gamma : x_1 = 0\ [\mathrm{m}]\} \times \Upsilon \\
\gamma_1^- u(\mathbf{x},t) + \kappa_1 \gamma_0^- \partial_t u(\mathbf{x},t) &= f_1(t) \quad \forall \quad (\mathbf{x},t) \in \{\mathbf{x} \in \Gamma : x_1 = L\ [\mathrm{m}]\} \times \Upsilon \\
\gamma_1^- u(\mathbf{x},t) &= 0 \qquad \forall \quad (\mathbf{x},t) \in \{\mathbf{x} \in \Gamma : x_1 \in (0,L)\ [\mathrm{m}]\} \times \Upsilon \quad .
\end{aligned}$$

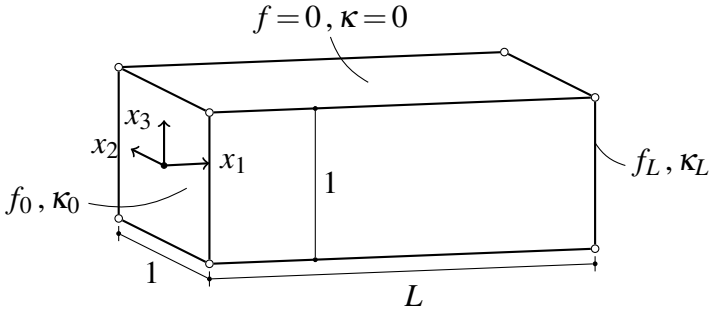

Figure 7.5: Schematic sketch of rod under consideration.

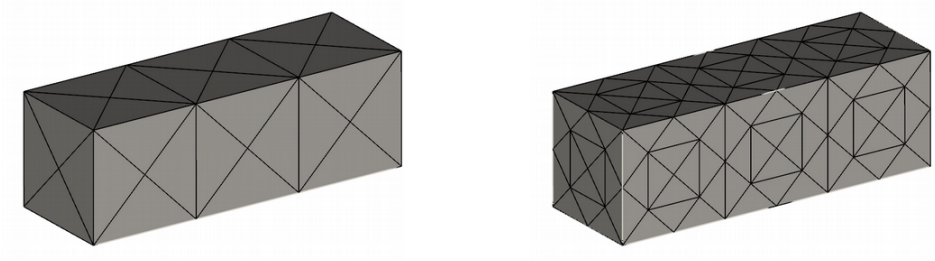

Figure 7.6: Triangulations of the rod with $N = 56$ and $N = 224$.

For the direct method we consider the error in the Cauchy data measured in the $L_2(\Gamma \times \Upsilon)$ norm, which is the L_2 norm on the lateral boundaries of the space-time cylinder. The integration in time is approximated by the trapezoidal rule, leading to the estimated errors

$$\begin{aligned}
e^D_{\Gamma\times\Upsilon} &:= \left(\Delta t \sum_{n=0}^{N_t} \| \gamma_0^- u(\cdot,t_n) - u_h^D(\cdot,t_n) \|^2_{L_2(\Gamma)} \right)^{1/2} \approx \| \gamma_0^- u - u_h^D \|_{L_2(\Gamma\times\Upsilon)} \\
e^N_{\Gamma\times\Upsilon} &:= \left(\Delta t \sum_{n=0}^{N_t} \| \gamma_1^- u(\cdot,t_n) - u_h^N(\cdot,t_n) \|^2_{L_2(\Gamma)} \right)^{1/2} \approx \| \gamma_1^- u - u_h^N \|_{L_2(\Gamma\times\Upsilon)} \quad .
\end{aligned}$$

When it comes to the computation of interior results we consider a set of 88 interior points located on the prism $(0.5, 2.5) \times (-0.2, 0.2) \times (-0.2, 0.2)$ [m], which is fully contained in the rod. We define the vector of interior solutions $\mathbf{u}^{\mathrm{int}}(t_n)$ for each time step n similary to before. Hence, we may approximate the error at these points using

$$e_{\Omega\times\Upsilon} := \left(\Delta t \sum_{n=0}^{N_t} \| \mathbf{u}^{\mathrm{int}}(t_n) - \mathbf{u}_h^{\mathrm{int}}(t_n) \|^2_{l^2} \right)^{1/2} \approx \| \| \mathbf{u}^{\mathrm{int}}(\cdot) - \mathbf{u}_h^{\mathrm{int}}(\cdot) \|_{l^2} \|_{L_2(\Upsilon)} \quad .$$

Note that the error introduced by using the trapezoidal rule instead of the actual time integrals is $\mathcal{O}(\Delta t^2)$. Thus the maximal order of covergence that is observable with above error measurements is also $\mathcal{O}(\Delta t^2)$. Since the employed methods are expected to permit quadratic convergence at most, this circumstance poses no actual problem. A detailed error analysis of a boundary element method based on the CQM utilizing the BDF-2 scheme can be found in [2]. It is stated that the error in the density function, measured in the energy norm, optimally decays like $\mathcal{O}(\Delta t^2)$ when considering an indirect SLP ansatz for a Dirichlet problem. The experimental evidence presented in the remainder of this section suggests that this estimate is applicable to the considered methods as well.

Moreover, it shall be kept in mind that the right hand side $f_i,\ i = 0,1$ is piecewise constant and can therefore be represented exactly in the boundary element code, i.e. $f_{h,i} = \mathcal{Q}_h^{d_1} f_i = \mathcal{I}_h^{d_1} f_i = f_i,\ i = 0,1$.

In the sequel we consider a sequence of five meshes, where both space and time are refined uniformly. The properties of these triangulations are shown in table 7.6, where we note that $h_l = \Delta t_l\ ,\ l = 0,\ldots,4$. The index l denotes the *level of refinement*. Figure 7.6 depicts two of the considered spatial meshes.

l	N	h	N_t	Δt
0	56	0.5	8	0.5
1	224	0.25	16	0.25
2	896	0.125	32	0.125
3	3584	0.0625	64	0.0625
4	14336	0.03125	128	0.03125

Table 7.6: Levels of refinement under consideration.

Table 7.7 shows the space-time error for the interior evaluation of both indirect methods. The SLP BEM basically reaches the same order of convergence as already observed in the experiment in Laplace domain. Similarly to before, the rod has edges and corners, hence the regularity of the underlying density function is strictly limited. The observed behaviour suggests that the lacking smoothness of density on Γ predominates the error for the SLP BEM.

In contrast, the DLP BEM reaches the optimal quadratic rate of convergence. Although the errors in the Laplace domain decay like $\mathcal{O}(h^3)$, the discretization via the BDF-2 scheme used in the CQM seems to permit a $\mathcal{O}(\Delta t^2)$ behaviour in time. Due to the uniformity of the space-time refinement, the considered error measure vanishes in a quadratic fashion.

Moreover, table 7.8 shows the errors in the Cauchy data as well as the interior evaluation for the direct BEM. As expected, the Dirichlet data converges at a quadratic rate. Although the Neumann data are expected to show a linear rate, the numerical experiment shows a better rate. This might be induced by the fact that the Neumann data are actually zero on

	SLP BEM		DLP BEM	
l	$e_{\Omega\times\Upsilon}$	eoc	$e_{\Omega\times\Upsilon}$	eoc
0	2.96E+00		2.05E+00	
1	8.69E-01	1.77	5.62E-01	1.87
2	2.41E-01	1.85	1.47E-01	1.93
3	6.59E-02	1.87	3.77E-02	1.97
4	1.80E-02	1.87	9.59E-03	1.97
eoc_{opt}		2		2

Table 7.7: Error and rate of convergence for the interior evaluation for the rod, indirect BEM.

most of Γ. The error in the interior evaluation vanishes quadratically. Similarly to the DLP BEM the time discretization seems to dominate the error and the cubic convergence of the experiment in Laplace domain cannot be achieved.

As a concluding remark it shall be noted that the direct method could not solve level $l = 4$ in a reasonable time with the resources available.

	direct BEM					
l	$e^D_{\Gamma\times\Upsilon}$	eoc	$e^N_{\Gamma\times\Upsilon}$	eoc	$e_{\Omega\times\Upsilon}$	eoc
0	1.18E+00		1.11E+00		2.07E+00	
1	3.09E-01	1.94	4.86E-01	1.20	5.68E-01	1.87
2	7.96E-02	1.96	1.76E-01	1.46	1.48E-01	1.94
3	2.02E-02	1.98	6.33E-02	1.48	3.78E-02	1.97
theory		2		1		2

Table 7.8: Error and rate of convergence for the Cauchy data and interior evaluation for the rod, direct BEM.

7.3 Applications

To underline the potential of the discussed methods, we shift our attention to an actual problem of architectural acoustics. The main goal is to show that the employed procedures are indeed capable of reproducing the absorption of incoming waves at the boundary. It seems adequate to consider a domain which has a lot of edges and nooks, such that a rather complex state in terms of superposition of the waves is reached. To this extent we consider an atrium[1] whose model is depicted in figure 7.7.

[1] The considered atrium is an abstract model of areas of an actual structure. This building belongs to the Irchel campus of the Univeristy of Zurich and its address is *Winterthurerstrasse 190, 8057 Zurich*.

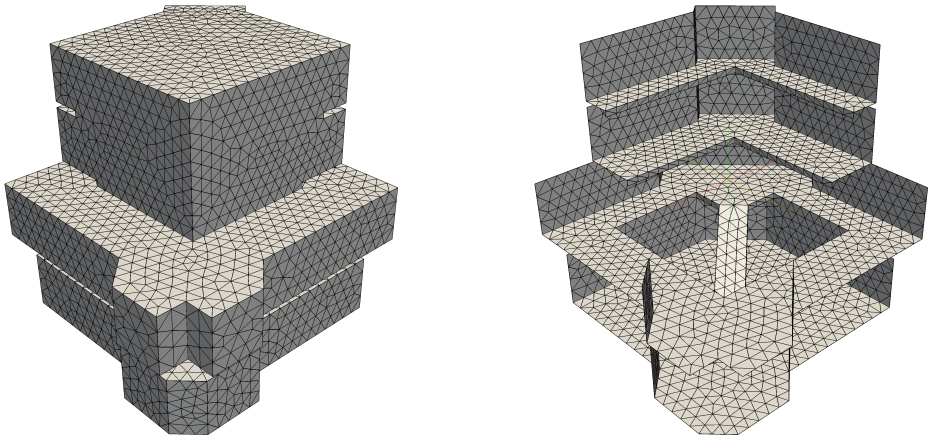

Figure 7.7: The considered atrium, discretized by a mesh comprised of $N = 7100$ elements.

The experiment conducted in the sequel is rather straightforward. The coefficient of absorption is set to $\alpha = 0$ for the walls and floors, as they are assumed to be acoustically hard. The ceilings, on the other hand, are furnished with some sort of absorbing material. Hence, we consider the decomposition of the boundary $\Gamma = \Gamma_0 \cup \Gamma_\alpha$ and $\Gamma_0 \cap \Gamma_\alpha = 0$, where $\alpha = 0$ on Γ_0 and $\alpha > 0$ on Γ_α holds. The considered degrees of absorption are divided into the following three levels:

- low level of insulation: $\alpha = 0.05$ on Γ_α
- intermediate level of insulation: $\alpha = 0.40$ on Γ_α
- high level of insulation: $\alpha = 0.80$ on Γ_α

The ceilings that are equipped with an absorbing material are depicted in figure 7.8. Moreover, we set up a mesh of sampling points to evaluate the pressure in the interior of the atrium. The pressure distribution on this mesh is interpolated in a linear continuous manner. This mesh is shown in figure 7.8.

To apply a suitable loading scenario to this problem we consider an impulse imposed by an incoming wave u^{inc}. The scattered response of the system to this load u^{scat} is obtained by solving the initial-boundary value problem (2.10) with the right hand side

$$f(\mathbf{x},t) = -\left[\gamma_1^- u^{\text{inc}}(\mathbf{x},t) + \frac{\alpha(\mathbf{x})}{c_0}\gamma_0^- \partial_t u^{\text{inc}}(\mathbf{x},t)\right] \quad \forall\,(\mathbf{x},t) \in \Gamma \times (0,\infty) \quad . \tag{7.2}$$

The final pressure function is obtained by superposition $u := u^{\text{inc}} + u^{\text{scat}}$.

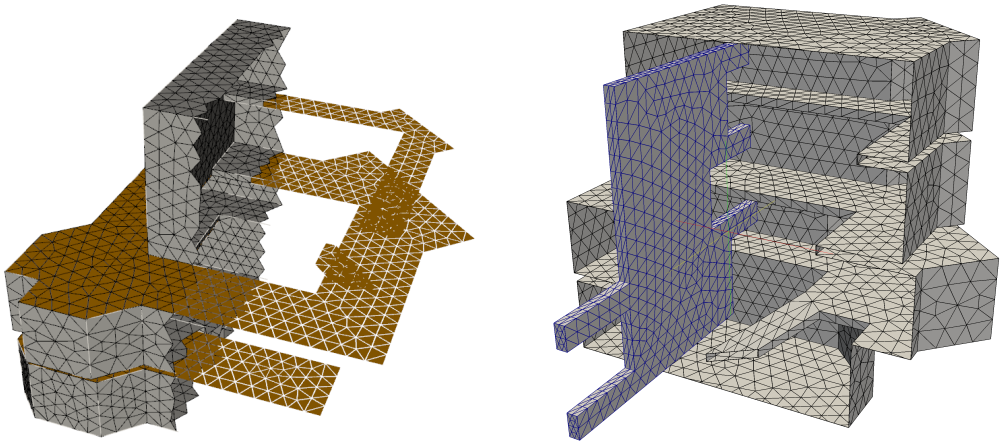

Figure 7.8: Cross sections of the meshed courtyard. On the left hand side the ceilings equipped with an absorbing material, i.e. Γ_α, are coloured, whereas Γ_0 is left grey. On the right hand side the interior sampling mesh is drawn in blue.

The incoming wave function considered throughout the following experiments reads

$$u^{\text{inc}}(\tilde{\mathbf{x}},t) = \frac{1}{4\pi r(\tilde{\mathbf{x}})} \sin\left(\frac{2\pi}{a}\left(t - \frac{r(\tilde{\mathbf{x}})}{c_0}\right)\right)\left[\Theta\left(t - \frac{r(\tilde{\mathbf{x}})}{c_0}\right) - \Theta\left(t - \frac{r(\tilde{\mathbf{x}})}{c_0} - an\right)\right] \quad \forall\,(\tilde{\mathbf{x}},t) \in \Omega^- \times (0,\infty) \tag{7.3}$$

where $r(\tilde{\mathbf{x}}) = \|\tilde{\mathbf{x}} - \tilde{\mathbf{y}}_0\|$ and $\tilde{\mathbf{y}}_0 \in \Omega^-$ is the source point of the impulse. Furthermore, we have the frequency scaling $a := \frac{2}{c_0}$ [s] and the number of periods the incoming sine goes through before fading out $n := 1$. For the positioning of the source point $\tilde{\mathbf{y}}_0$ we consider two locations. The first one is established in the upper region of the atrium, rather far from the boundary, while the second one is stationed in the lower region at the very bottom of the central stairs.

For all following considerations we assume the adiabatic bulk modulus $K = 1.42 \times 10^5$ [Pa] and the mean density $\rho_0 = 1.2041$ [kg m^{-3}], which correspond to the recommended value for a room temperature of 20 [°C]. This leads to a speed of sound of $c_0 \approx 343.41$ [m s^{-1}] and thus the frequency of the imposed impulse (7.3) is roughly 172 [Hz].

In terms of discretization we opt for a rather coarse mesh, since the dense Galerkin BEM employed throughout this thesis is rather expensive in terms of computational cost and the available resources are somewhat limited. The considered mesh features $N = 7100$ elements and has a mean mesh size of roughly $h_{\text{mean}} \approx 0.52$ [m]. The time step size $\Delta t = 1.5 \times 10^{-3}$ [s] is chosen such that $\beta := \frac{c_0 \Delta t}{h_{\text{mean}}}$ is approximately one.

Most of the computations are performed using the direct Galerkin BEM to obtain the Dirichlet data, i.e. the pressure distribution on the surface, immediately. However, we used the indirect DLP BEM to compute the interior results depicted in figure 7.9.

Figure 7.9 shows the interior pressure distribution due to an impulse situated in the upper area of the atrium for all three considered configurations of insulation at an intermediate time level. We clearly observe that the overall pressure is reduced and the pressure peaks are less pronounced for acoustically softer materials.

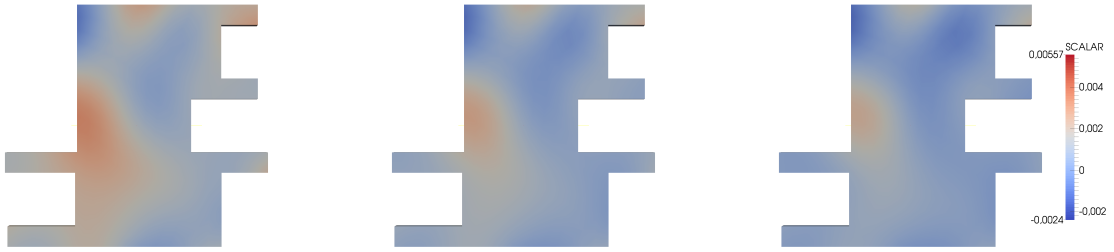

(a) $\alpha = 0.05$, $t = 0.096$ s (b) $\alpha = 0.40$, $t = 0.096$ s (c) $\alpha = 0.80$, $t = 0.096$ s

Figure 7.9: Sound pressure at the interior sampling mesh due to an excitation located in the upper area of the atrium.

The pressure distribution on the surface corresponding to the same impulse is depicted in figure 7.10. In contrast to the previous consideration, we observe three time levels and realize that the difference gets more evident as time advances. While all three configurations show roughly the same pressure distribution at the early time level it is evident that the softer materials already absorbed large parts of the wave in the later time levels. Furthermore, figure 7.11 shows the interior of the atrium for the lowest and highest level of insulation at the intermediate time step, whereas figure 7.12 depicts a cross-section of the same scenario. These plots confirm the previous observations and suggest that the acoustic waves are indeed absorbed by the different surfaces in a distinct manner.

A similar behaviour is shown in figure 7.13, where an excitation at the bottom of the central stair is considered. Especially for the lowest level of insulation we observe quite large pressure peaks in the depicted areas, which might be induced by the fact that the waves are reflected back and forth in the confined space around the source point. Similarly to the previous case, the configurations equipped with higher levels of acoustic insulation were already capable of dissipating a siginificant share of the incoming wave at the advanced time levels. Moreover, figure 7.14 depicts the inner of the atrium for the lowest and highest level of insulation at the intermediate time step, while figure 7.15 shows a cross-section of the same situation. Interestingly, the acoustic pressure is quite large in the top floors for the configuration featuring only negligible absorption. This behaviour would suggest that noise created at the ground floor is clearly audible in the entire atrium. This circumstance is also observed by the users of the actual structure this model is based on. However, if the atrium is furnished with insulating material these effects can be diminished decisively.

To conclude these numerical experiments we state that the results suggest that the employed methods are capable of representing the absorption of acoustic waves on the surface in varying magnitudes. Moreover, the calculations suggest that the overall level of noise in the atrium might be quite uncomfortable if no acoustic insulation is employed. Additionally, it is indicated that applying an absorbing material to the ceilings of the structure may lead to a significant reduction of these intrusive effects.

The very intention of this example is to apply the boundary element method, which was discussed in a slightly abstract fashion throughout this thesis, to an actual problem of enginnering science. The presented computations should be considered a mere *proof of concept* rather than a precise simulation in terms of acoustic design. To provide a reasonable simulation for the purpose of creating acoustic design concepts, one would have to consider further levels of refinement in order to verify that the results are not distorted by any errors of the numerical approximation. Moreover, one would have to test more frequencies and observe a longer time interval in order to compute actual reverberation times for different configurations of insulation. Furthermore, the geometric model of the atrium features quite a high level of abstraction compared to the real structure, as many details are left out for the sake of simplicity.

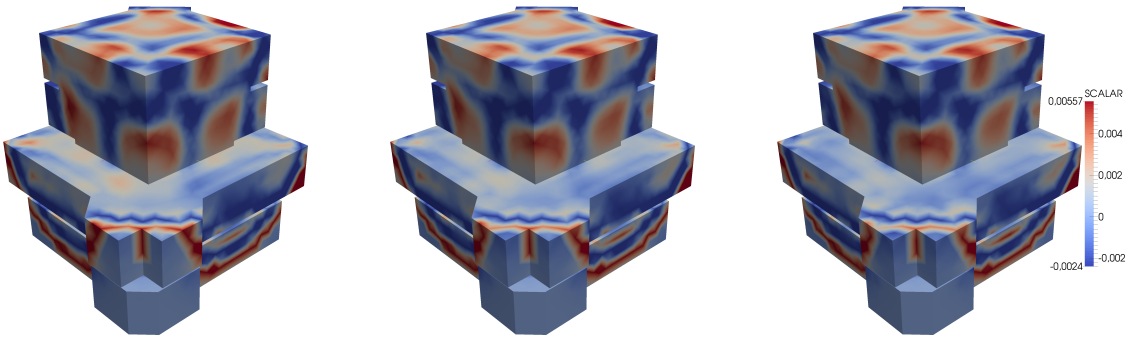

(a) $\alpha = 0.05$, $t = 0.036$ s (b) $\alpha = 0.40$, $t = 0.036$ s (c) $\alpha = 0.80$, $t = 0.036$ s

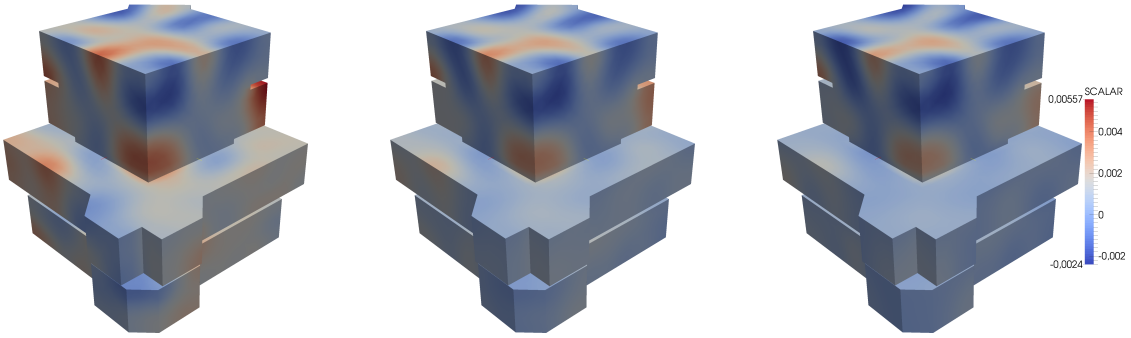

(d) $\alpha = 0.05$, $t = 0.096$ s (e) $\alpha = 0.40$, $t = 0.096$ s (f) $\alpha = 0.80$, $t = 0.096$ s

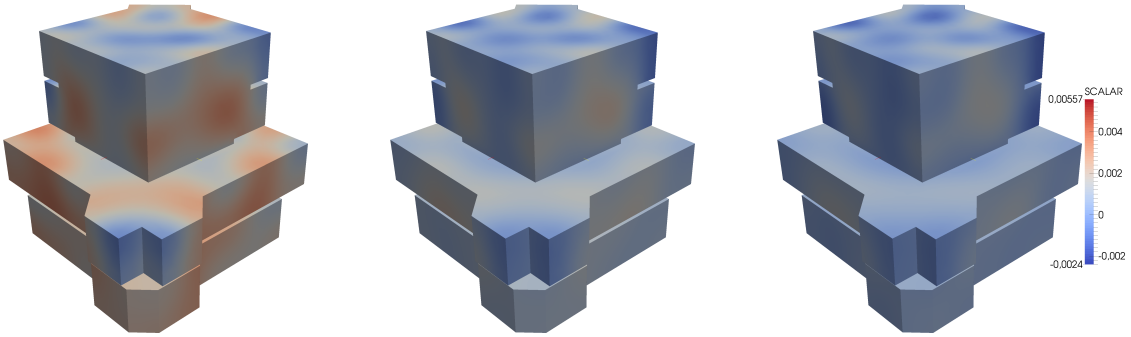

(g) $\alpha = 0.05$, $t = 0.138$ s (h) $\alpha = 0.40$, $t = 0.138$ s (i) $\alpha = 0.80$, $t = 0.138$ s

Figure 7.10: Sound pressure on the surface due to an impulse located in the upper area of the staircase.

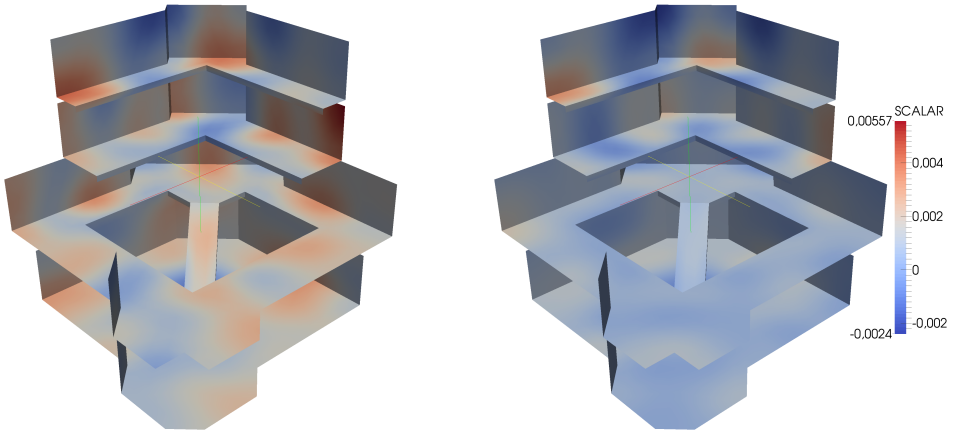

(a) $\alpha = 0.05$, $t = 0.096$ s (b) $\alpha = 0.80$, $t = 0.096$ s

Figure 7.11: Sound pressure on the surface due to an impulse located in the upper area of the atrium.

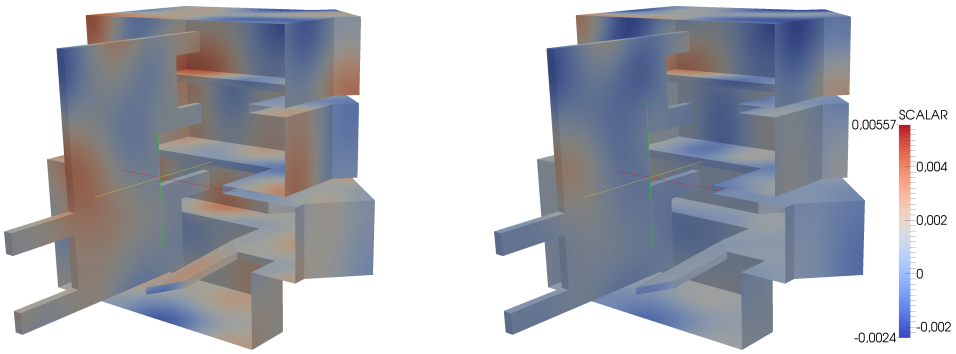

(a) $\alpha = 0.05$, $t = 0.096$ s (b) $\alpha = 0.80$, $t = 0.096$ s

Figure 7.12: Sound pressure on the surface and at the interior sampling points due to an impulse located in the upper area of the atrium.

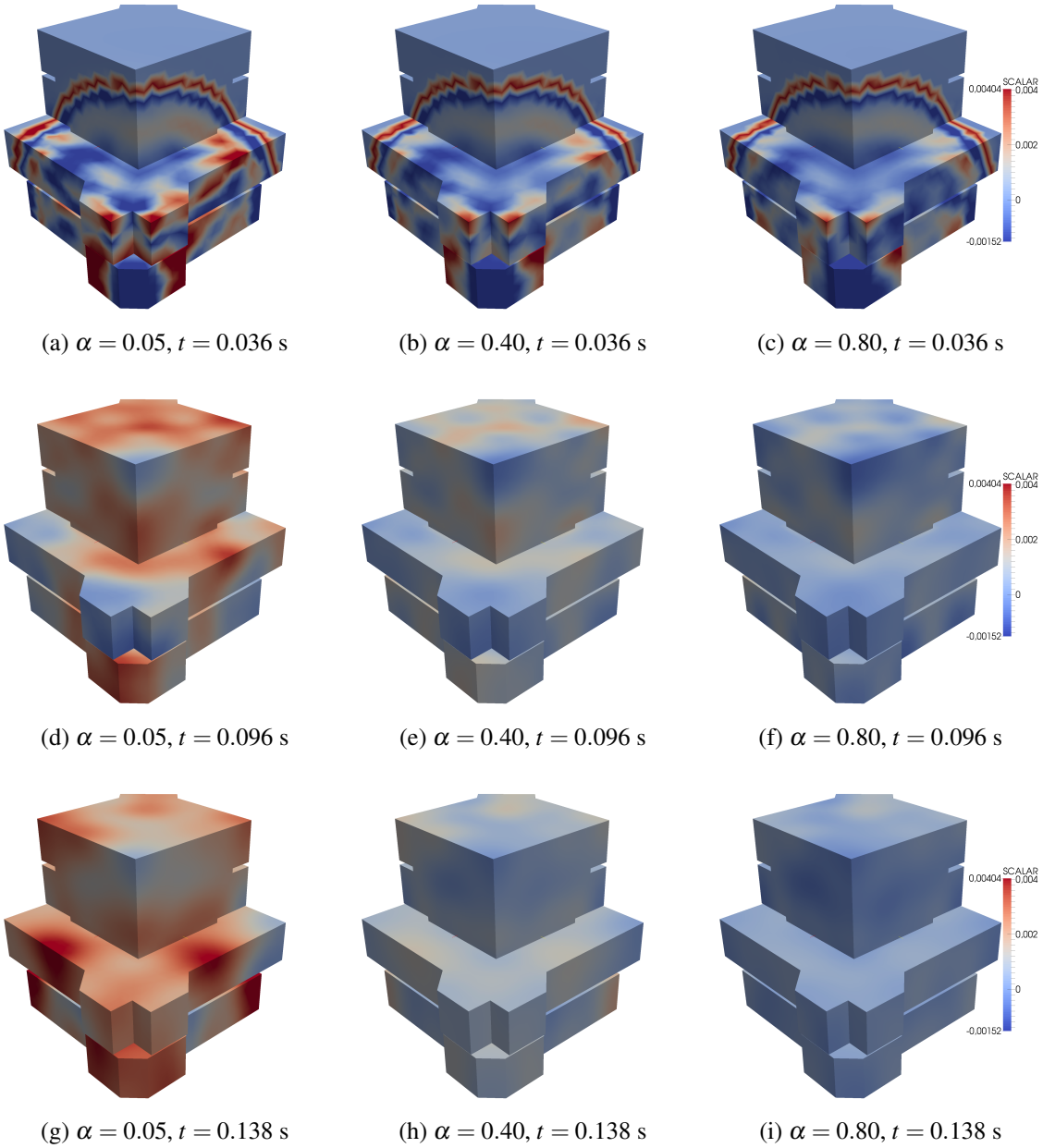

(a) $\alpha = 0.05$, $t = 0.036$ s (b) $\alpha = 0.40$, $t = 0.036$ s (c) $\alpha = 0.80$, $t = 0.036$ s

(d) $\alpha = 0.05$, $t = 0.096$ s (e) $\alpha = 0.40$, $t = 0.096$ s (f) $\alpha = 0.80$, $t = 0.096$ s

(g) $\alpha = 0.05$, $t = 0.138$ s (h) $\alpha = 0.40$, $t = 0.138$ s (i) $\alpha = 0.80$, $t = 0.138$ s

Figure 7.13: Sound pressure on the surface due to an impulse located in the lower area of the staircase.

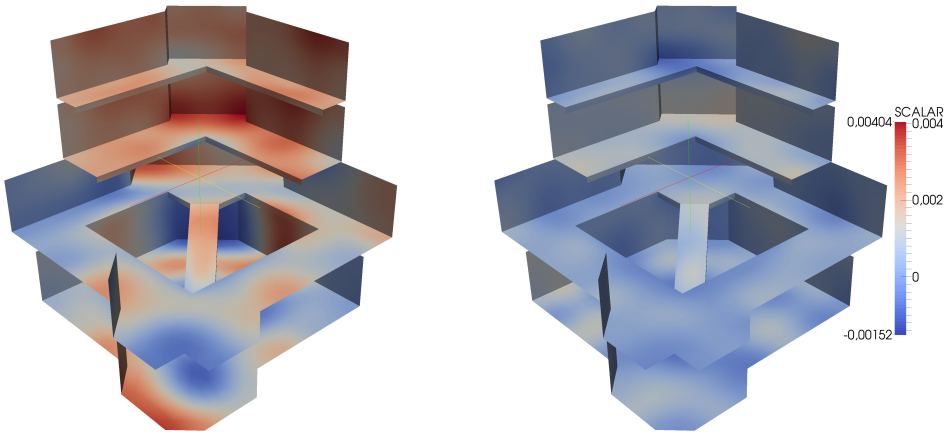

(a) $\alpha = 0.05$, $t = 0.096$ s (b) $\alpha = 0.80$, $t = 0.096$ s

Figure 7.14: Sound pressure on the surface due to an impulse located in the lower area of the staircase.

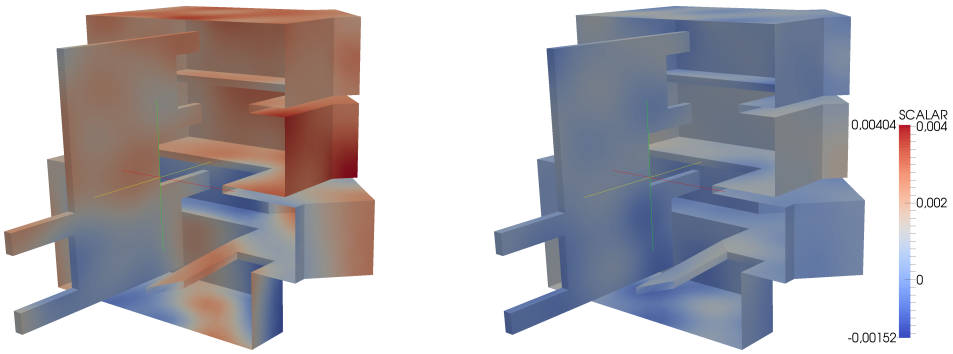

(a) $\alpha = 0.05$, $t = 0.096$ s (b) $\alpha = 0.80$, $t = 0.096$ s

Figure 7.15: Sound pressure on the surface and at the interior sampling points due to an impulse located in the lower area of the staircase.

8 CONCLUSION

The goal of this thesis is to simulate the absorption of acoustic waves as they interact with different types of surfaces. To do so the linear acoustic wave equation is used in conjuction with a special impedance boundary condition. The resulting initial-boundary value problem is transformed to Laplace domain and converted to an equivalent integral equation. The solution in time domain is then retrieved from the one in Laplace domain via the CQM. The boundary integral equations in Laplace domain are discretized utilizing the well-established Galerkin BEM, where three different methods are considered. The principles of spatial discretization by means of boundary elements are stated rather extensively to give the reader an introduction to these methods. Furthermore, some fundamental properties of the approximations generated by the Galerkin BEM are discussed. The given methods are implemented in an existing BEM code and their correctness is validated by numerical experiments in both Laplace and time domain. Finally, these methods are applied to a problem of architectural acoustics, where the results are deemed satisfactory.

The fact that a naive discretization of boundary integral operators leads to fully populated matrices in conjunction with the Galerkin method causes the presented numerical methods to be awfully expensive in terms of computational cost. Thus, it has to be emphasized that the dense Galerkin BEM treated throughout this work is not competitive with other numerical procedures for many problems posed on interior domains. However, the given boundary element formulations can be applied to exterior problems by mere change of sign, cf. [28,30]. In such applications the discussed methods might prove viable due to the inherent advantages gained by transforming the problem to the surface of the unbounded domain.

To alleviate the drawback of dense matrices one could employ fast boundary element methods, which seek sparse representations of the occurring stiffness matrices. For such matrices the use of an iterative solver is particularly appealing as it enables an efficient solution of the algebraic system. Since the condition number grows as $h \to 0$ one might have to employ a suitable preconditioner to prevent the number of required iterations from growing as well. As already pointed out in the introduction fast boundary element methods are competitive to domain-based methods and might eventually prove superior to them if the scale of the problem is sufficiently large.

Moreover, one could resort to a more refined mechanical model. The impedance boundary condition employed throughout this work is a widely used concept when it comes to acoustic absorption, however, there are certainly more sophisticated models for this purpose. Instead of a mere boundary condition one could consider an actual layer of porous

material located on the surface. In essence there would be two domains, the air and the porous layer, that have to be coupled appropriately. One could even utilize a nonlinear model for the porous material, which might be discretized by a finite element method, and couple this approach with a boundary element method discretizing the surface of the surrounding body of air. Such combinations of finite and boundary element methods seem particularly attractive as they merge the advantages of both underlying procedures.

A MATHEMATICAL PRELIMINARIES

Note that most of the following definitions are taken from [30].

Considering the open domain $\Omega \subset \mathbb{R}^d$ we define the *support* of a function $u(\tilde{\mathbf{x}}),\ \tilde{\mathbf{x}} \in \Omega$ by

$$\operatorname{supp}(u) := \overline{\{\tilde{\mathbf{x}} \in \Omega : u(\tilde{\mathbf{x}}) \neq 0\}}$$

and we say a function u has *compact support* if

$$\operatorname{supp}(u) \subset \Omega$$

holds.

By $L_p(\Omega)$ we denote the space of all functions on Ω whose powers of order p are integrable. The associated norm reads as

$$\|u\|_{L_p(\Omega)} := \left\{ \int_\Omega |u(\tilde{\mathbf{x}})|^p d\tilde{\mathbf{x}} \right\}^{1/p} \qquad \text{for } p \in [1,\infty) \quad .$$

Two functions $u, v \in L_p(\Omega)$ are identified with each other if they are different only on a set of zero measure. Consider the Heaviside step function

$$\Theta(x) = \begin{cases} 1 & \text{for } x > 0 \\ 0 & \text{for } x < 0 \end{cases}$$

for $x \in (-1,1)$. Regardless of the definition at $x = 0$ its norm is given by

$$\|u\|^p_{L_p((0,1))} = \int_{-1}^{1} |\Theta(x)|^p dx = \int_0^1 1^p dx = 1$$

since the integral occuring in the norm cannot reflect the deviation at single points.

Probably the most important Lebesgue space is obtained by setting $p = 2$, which is the space of *square integrable functions*. Its norm is induced by the scalar product

$$(u,v)_{L_2(\Omega)} = \int_\Omega u(\tilde{\mathbf{x}}) \overline{v}(\tilde{\mathbf{x}}) d\tilde{\mathbf{x}}$$

such that $(u,u)_{L_2(\Omega)} = \|u\|^2_{L_2(\Omega)}$ holds. Note that $\bar{v}$ denotes the complex conjugate of v satisfying $\Re v = \Re \bar{v}$ and $\Im v = -\Im \bar{v}$.

The concept of square integrability may be extended to the derivatives of a function as well leading to the *Sobolev spaces* in the process. For a more comprehensive discussion of these spaces refer to the introductions in [30] or [28]. The Sobolev space $H^s(\mathbb{R}^d)$ is equipped with the norm

$$\|v\|^2_{H^s(\mathbb{R}^d)} := \int_{\mathbb{R}^d} (1+|\xi|^2)^s |\mathcal{F}v(\xi)|^2 d\xi$$

for real $s \geq 0$ and $\mathcal{F}v$ being the Fourier transform of v. The space $H^s(\Omega)$ is obtained by restriction

$$H^s(\Omega) := \left\{ v = \tilde{v}_{|\Omega} : \tilde{v} \in H^s(\mathbb{R}^d) \right\}$$

with the norm

$$\|v\|_{H^s(\Omega)} := \inf_{\tilde{v} \in H^s(\mathbb{R}^d), \tilde{v}_{|\Omega} = v} \|\tilde{v}\|_{H^s(\mathbb{R}^d)} \quad .$$

Furthermore the application of the trace operator to functions induces function spaces on the boundary. The space of square integrable functions on the surface is defined by the norm

$$\|v\|_{L_2(\Gamma)} := \left\{ \int_\Gamma |v(\mathbf{x})|^2 ds_\mathbf{x} \right\}^{1/2}$$

induced by the scalar product

$$(u,v)_{L_2(\Gamma)} = \int_\Gamma u(\mathbf{x}) \bar{v}(\mathbf{x}) ds_\mathbf{x} \quad .$$

Additionally, we define the weighted scalar product

$$(u,v)_{L_2(\Gamma),w} = \int_\Gamma w(\mathbf{x}) u(\mathbf{x}) \bar{v}(\mathbf{x}) ds_\mathbf{x} \quad .$$

where $w : \Gamma \to \mathbb{R}_{\geq 0}$ denotes the weight. For $s \in (0,1)$ the Sobolev-Slobodeckii norm reads

$$\|v\|_{H^s(\Gamma)} := \left\{ \|v\|^2_{L_2(\Gamma)} + \int_{\Gamma\times\Gamma} \frac{|v(\mathbf{x}) - v(\mathbf{y})|^2}{\|\mathbf{x}-\mathbf{y}\|^{d-1+2s}} ds_\mathbf{x} ds_\mathbf{y} \right\} \quad .$$

For $s < 0$ the Sobolev spaces are defined by duality

$$H^s(\Gamma) := \left[H^{-s}(\Gamma) \right]'$$

when Γ is a closed surface, cf. [28, chapter 2.4]. They are equipped with the norm

$$\|w\|_{H^s(\Gamma)} := \sup_{0\neq v\in H^{-s}(\Gamma)} \frac{\langle w, v\rangle}{\|v\|_{H^{-s}(\Gamma)}}$$

with respect to the duality pairing $\langle\cdot,\cdot\rangle : H^s(\Gamma)\times H^{-s}(\Gamma)\to\mathbb{C}$

$$\langle w, v\rangle := \int_\Gamma w(\mathbf{x})\overline{v}(\mathbf{x})ds_{\mathbf{x}} \quad .$$

Moreover, for $s > 0$ we define the space of piecewise smooth functions

$$H^s_{pw}(\Gamma) := \left\{w \in L_2(\Gamma) : w_{|\Gamma_k} \in H^s(\Gamma_k),\ k = 1,\dots,N\right\}$$

with the norm

$$\|w\|_{H^s_{pw}(\Gamma)} := \left\{\sum_{k=1}^{N} \|w_{|\Gamma_k}\|^2_{H^s(\Gamma_k)}\right\}^{1/2} \quad .$$

B EXPLICIT REPRESENTATION OF THE BOUNDARY INTEGRAL OPERATORS

B.1 Boundary integral operators in time domain

With the fundamental solution of the wave equation

$$U(\tilde{\mathbf{z}},t) = \frac{1}{4\pi\|\tilde{\mathbf{z}}\|}\delta_0\left(t - \frac{\|\tilde{\mathbf{z}}\|}{c_0}\right) \quad \forall\,(\tilde{\mathbf{z}},t) \in \mathbb{R}^3 \times (0,\infty)$$

and the sifting property of the Dirac distribution δ_0 we obtain the single layer potential

$$\begin{aligned}\left(\tilde{\mathcal{V}} * \varphi\right)(\tilde{\mathbf{x}},t) &:= \int_\Gamma \int_0^t U(\tilde{\mathbf{x}}-\mathbf{y}, t-\tau)\,\varphi(\mathbf{y},t)\,d\tau\,ds_\mathbf{y} \\ &= \int_\Gamma \frac{\varphi\left(\mathbf{y}, t - \frac{1}{c_0}\|\tilde{\mathbf{x}}-\mathbf{y}\|\right)}{4\pi\|\tilde{\mathbf{x}}-\mathbf{y}\|}\,ds_\mathbf{y} \quad \forall\,(\tilde{\mathbf{x}},t) \in \Omega^- \times (0,\infty)\end{aligned}$$

for any suitable φ. To compute the double layer potential we employ several results. First, we note

$$\operatorname{grad}_{\tilde{\mathbf{y}}}\|\tilde{\mathbf{x}}-\tilde{\mathbf{y}}\| = -\frac{\tilde{\mathbf{x}}-\tilde{\mathbf{y}}}{\|\tilde{\mathbf{x}}-\tilde{\mathbf{y}}\|}$$

furthermore we utilize two results obtained by application of the chain rule to

$$\underbrace{\delta_0\left(t - \tau - \frac{1}{c_0}\|\tilde{\mathbf{x}}-\tilde{\mathbf{y}}\|\right)}_{=:\, f(\tilde{\mathbf{x}},\tilde{\mathbf{y}},t,\tau)}$$

namely

$$\begin{aligned}\operatorname{grad}_{\tilde{\mathbf{y}}}\delta_0\left(f(\tilde{\mathbf{x}},\tilde{\mathbf{y}},t,\tau)\right) &= \partial_f\delta_0 \operatorname{grad}_{\tilde{\mathbf{y}}} f \\ \partial_t\delta_0\left(f(\tilde{\mathbf{x}},\tilde{\mathbf{y}},t,\tau)\right) &= \partial_f\delta_0 \underbrace{\partial_t f}_{=1}\end{aligned}$$

where we omitted the argument list on the right hand side. This finally yields the relation

$$\operatorname{grad}_{\tilde{\mathbf{y}}}\delta_0\left(f(\tilde{\mathbf{x}},\tilde{\mathbf{y}},t,\tau)\right) = \operatorname{grad}_{\tilde{\mathbf{y}}} f(\tilde{\mathbf{x}},\tilde{\mathbf{y}},t,\tau)\,\partial_t\delta_0\left(f(\tilde{\mathbf{x}},\tilde{\mathbf{y}},t,\tau)\right)$$

where $\operatorname{grad}_{\tilde{\mathbf{y}}} f(\tilde{\mathbf{x}},\tilde{\mathbf{y}},t,\tau) = \frac{\tilde{\mathbf{x}}-\tilde{\mathbf{y}}}{c_0\|\tilde{\mathbf{x}}-\tilde{\mathbf{y}}\|}$. By using

$$\int_0^T \partial_t \delta_0(t-\tau) f(\tau) d\tau = -\partial_t f(t) \quad \forall\, t \in (0,T)$$

we obtain the explicit representation of the double layer potential for the wave equation

$$\begin{aligned}(\mathcal{W} * \psi)(\tilde{\mathbf{x}},t) &:= \int_\Gamma \int_0^t \gamma_{1,\mathbf{y}}^- U(\tilde{\mathbf{x}}-\mathbf{y},t-\tau)\,\psi(\mathbf{y},\tau) d\tau ds_{\mathbf{y}} \\ &= \int_\Gamma \frac{(\mathbf{n}(\mathbf{y}),\tilde{\mathbf{x}}-\mathbf{y})}{4\pi\|\tilde{\mathbf{x}}-\mathbf{y}\|^2} \left(\frac{\psi\left(\mathbf{y},t-\frac{1}{c_0}\|\tilde{\mathbf{x}}-\mathbf{y}\|\right)}{\|\tilde{\mathbf{x}}-\mathbf{y}\|} + \frac{1}{c_0}\partial_t \psi\left(\mathbf{y},t-\frac{1}{c_0}\|\tilde{\mathbf{x}}-\mathbf{y}\|\right)\right) ds_{\mathbf{y}} \\ &\qquad\qquad \forall\,(\tilde{\mathbf{x}},t) \in \Omega^- \times (0,\infty)\end{aligned}$$

for any suitable ψ.

B.2 Boundary integral operators in Laplace domain

By either applying the Laplace transform to the single and double layer potentials in time domain or inserting the fundamental solution of the Helmholtz equation[1]

$$\hat{U}_s(\tilde{\mathbf{z}}) = \frac{\exp\left(-\frac{s}{c_0}\|\tilde{\mathbf{z}}\|\right)}{4\pi\|\tilde{\mathbf{z}}\|} \quad \forall\, \tilde{\mathbf{z}} \in \mathbb{R}^3$$

we get the explicit representations of the layer potentials associated with the Laplace transformed wave equation. We obtain the single layer potential

$$\left(\tilde{\mathcal{V}}_s \hat{\varphi}\right)(\tilde{\mathbf{x}}) := \int_\Gamma \hat{U}_s(\tilde{\mathbf{x}}-\mathbf{y})\,\hat{\varphi}(\mathbf{y})(\mathbf{y}) ds_{\mathbf{y}} = \int_\Gamma \frac{\exp(-\frac{s}{c_0}\|\tilde{\mathbf{x}}-\mathbf{y}\|)}{4\pi\|\tilde{\mathbf{x}}-\mathbf{y}\|}\hat{\varphi}(\mathbf{y}) ds_{\mathbf{y}}$$

as well as the double layer potential

$$\begin{aligned}(\mathcal{W}_s \hat{\psi})(\tilde{\mathbf{x}}) &:= \int_\Gamma \gamma_{1,\mathbf{y}}^- \hat{U}_s(\tilde{\mathbf{x}}-\mathbf{y})\,\hat{\psi}(\mathbf{y}) ds_{\mathbf{y}} \\ &= \int_\Gamma \frac{(\mathbf{n}(\mathbf{y}),\tilde{\mathbf{x}}-\mathbf{y})\exp(-\frac{s}{c_0}\|\tilde{\mathbf{x}}-\mathbf{y}\|)}{4\pi\|\tilde{\mathbf{x}}-\mathbf{y}\|^2}\left(\frac{1}{\|\tilde{\mathbf{x}}-\mathbf{y}\|}+\frac{s}{c_0}\right)\hat{\psi}(\mathbf{y}) ds_{\mathbf{y}}\end{aligned}$$

both for any suitable $\hat{\varphi}$ and $\hat{\psi}$ respectively.

[1] The Helmholtz operator and the Yukawa operator are interpreted in a unified fashion.

C ERRORS IN FUNCTIONALS OF THE BOUNDARY ELEMENT SOLUTION

The following explanations are based on [28, theorem 4.2.14].

With the notation of chapter 6 the abstract variational formulation of a boundary integral equation reads as

$$\text{find } u \in H : b(u,v) = F(v) \quad \forall\, v \in H \quad . \tag{C.1}$$

By considering a family of conforming trial spaces $\{H_K\}_K \subset H$ we obtain the Galerkin discretized incarnation of (C.1)

$$\text{find } u_K \in H_K : b(u_K, v_K) = F(v_K) \quad \forall\, v_K \in H_K \tag{C.2}$$

where the Galerkin orthogonality

$$b(u - u_K, v_K) = 0 \quad \forall\, v_K \in H_K \tag{C.3}$$

holds. Furthermore, we consider the dual problem

$$\text{find } \varphi \in H : b(\eta, \varphi) = \sigma(\eta) \quad \forall\, \eta \in H \tag{C.4}$$

with the continuous linear functional $\sigma \in H'$. Due to the inclusion $u_K \in H_K \subset H$ we may insert u_K in σ and get the difference

$$|\sigma(u) - \sigma(u_K)| = |\sigma(u - u_K)| = |b(u - u_K, \varphi)|$$

by the linearity of σ. Using the Galerkin orthogonality (C.3) we obtain

$$|\sigma(u - u_K)| = |b(u - u_K, \varphi - v_K)| \quad \forall\, v_K \in H_K$$

and due to the boundedness of $b(\cdot,\cdot)$ we end up with

$$|\sigma(u - u_K)| = |b(u - u_K, \varphi - v_K)| \leq c\|u - u_K\|_H \|\varphi - v_K\|_H \quad \forall\, v_K \in H_K \quad .$$

Due to the quasi-optimality of the error implied by (C.3) we get

$$|\sigma(u - u_K)| \leq c \inf_{v_K \in H_K} \|u - v_K\|_H \inf_{\eta_K \in H_K} \|\varphi - \eta_K\|_H \quad . \tag{C.5}$$

Statement (C.5) tells us that if u and φ are sufficiently smooth the rate of convergence in functionals of the solution is two times the rate of convergence of the solution in the energy norm.

As a model problem we consider the single layer potential ansatz for a fixed $\tilde{\mathbf{x}} \in \Omega$

$$u(\tilde{\mathbf{x}}) := \left(\tilde{\mathcal{V}}_s w\right)(\tilde{\mathbf{x}}) = \int_\Gamma \hat{U}_s(\tilde{\mathbf{x}} - \mathbf{y})\, w(\mathbf{y})\, ds_\mathbf{y}$$

with the spaces $H := H^{-1/2}(\Gamma)$ and $H' := H^{1/2}(\Gamma)$. By interpreting the integral as duality pairing $\langle \cdot, \cdot \rangle_{H^{1/2}(\Gamma) \times H^{-1/2}(\Gamma)}$ we learn

$$\left| \int_\Gamma \hat{U}_s(\tilde{\mathbf{x}} - \mathbf{y})\, w(\mathbf{y})\, ds_\mathbf{y} \right| \leq \underbrace{\| \hat{U}_s(\tilde{\mathbf{x}} - \cdot) \|_{H^{1/2}(\Gamma)}}_{c(\tilde{\mathbf{x}})} \| w \|_{H^{-1/2}(\Gamma)}$$

and thus the solution $u(\tilde{\mathbf{x}})$, $\tilde{\mathbf{x}} \in \Omega$ is governed by the linear continuous functional $\sigma(w)$, implying the error estimate (C.5). By employing the approximation property of the piecewise discontinuous boundary element space $S_h^{d_p}$ (6.12) we obtain

$$|u(\tilde{\mathbf{x}}) - u_h(\tilde{\mathbf{x}})| \leq c h^{1/2+\min(p+1,s)} \|w\|_{H^s(\Gamma)}\, h^{1/2+\min(p+1,t)} \|\varphi\|_{H^t(\Gamma)}$$

for $s, t \geq 1/2$. If the solutions are sufficiently regular we obtain for the space of piecewise constant basis functions, i.e. $p = 0$, the error estimate

$$|u(\tilde{\mathbf{x}}) - u_h(\tilde{\mathbf{x}})| \leq c h^3 \|w\|_{H^1(\Gamma)}\, \|\varphi\|_{H^1(\Gamma)} \quad .$$

Note that since the fundamental solution $\hat{U}_s(\tilde{\mathbf{x}} - \mathbf{y})$ is analytic for $\tilde{\mathbf{x}} \neq \mathbf{y}$ any derivative of it is also in $H^{1/2}(\Gamma)$. Thus the obtained order of convergence is valid for the function u itself as well as any quantity defined by derivatives of u inside Ω. As a result the observed rates of convergence only depend on the regularity of w and φ, which highly depend on the smoothness of the domain. For the dual problem (C.4) in conjuction with the single layer potential ansatz there holds

$$\|\varphi\|_{H^{-1/2+s}(\Gamma)} \leq c \|\hat{U}_s(\tilde{\mathbf{x}} - \cdot)\|_{H^{1/2+s}(\Gamma)}$$

on a globally smooth boundary for any $s \geq 0$, see [28, theorem 3.2.2]. Due to the analyticity of $\hat{U}_s(\tilde{\mathbf{x}} - \cdot)$ already mentioned in the prequel its norm exists for any s. Hence we get

$$\|\varphi\|_{H^1(\Gamma)} \leq c \|\hat{U}_s(\tilde{\mathbf{x}} - \cdot)\|_{H^2(\Gamma)} =: c_{\text{int}}(\tilde{\mathbf{x}})$$

which leads to the final error estimate of the single layer potential ansatz

$$|u(\tilde{\mathbf{x}}) - u_h(\tilde{\mathbf{x}})| \leq c(\tilde{\mathbf{x}})\, h^3 \|w\|_{H^1(\Gamma)}$$

for smooth boundaries Γ. Note that the constant $c(\tilde{\mathbf{x}})$ becomes very large when $\tilde{\mathbf{x}}$ is close to the surface, thus one should only compute interior solutions sufficiently far from the boundary.

Furthermore, these concepts can be expanded to the double layer potential in a rather straightforward way. Since the interior evaluation of the direct method is merely an addition of single and double layer potential the obtained results remain valid for it as well.

D SYMMETRY OF GALERKIN BEM MATRICES

Throughout this appendix we consider the generic ansatz functions $\varphi \in H_1$ and $\psi \in H_2$ whose actual representation does not matter as long as they are contained in the function spaces associated with the respective sesquilinear forms.

D.1 Single layer potential and hypersingular operator

Consider the single layer potential matrix

$$\mathsf{V}_h[k,l] = \int\limits_{\Gamma\times\Gamma} \hat{U}_s(\mathbf{x}-\mathbf{y})\,\psi_k(\mathbf{x})\psi_l(\mathbf{y})\,ds_{\mathbf{y}}\,ds_{\mathbf{x}}$$

whose transposed reads as

$$\mathsf{V}_h[l,k] = \int\limits_{\Gamma\times\Gamma} \hat{U}_s(\mathbf{x}-\mathbf{y})\,\psi_l(\mathbf{x})\psi_k(\mathbf{y})\,ds_{\mathbf{y}}\,ds_{\mathbf{x}} \quad ,$$

and since $\mathbf{x},\mathbf{y} \in \Gamma$ we may change their roles, leading to

$$\mathsf{V}_h[l,k] = \int\limits_{\Gamma\times\Gamma} \hat{U}_s(\mathbf{y}-\mathbf{x})\,\psi_l(\mathbf{y})\psi_k(\mathbf{x})\,ds_{\mathbf{x}}\,ds_{\mathbf{y}} \quad .$$

Due to the radial-symmetry of the fundamental solution, i.e. it only depends on the norm of the argument, we have $\hat{U}_s(\mathbf{y}-\mathbf{x}) = \hat{U}_s(\mathbf{x}-\mathbf{y})$, which gives

$$\mathsf{V}_h[l,k] = \int\limits_{\Gamma\times\Gamma} \hat{U}_s(\mathbf{x}-\mathbf{y})\,\psi_l(\mathbf{y})\psi_k(\mathbf{x})\,ds_{\mathbf{x}}\,ds_{\mathbf{y}} = \mathsf{V}_h[k,l].$$

Thus the single layer potential matrix is symmetric $\mathsf{V}_h = \mathsf{V}_h^T$. This argument can be applied in a very straightforward manner to the matrix of the hypersingular boundary integral operator as well. By using the symmetry of the Euclidean scalar product one obtains the symmetry $\mathsf{D}_h = \mathsf{D}_h^T$.

Note that the SLP matrix associated to the weighted $L_2(\Gamma)$ scalar product is not symmetric

$$\begin{aligned}
\mathsf{V}_h^{\kappa}[k,l] &= \int_{\Gamma\times\Gamma} \hat{U}_s(\mathbf{x}-\mathbf{y})\,\kappa(\mathbf{x})\psi_k(\mathbf{x})\psi_l(\mathbf{y})\,ds_{\mathbf{y}}\,ds_{\mathbf{x}} \\
\mathsf{V}_h^{\kappa}[l,k] &= \int_{\Gamma\times\Gamma} \hat{U}_s(\mathbf{x}-\mathbf{y})\,\kappa(\mathbf{x})\psi_l(\mathbf{x})\psi_k(\mathbf{y})\,ds_{\mathbf{y}}\,ds_{\mathbf{x}} \\
&= \int_{\Gamma\times\Gamma} \hat{U}_s(\mathbf{y}-\mathbf{x})\,\kappa(\mathbf{y})\psi_l(\mathbf{y})\psi_k(\mathbf{x})\,ds_{\mathbf{x}}\,ds_{\mathbf{y}} \\
&= \int_{\Gamma\times\Gamma} \hat{U}_s(\mathbf{x}-\mathbf{y})\,\kappa(\mathbf{y})\psi_l(\mathbf{y})\psi_k(\mathbf{x})\,ds_{\mathbf{y}}\,ds_{\mathbf{x}} \quad \neq \quad \mathsf{V}_h^{\kappa}[k,l] \quad .
\end{aligned}$$

D.2 Double layer potential and adjoint double layer potential

Consider the double layer potential matrix

$$\mathsf{K}_h[k,l] = \int_{\Gamma\times\Gamma} \gamma_{1,\mathbf{y}}^{-}\hat{U}_s(\mathbf{x}-\mathbf{y})\,\psi_k(\mathbf{x})\varphi_l(\mathbf{y})\,ds_{\mathbf{y}}\,ds_{\mathbf{x}}$$

whose transpose is

$$\mathsf{K}_h[l,k] = \int_{\Gamma\times\Gamma} \gamma_{1,\mathbf{y}}^{-}\hat{U}_s(\mathbf{x}-\mathbf{y})\,\psi_l(\mathbf{x})\varphi_k(\mathbf{y})\,ds_{\mathbf{y}}\,ds_{\mathbf{x}}$$

and by changing the roles of $\mathbf{x}$ and $\mathbf{y}$ we get

$$\mathsf{K}_h[l,k] = \int_{\Gamma\times\Gamma} \gamma_{1,\mathbf{y}}^{-}\hat{U}_s(\mathbf{y}-\mathbf{x})\,\psi_l(\mathbf{y})\varphi_k(\mathbf{x})\,ds_{\mathbf{x}}\,ds_{\mathbf{y}} \quad . \tag{D.1}$$

Using the chain rule for differentiation one finds $\gamma_{1,\mathbf{y}}^{-}\hat{U}_s(\mathbf{y}-\mathbf{x}) = -\gamma_{1,\mathbf{x}}^{-}\hat{U}_s(\mathbf{y}-\mathbf{x})$ and by employing the the point symmetry $\gamma_{1,\mathbf{x}}^{-}\hat{U}_s(\mathbf{y}-\mathbf{x}) = -\gamma_{1,\mathbf{x}}^{-}\hat{U}_s(\mathbf{x}-\mathbf{y})$ we obtain

$$\gamma_{1,\mathbf{y}}^{-}\hat{U}_s(\mathbf{y}-\mathbf{x}) = \gamma_{1,\mathbf{x}}^{-}\hat{U}_s(\mathbf{x}-\mathbf{y}) \quad . \tag{D.2}$$

Insertion of (D.2) into (D.1) yields

$$\mathsf{K}_h[l,k] = \int_{\Gamma\times\Gamma} \gamma_{1,\mathbf{y}}^{-}\hat{U}_s(\mathbf{y}-\mathbf{x})\,\psi_l(\mathbf{y})\varphi_k(\mathbf{x})\,ds_{\mathbf{x}}\,ds_{\mathbf{y}} = \int_{\Gamma\times\Gamma} \gamma_{1,\mathbf{x}}^{-}\hat{U}_s(\mathbf{x}-\mathbf{y})\,\psi_l(\mathbf{y})\varphi_k(\mathbf{x})\,ds_{\mathbf{x}}\,ds_{\mathbf{y}}$$

and recalling the definition of the adjoint double layer potential matrix

$$\mathsf{K}'_h[l,k] = \int_{\Gamma\times\Gamma} \gamma^-_{1,\mathbf{x}} \hat{U}_s(\mathbf{x}-\mathbf{y})\, \varphi_k(\mathbf{x})\psi_l(\mathbf{y})\, ds_{\mathbf{y}}\, ds_{\mathbf{x}}$$

we obtain $\mathsf{K}_h^T = \mathsf{K}'_h$. Therefore, only one of these two operators has to be considered when using the direct method, as the other one can be retrieved by transposition.

D.3 Mass matrices

For the sake of completeness we consider the mass matrix of the jump term of the double layer potential

$$\mathsf{M}_h[k,l] = \int_{\Gamma} \psi_k(\mathbf{x})\varphi_l(\mathbf{x})\, ds_{\mathbf{x}}$$

whose transpose

$$\mathsf{M}_h[l,k] = \int_{\Gamma} \psi_l(\mathbf{x})\varphi_k(\mathbf{x})\, ds_{\mathbf{x}}$$

coincides with the jump term of the adjoint double layer potential

$$\mathsf{M}'_h[l,k] = \int_{\Gamma} \varphi_k(\mathbf{x})\psi_l(\mathbf{x})\, ds_{\mathbf{x}} \quad .$$

Once again, only the mass matrix of the double layer potential has to be computed and the mass matrix of the adjoint double layer potential may be obtained by transposition.

Note that the weighted mass matrix M_h^κ remains symmetric.

E A SAMPLE SOLUTION FOR THE WAVE EQUATION

We observe the open one-dimensional spatial domain $\Omega = (0,L) \subset \mathbb{R}$. The considered initial-boundary value problem reads

$$\begin{aligned} \left(c_0^{-2}\partial_{tt} - \partial_{xx}\right) u(x,t) &= 0 \qquad \forall\, (x,t) \in \Omega \times (0,\infty) \quad , \\ u(x,0) = \partial_t u(x,0) &= 0 \qquad \forall\, x \in \Omega \quad , \\ -\partial_x u(0,t) + \kappa_0 \partial_t u(0,t) &= f_0(t) \quad \forall\, t \in (0,\infty) \quad , \\ \partial_x u(L,t) + \kappa_L \partial_t u(L,t) &= f_L(t) \quad \forall\, t \in (0,\infty) \quad , \end{aligned} \tag{E.1}$$

where both the differential equation and the initial conditions are homogeneous, while the Robin boundary conditions are inhomogeneous.

E.1 General solution in Laplace domain

In order to derive a sample solution for the previously described problem we switch from time domain to Laplace domain. The Laplace transform of a function $u(x,t)$ is once again denoted by $\hat{u}(x,s)$.

Application of the Laplace transform to the partial differential equation yields

$$s^2\hat{u}(x,s) - s\underbrace{u(x,0)}_{=0\ \forall x\in\Omega} - \underbrace{\partial_t u(x,0)}_{=0\ \forall x\in\Omega} - c_0^2\partial_{xx}\hat{u}(x,s) = 0$$

where we used the vanishing intial conditions. Hence, we obtain the ordinary differential equation

$$s^2\hat{u}(x,s) - c_0^2\partial_{xx}\hat{u}(x,s) = 0 \quad \forall\, x \in \Omega$$

for some suitable $s \in \mathbb{C}$. Note that this equation is the Helmholtz equation for complex-valued wave numbers in one dimension. By inserting the ansatz

$$\begin{aligned} \hat{u}(x,\lambda) &= C\exp(\lambda x) \quad , \\ \partial_x\hat{u}(x,\lambda) &= C\lambda\exp(\lambda x) \quad , \\ \partial_{xx}\hat{u}(x,\lambda) &= C\lambda^2\exp(\lambda x) \end{aligned}$$

into the differential equation (E.1), we obtain

$$\begin{aligned} s^2 C\exp(\lambda x) - c_0^2 C\lambda^2\exp(\lambda x) &= 0 \\ C\exp(\lambda x)(s^2 - c_0^2\lambda^2) &= 0 \end{aligned}$$

and since above equation has to hold for any $x \in \Omega$ we get $\lambda = \pm\frac{s}{c_0}$. Hence, the general solution of the differential equation reads

$$\hat{u}(x,s) = A(s)\exp(\tfrac{s}{c_0}x) + B(s)\exp(-\tfrac{s}{c_0}x) \quad , \tag{E.2}$$

which still has to be tailored to satisfy the boundary conditions. This step will be performed in the sequel.

Application of the Laplace transform to the boundary conditions in (E.1) yields

$$\begin{aligned} \lim_{\substack{x\to 0\\ x>0}} \left[-\partial_x \hat{u}(x,s) + \kappa_0 \big(s\hat{u}(x,s) - \underbrace{\partial_t u(x,s)}_{=0} \big) \right] &= \hat{f}_0(s) \quad , \\ \lim_{\substack{x\to L\\ x<L}} \left[\partial_x \hat{u}(x,s) + \kappa_L \big(s\hat{u}(x,s) - \underbrace{\partial_t u(x,s)}_{=0} \big) \right] &= \hat{f}_L(s) \quad , \end{aligned}$$

where the homogeneous initial conditions were employed once again. The general solution previously (E.2) has to be adapted such that it satisfies the boundary conditions

$$\begin{aligned} -\partial_x \hat{u}(0,s) + \kappa_0 s\hat{u}(0,s) &= \hat{f}_0(s) \quad , \\ \partial_x \hat{u}(L,s) + \kappa_L s\hat{u}(L,s) &= \hat{f}_L(s) \quad . \end{aligned}$$

By inserting the ansatz (E.2) into both boundary conditions we find

$$\begin{aligned} -A(s)\tfrac{s}{c_0} + B(s)\tfrac{s}{c_0} + \kappa_0 s(A(s)+B(s)) &= \hat{f}_0(s) \\ A(s)\tfrac{s}{c_0}\exp(\tfrac{L}{c_0}s) - B(s)\tfrac{s}{c_0}\exp(-\tfrac{L}{c_0}s) + \kappa_L s(A(s)\exp(\tfrac{L}{c_0}s) + B(s)\exp(-\tfrac{L}{c_0}s)) &= \hat{f}_L(s) \end{aligned}$$

which corresponds to the system

$$s \begin{bmatrix} -\frac{1}{c_0} + \kappa_0 & \frac{1}{c_0} + \kappa_0 \\ \exp(\frac{L}{c_0}s)(\frac{1}{c_0} + \kappa_L) & \exp(-\frac{L}{c_0}s)(-\frac{1}{c_0} + \kappa_L) \end{bmatrix} \begin{bmatrix} A(s) \\ B(s) \end{bmatrix} = \begin{bmatrix} \hat{f}_0(s) \\ \hat{f}_L(s) \end{bmatrix} \quad . \tag{E.3}$$

The goal is to choose $F_0(s)$ and $F_L(s)$, which implies the choice of $f_0(t)$ and $f_L(t)$, such that the final solution can be transformed back to time domain easily. To do so we set $A := 0$, which reduces the first equation in (E.3) to

$$s(\tfrac{1}{c_0} + \kappa_0)B(s) = \hat{f}_0(s)$$

leading to

$$B(s) = \frac{1}{s}\frac{\hat{f}_0(s)}{\frac{1}{c_0} + \kappa_0} \quad . \tag{E.4}$$

For a vanishing A the second equation in (E.3) becomes

$$s\exp(-\tfrac{L}{c_0}s)(-\tfrac{1}{c_0}+\kappa_L)B(s)=\hat{f}_L(s)$$

and insertion of (E.4) yields the following equation

$$\hat{f}_L(s)=\hat{f}_0(s)\exp(-\tfrac{L}{c_0}s)\frac{-\frac{1}{c_0}+\kappa_L}{\frac{1}{c_0}+\kappa_0} \tag{E.5}$$

which determines $\hat{f}_L(s)$ such that $A=0$.

The choice of $f_0(t)$, which implies $\hat{f}_0(s)$, is crucial in order to get a practical solution. Recall the relation

$$t^n\Theta(t)\circ\!\!-\!\!\bullet\,\frac{n!}{s^{n+1}}$$

for some $n\in\mathbb{N}^0$, where $\mathbb{N}^0$ is the set of nonnegative integers and $\Theta(t)$ is the Heaviside step function.

Let $f_0(t)=(\frac{1}{c_0}+\kappa_0)\frac{1}{(p-1)!}t^{p-1}\Theta(t)$ for some $p\in\mathbb{N}\subset\mathbb{N}^0$, where $\mathbb{N}$ is the set of positive integers. We obtain the Laplace transformed signal

$$f_0(t)=(\tfrac{1}{c_0}+\kappa_0)\frac{1}{(p-1)!}t^{p-1}\Theta(t)\circ\!\!-\!\!\bullet\,(\tfrac{1}{c_0}+\kappa_0)\frac{1}{s^p}=\hat{f}_0(s) \tag{E.6}$$

and the signal at the other end is obtained by inserting $\hat{f}_0(s)$ into (E.5)

$$\hat{f}_L(s)=(-\tfrac{1}{c_0}+\kappa_L)\frac{1}{s^p}\exp(-\tfrac{L}{c_0}s)\;\bullet\!\!-\!\!\circ\;(-\tfrac{1}{c_0}+\kappa_L)\frac{1}{(p-1)!}(t-\tfrac{L}{c_0})^{p-1}\Theta(t-\tfrac{L}{c_0})=f_L(t) \tag{E.7}$$

where we used the rule of translation in time domain.

E.2 Final solution in Laplace and time domain

With (E.4) and (E.6) we find

$$B(s)=\frac{1}{s^{p+1}}$$

and inserting this result into (E.2) we obtain a solution of the boundary value problem in Laplace domain

$$\hat{u}(x,s)=\frac{1}{s^{p+1}}\exp(-\tfrac{s}{c_0}x)\quad .$$

By applying the inverse Laplace transform, we retrieve the solution of the initial-boundary value problem in time domain

$$\frac{1}{s^{p+1}}\exp(-\tfrac{s}{c_0}x)\;\bullet\!\!-\!\!\circ\;\frac{1}{p!}(t-\tfrac{x}{c_0})^p\Theta(t-\tfrac{x}{c_0})=u(x,t)\quad\forall\,(x,t)\in\Omega\times(0,\infty)$$

for some $p \in \mathbb{N}$. Note that the choice of p determines the smoothness of $u(x,t)$ in $\Omega \times (0,\infty)$, where higher values correspond to smoother functions.

E.3 Summary and solution in three spatial dimensions

Right hand side in time domain:

$$\begin{aligned} f_0(t) &= (\tfrac{1}{c_0} + \kappa_0)\frac{1}{(p-1)!}t^{p-1}\Theta(t) \\ f_L(t) &= (-\tfrac{1}{c_0} + \kappa_L)\frac{1}{(p-1)!}(t-\tfrac{L}{c_0})^{p-1}\Theta(t-\tfrac{L}{c_0}) \end{aligned}$$

Right hand side in Laplace domain:

$$\begin{aligned} F_0(s) &= (\tfrac{1}{c_0} + \kappa_0)\frac{1}{s^p} \\ F_L(s) &= (-\tfrac{1}{c_0} + \kappa_L)\frac{1}{s^p}\exp(-\tfrac{L}{c_0}s) \end{aligned}$$

Solution in Laplace domain:

$$\begin{aligned} U(x,s) &= \frac{1}{s^{p+1}}\exp(-\tfrac{s}{c_0}x) \\ \partial_x U(x,s) &= -\frac{1}{c_0\, s^p}\exp(-\tfrac{s}{c_0}x) \end{aligned}$$

Solution in time domain:

$$\begin{aligned} u(x,t) &= \frac{1}{p!}(t-\tfrac{x}{c_0})^p\Theta(t-\tfrac{x}{c_0}) \\ \partial_x u(x,t) &= -\frac{1}{c_0(p-1)!}(t-\tfrac{x}{c_0})^{p-1}\Theta(t-\tfrac{x}{c_0}) \quad . \end{aligned}$$

It shall be noted that above solution is not defined at $t = \frac{x}{c_0}$, since we left $\Theta(0)$ intentionally undefined. As we seek a continuous extension of $u(x,t)$ to the entire domain $\Omega \times (0,\infty)$ we introduce the retarded time $\xi = t - \frac{x}{c_0}$ and obtain the function

$$\bar{u}(\xi) = \xi^p \Theta(\xi) \quad .$$

This function is in $C^\infty(\mathbb{R}\setminus\{0\})$, since it is defined by a polynomial for $\xi > 0$ and zero for $\xi < 0$. Performing the limit $\xi \to 0$ from both sides yields

$$\begin{aligned} \lim_{\substack{\epsilon\to 0 \\ \epsilon>0}} \bar{u}(\epsilon) &= \lim_{\substack{\epsilon\to 0 \\ \epsilon>0}} \epsilon^p = 0 \\ \lim_{\substack{\epsilon\to 0 \\ \epsilon>0}} \bar{u}(-\epsilon) &= \lim_{\substack{\epsilon\to 0 \\ \epsilon>0}} 0 = 0 \end{aligned}$$

where $p \geq 1$ and thus there exists a continuous extension of $\bar{u}$ to the entire real line, satisfying $\bar{u}(0) = 0$. We denote this extension of $\bar{u}$ by $\tilde{\bar{u}}$, which reads

$$\tilde{\bar{u}}(\xi) = \begin{cases} 0 & \text{for } \xi = 0 \\ \bar{u}(\xi) & \text{elsewhere} \end{cases} = \begin{cases} 0 & \text{for } \xi = 0 \\ \xi^p \Theta(\xi) & \text{elsewhere} \end{cases} \quad .$$

If $p \geq 2$ then $\tilde{\bar{u}}(\xi)$ is differentiable at $\xi = 0$

$$\lim_{\substack{\epsilon \to 0 \\ \epsilon > 0}} \frac{1}{\epsilon} [\tilde{\bar{u}}(\epsilon) - \tilde{\bar{u}}(0)] = \lim_{\substack{\epsilon \to 0 \\ \epsilon > 0}} \frac{1}{\epsilon} [\epsilon^p - 0] = \lim_{\substack{\epsilon \to 0 \\ \epsilon > 0}} \epsilon^{p-1} = 0 \quad .$$

By repeated differentiation we induce that $\tilde{\bar{u}} \in C^{p-1}(\mathbb{R})$. As a result, we define the continuous extension of $u(x,t)$

$$\tilde{u}(x,t) = \begin{cases} 0 & \text{for } t = \frac{x}{c_0} \\ \frac{1}{p!}(t - \frac{x}{c_0})^p \Theta(t - \frac{x}{c_0}) & \text{elsewhere} \end{cases}$$

where $\tilde{u}(x,t) \in C^{p-1}(\Omega \times (0,\infty))$ holds.

The solution derived in one spatial dimension solves a corresponding problem in $\Omega \subset \mathbb{R}^3$ as well. The open time interval remains unchanged while the considered open domain is a prism with a square base

$$\Omega \quad := \quad (0,L) \times (-\tfrac{a}{2}, \tfrac{a}{2}) \times (-\tfrac{a}{2}, \tfrac{a}{2}) \subset \mathbb{R}^3 \quad .$$

Applying the operator of the wave equation in three spatial dimensions

$$c_0^{-2} \partial_{tt} - (\partial_{x_1 x_1} + \partial_{x_2 x_2} + \partial_{x_3 x_3})$$

to the adapted one-dimensional solution

$$u(x,t) := \begin{cases} 0 & \text{for } t = \frac{x_1}{c_0} \\ \frac{1}{p!}(t - \frac{x_1}{c_0})^p \Theta(t - \frac{x_1}{c_0}) & \text{elsewhere} \end{cases}$$

yields zero in $\Omega \times (0,\infty)$, thus the differential equation is satisfied. The boundary conditions at $x_1 = 0$ and $x_1 = L$ remain unaltered, however, at the lateral boundaries (either $x_2 = \pm\frac{a}{2}$ or $x_3 = \pm\frac{a}{2}$) we have to enforce a different condition. Since the derivatives of the one dimensional solution with respect to the x_2- or x_3- direction vanish, we have to demand homogeneous Neumann conditions along the lateral boundaries, i.e. $\gamma_1^- u = 0$. Then the adapted one-dimensional solution is a solution of the three-dimensional problem and can be used for a convergence study.

REFERENCES

[1] J. Baaran. Schallfeldanalyse bei sich bewegenden schallerzeugenden körpern. In H. Antes, editor, *Braunschweiger Schriften zur Mechanik*. Mechanik-Zentrum der Technischen Univeristät Braunschweig, 1999.

[2] L. Banjai and S. Sauter. Rapid solution of the wave equation in unbounded domains. *SIAM Journal on Numerical Analysis*, 47.1:227–249, 2008.

[3] L. Banjai and M. Schanz. Wave propagation problems treated with convolution quadrature and bem. In *Fast boundary element methods in engineering and industrial applications*, pages 145–184. Springer Berlin Heidelberg, 2012.

[4] K.-J. Bathe. *Finite-Elemente-Methoden*. Springer, Berlin, 2002.

[5] J. P. Boyd. *Fourier and Chebyshev Spectral Methods*. Dover Publications, New York, 2000.

[6] E. O. Brigham. *FFT - Schnelle Fourier-Transformation*. R. Oldenbourg Verlag GmbH, München, 1987.

[7] M. Costabel. Boundary integral operators on Lipschitz domains: Elementary results. *SIAM Journal on Mathematical Analysis*, 19:613–626, 1988.

[8] M. Costabel. Time-dependent problems with the boundary integral equation method. In *Encyclopedia of computational mechanics*, chapter 25, pages 703–721. Wiley, 2004.

[9] G. Doetsch. *Anleitung zum praktischen Gebrauch der Laplace-Transformation und der Z-Transformation*. R. Oldenbourg Verlag GmbH, München, 1989.

[10] J. Dominguez. *Boundary Elements in Dynamics*. Computational Mechanics Publications, Southampton, 1993.

[11] L. Gaul, M. Kögl, and M. Wagner. *Boundary Element Methods for Engineers and Scientists*. Springer-Verlag, Berlin Heidelberg, 2003.

[12] W. C. Gibson. *The Method of Moments in Electromagnetics*. Taylor & Francis Group, Boca Raton, 2008.

[13] T. Ha-Duong, B. Ludwig, and I. Terrasse. A galerkin bem for transient acoustic scattering by an absorbing obstacle. *International Journal for Numerical Methods in Engineering*, 57.13:1845–1882, 2003.

[14] W. Hackbusch. Panel clustering techniques and hierarchical matrices for bem and fem. In *Encyclopedia of computational mechanics*, chapter 21, pages 597–615. Wiley, 2004.

[15] G. A. Holzapfel. *Nonlinear sold mechanics*. Wiley, Chichester, 2010.

[16] M. Jung and U. Langer. *Methode der finiten Elemente für Ingenieure*. Springer Fachmedien Wiesbaden, Wiesbaden, 2013.

[17] B. Kager. Efficient convolution quadrature based boundary element formulation for time-domain elastodynamics. In G. Brenn, G. A. Holzapfel, W. von der Linden, M. Schanz, and O. Steinbach, editors, *Monographic Series TU Graz,* volume 26 of *Computation in Engineering and Sciences*. Verlag der Technischen Univeristät Graz, 2015.

[18] L. Kielhorn. A time-domain symmetric galerkin BEM for viscoelastodynamics. In G. Brenn, G. A. Holzapfel, W. von der Linden, M. Schanz, and O. Steinbach, editors, *Monographic Series TU Graz,* volume 5 of *Computation in Engineering and Sciences*. Verlag der Technischen Univeristät Graz, 2009.

[19] C. Lubich. On the multistep discretization of linear initial-boundary value problems and their boundary integral equations. *Numerische Mathematik*, 67:365–389, 1994.

[20] W. J. Mansur. *A time-stepping technique to solve wave propagation problems using the boundary element method*. PhD thesis, University of Southampton, 1983.

[21] M. Messner, M. Messner, F. Rammerstorfer, P. Urthaler, T. Traub, and B. Kager. HyENA - Hyperbolic and Elliptic Numerical Analysis C++ BEM library. `www.mech.tugraz.at/HyENA`, 2015.

[22] P. M. Morse and K. U. Ingard. *Theoretical Acoustics*. Princeton University Press, Princeton, 1968.

[23] M. Möser. *Technische Akustik*. Springer-Verlag, Berlin-Heidelberg, 2012.

[24] *ÖNORM EN 12354-6, Bauakustik - Berechnung der akustischen Eigenschaften von Gebäuden aus den Bauteileigenschaften*, 2004.

[25] W.H. Press, S.A. Teukolsky, W.T. Vetterling, and B.P. Flannery. *Numerical Recipes in FORTRAN*. Cambridge University Press, 1992.

[26] S. W. Rienstra and A. Hirschberg. *An Introduction to Acoustics*. Eindhoven University of Technology, Eindhoven, 2004.

[27] S. Rjasanow and O. Steinbach. *The Fast Solution of Boundary Integral Equations*. Springer, New York, 2010.

[28] S. Sauter and C. Schwab. *Randelementmethoden*. B.G. Teubner Verlag, Wiesbaden, 2004.

[29] M. Schanz. Eine Randelementformulierung im Zeitbereich mit verallgemeinerten viskoelastischen Stoffgesetzen. Technical Report 1/1994, Institut A Mechanik, Univeristät Stuttgart, 1994.

[30] O. Steinbach. *Numerical Approximation Methods for Elliptic Boundary Value Problems*. Springer Science+Business Media, New York, 2010.

[31] G. Strang. *Computational Science and Engineering*. Wellesley-Cambridge Press, Wellesley, 2007.

[32] T. von Petersdorff and C. Schwab. Wavelet discretization of first kind boundary integral equations of polygons. *Numerische Mathematik*, 74:479–519, 1996.

[33] L.C. Wrobel. *The Boundary Element Method*. John Wiley & Sons, West Sussex, 2002.